

2019-07-16

# Porcine Circovirus Cap-Induced Apoptosis of Non-Infected PK15 Cells

Rowell, Jared S.

---

Rowell, J. S. (2019). Porcine Circovirus Cap-Induced Apoptosis of Non-Infected PK15 Cells (Master's thesis, University of Calgary, Calgary, Canada). Retrieved from <https://prism.ucalgary.ca>.  
<http://hdl.handle.net/1880/110647>

*Downloaded from PRISM Repository, University of Calgary*

UNIVERSITY OF CALGARY

Porcine Circovirus Cap-Induced Apoptosis of Non-Infected PK15 Cells

by

Jared S. Rowell

A THESIS

SUBMITTED TO THE FACULTY OF GRADUATE STUDIES

IN PARTIAL FULFILMENT OF THE REQUIREMENTS FOR THE

DEGREE OF MASTER OF SCIENCE

GRADUATE PROGRAM IN MICROBIOLOGY AND INFECTIOUS DISEASES

CALGARY, ALBERTA

JULY, 2019

© Jared S. Rowell 2019

## **Abstract**

Porcine Circovirus 2 (PCV2) is a pathogen of major importance for swine production around the world. Despite development of several vaccines and robust vaccination programs, PCV2 continues to persistently transmit within and between swine herds causing infections marked by immunosuppression via lymphocyte depletion. This study aims to improve understanding of porcine circovirus diseases (PCVD) pathogenesis caused by PCV capsid cytotoxicity which activates apoptosis in non-infected bystander cells.

Putatively non-pathogenic Porcine Circovirus 1 (PCV1) was also included to help understand why there is a difference in pathogenicity between PCV1 and PCV2. Porcine Circovirus 3 (PCV3) has recently emerged worldwide as a possible etiological agent of clinical syndromes observed in swine that are similar to PCVD caused by PCV2. The capsid protein of PCV3 (PCV 3 Cap) was also included in this study to provide initial information regarding the cytotoxicity of this protein.

Results were obtained through flow cytometric analysis of apoptosis using Annexin V-FITC and 7-AAD to measure apoptosis markers and cell death respectively. Flow cytometry results were reinforced by also utilizing a TUNEL assay in conjunction with confocal imaging to detect cells undergoing DNA fragmentation leading to apoptosis. Results show that monomeric PCV2 Cap, 1% formaldehyde inactivated and dialyzed PCV2, PCV1 virus-like particles (VLPs), PCV2 VLPs, and PCV3 VLPs are all able to activate apoptosis in porcine kidney (PK15) cells at a rate of ~%30 after a 24-hour exposure; this apoptotic similar to apoptosis caused by 50  $\mu$ M etoposide, which is a strong chemical inducer of apoptosis. These results coupled with preliminary data obtained by pre-treating PK15 cells with caspase-8 or caspase-9 inhibitors suggest the involvement of caspase-8 and caspase-9 in PCV2 Cap induced apoptosis and lend weight to the idea of PCV2 Cap as a primary virulence factor during infections. In contrast, PCV1 Cap induced apoptosis does not appear to involve caspase-8 or caspase-9 indicating an alternate pathway to PK15 cell apoptosis, while PCV3 Cap appears to induce PK15 cell apoptosis with some involvement of caspase-9.

**Keywords:** Porcine circovirus, baculovirus, apoptosis, immunosuppression, virus-like-particles

## **Acknowledgements**

Dr. Markus Czub

Victor Palomino

Dr. Xi-Long Xheng

Keith Lau

Dr. Frank Jirik

Aaron Hawkes

Dr. Cameron Knight

Narges Nourozieh

Dr. Faizal Careem

Alessa Schmidt

Dr. Nathan Peters

William Bremner

Dr. Frank van der Meer

Sarjoon-Mohammed Cader

Dr. Guido van Marle

Upasama Senapathi

Dr. Jennifer Corcoran

Paul Gajda

Dr. Rkia Dardari

Laurie Kennedy

Dr. Cristina Solis-Worsfold

Danielle Grant

Dr. Jana Hundt

Illia Bright

Dr. Antonia Klein

Gia Luu

Dr. Sabine Gilch

Katie Green

Dr. Robin Yates

Cameron Semper

Dr. Aruna Amarasinghe

Nawaf Nasir Jamil Bogari

Dr. Su Shim

## **Dedication**

I dedicate this thesis to the budding scientists whom I have had the honor and pleasure to work with these past few years. You represent the best in humanity to me and have helped me to find my niche in the world.

## Table of Contents

Abstract .....	ii
Acknowledgements .....	iii
Dedication .....	iv
Table of Contents .....	v
List of Tables .....	vii
List of Figures and Illustrations .....	viii
List of Symbols, Abbreviations and Nomenclature .....	xiv
 CHAPTER ONE: INTRODUCTION .....	 1
1.1 Porcine Circoviruses .....	1
1.1.1 Molecular Biology of Porcine Circoviruses .....	2
1.1.2 Porcine Circovirus Type 1 .....	4
1.1.3 Porcine Circovirus Type 2 .....	5
1.1.4 Porcine Circovirus Type 3 .....	7
1.2 Immunosuppression Caused by PCV2 Infection .....	8
1.2.1 PCV2 Dysregulates IL-10 Expression .....	9
1.2.2 PCV2 Upregulates Expression of Programmed Death-1 Receptor (PD-1) .....	10
1.2.3 PCV2 Upregulates Expression of Fas/FasL Activation-Induced Cell Death .....	10
1.2.4 PCV2 Cap Protein Drives Cellular Apoptosis Regardless of Subcellular Localization .....	11
1.3 Mechanisms of Cell Death .....	11
1.4 Hypothesis and Objectives of the Study .....	12
 CHAPTER TWO: MATERIALS AND METHODS .....	 14
2.1 Cell Culture .....	14
2.1.1 Hemocytometer Cell Counting .....	14
2.2 PCV2 Virus Stock Production .....	15
2.2.1 Stock PCV2 Virus Precipitation and Purification .....	16
2.3 PCV2 Capsid Protein Production in Rosetta Blue BL21(DE3) <i>Escherichia coli</i> .....	17
2.3.1 PCV2 Capsid Protein Purification from BL21(DE3) <i>E. coli</i> .....	18
2.4 Colony PCR .....	18
2.5 Virus Inactivation with 1% Formaldehyde Solution .....	20
2.6 Dialysis of Purified PCV2 Cap, Inactivated PCV2 Virus, and all PCV VLP Preparations .....	21
2.7 PCV Cap Protein Detection and Confirmation .....	22
2.7.1 SDS-PAGE, Coomassie Staining and Western Blot for PCV Cap Proteins .....	22
2.7.2 Immunofluorescence Assay (IFA) for Detection of PCV2 Infection .....	25
2.8 Virus Stock Titration by the Reed-Muench Method .....	25
2.9 PCV1 & PCV2 Capsid Proteins Restriction Enzyme Cloning into pFastBac Vector .....	28
2.9.1 PCV3 Capsid Gibson Cloning into pFastBac Vector .....	30
2.10 Recombinant Bacmids Production .....	30
2.10.1 Reverse Genetics Production of Recombinant Baculoviruses .....	31
2.11 PCV Capsid Protein Expression via Recombinant Bacmid Infection of Sf9 Cells .....	32
2.11.1 PCV Cap Inclusion Bodies & Virus-Like Particles (VLPs) Purification .....	33
2.11.2 Protein Quantification using Bio-Rad DC Protein Assay Kit .....	34

2.11.3 PCV Virus-Like Particles and Recombinant Baculoviruses Transmission	
Electron Microscopy .....	35
2.12 Cellular Apoptosis Assay Using Flow Cytometry.....	37
2.13 PCV-Induced Apoptosis TUNEL Assay Detection.....	39
CHAPTER THREE: RESULTS .....	42
3.1 Porcine Circovirus 2 Cap Protein Recombinantly Expressed in <i>E. coli</i> is Cytotoxic to PK15 Cells <i>in vitro</i> , Causing Apoptosis .....	42
3.2 Porcine Circovirus 2 Inactivated with 1% Formaldehyde is Cytotoxic to PK15 Cells <i>in vitro</i> .....	47
3.3 Live PCV2 Virus Does Not Cause Apoptosis of PK15 Cells at Low MOI.....	47
3.4 Porcine Circovirus 2 Virus-like Particles are Cytotoxic to PK15 Cells <i>in vitro</i> .....	48
3.5 Porcine Circovirus 1 Virus-like Particles are Cytotoxic to PK15 Cells <i>in vitro</i> .....	49
3.6 Porcine Circovirus 3 Virus-like Particles are Cytotoxic to PK15 Cells <i>in vitro</i> .....	51
3.7 PK15 Cell Apoptosis Caused by Porcine Circovirus 2 Cap is Reduced by Pre-treatment with Caspase-8 Inhibitor .....	52
3.8 PK15 Cell Apoptosis Caused by Porcine Circovirus 2 Cap and Porcine Circovirus 3 Cap is Reduced by Treatment with Caspase-9 Inhibitor .....	54
3.9 Statistical Analysis.....	55
CHAPTER FOUR: DISCUSSION .....	57
4.1 PCV2 Effectively Regulates Host Cell Processes to Control Host Apoptosis and PCV2 Cap is a Major Cytotoxic Mediator .....	57
4.2 PCV2 Cap Driven Apoptosis is Linked to Caspase-8 and Caspase-9 Dependant Pathways .....	59
4.3 Preliminary Results Indicate PCV 1 and 3 Cap are also Cytotoxic.....	60
4.3.1 PCV1 Activates Apoptosis Through a Caspase-Independent Mechanism.....	61
4.4 PCV1, PCV2, and PCV3 Capsid Proteins all Contain Mitochondrial Localization Sequences.....	62
4.5 Live PCV2 Virus at a low MOI Does Not Cause Apoptosis in PK15 Cells .....	64
4.6 Unanswered Questions and Future Directions.....	65
REFERENCES .....	68

## List of Tables

Table 1.1 Table overview summary of flow cytometric and TUNEL assay results. Live PCV2 Virus is unmodified stock virus exposed to cells at a MOI of 0.1. MOCK Infection samples were PK15 cells treated with only cell culture media and no additional treatments. Dialysis Buffer samples were collected after the last round of dialysis after formaldehyde treatments of stock virus and lysed PK15 cells. 1%F PK15 sample are cells lysed, treated with 1% formaldehyde, and then dialyzed to remove excess formaldehyde. The cBac sample is baculovirus containing a GUS insert and used as a wild-type control. Etoposide is a potent inducer of mammalian cell apoptosis at a final concentration of 50 $\mu$ M. 1%F PCV2 virus is 1% formaldehyde treated live virus post-dialysis. PCV VLPs represent virus-like-particles of each respective virus. C8i and C9i represent caspase-8 inhibitor II (Z-IE(OMe)TD(OMe)-FMK) and caspase-9 inhibitor II (LEHD-CHO), respectively. Recombinant and purified monomeric PCV2 cap is represented by rCap. ....	56
---	----



## List of Figures and Illustrations

- Figure 1.1 The evolutionary history of pathogenic circoviruses (except non-pathogenic PCV1) was inferred by using the Maximum Likelihood method and Tamura-Nei model<sup>22</sup>. The tree with the highest log likelihood (-30273.32) is shown. The percentage of trees in which the associated taxa clustered together is shown next to the branches. Initial tree(s) for the heuristic search were obtained automatically by applying Neighbor-Join and BioNJ algorithms to a matrix of pairwise distances estimated using the Maximum Composite Likelihood (MCL) approach, and then selecting the topology with superior log likelihood value. The tree is drawn to scale, with branch lengths measured in the number of substitutions per site. This analysis involved 16 nucleotide sequences. Codon positions included were 1st+2nd+3rd+Noncoding. There were a total of 2737 positions in the final dataset. Evolutionary analyses were conducted in MEGA X<sup>23</sup>. Porcine circoviruses are most closely linked to mink (MiCV) and canine circovirus (CCV). .....2
- Figure 1.3 Simplified diagram displaying the viral replication cycle of porcine circoviruses as currently known. Porcine circoviruses attach to the glycosaminoglycans (GAG) heparin sulphate and chondroitin sulphate B leading to clathrin-mediated endocytosis. The mechanism of virus uncoating and entry to the nucleus is unclear but does involve a nuclear localization signal present on Cap protein; however, replication takes place in the nucleus with host DNA replication enzymes. Expressed Rep and Rep' are re-imported into the nucleus to being rolling circle replication of the ssDNA genome before the formation of new virions. Progeny virus then exits the host cell through an unknown mechanism but is involved with cell death. .... 4
- Figure 2.2 Colony PCR agarose gel electrophoresis to detect colonies positive for PCV Cap insert into pFastBac plasmid. Positive colonies are denoted by a red circle and indicate an amplicon of expected band size of ~1600 bp which include full-length PCV Cap, WSSV IRES, and eGFP. These colonies were subsequently grown, and plasmids were extracted for sequence confirmation. Sequences confirmed for PCV1, PCV2, and PCV3 Cap were then transposed into parent bacmids by transforming DH10Bac *E. coli* with the confirmed pFastBac plasmids. .... 20
- Figure 2.3 Immunofluorescence assay to confirm PCV2 infection absence in PK15 cells infected 24 hours after dialysis. Left Image A represents PK15 cells treated with 1% formaldehyde inactivated stock PCV2 virus post-dialysis. Right Image B represents PK15 cells treated with stock PCV2 virus post-dialysis to confirm absence of infectivity was not due to dialysis treatment. Nuclei are stained blue with Hoescht 33342 and PCV2 Cap is stained with a primary rabbit anti-cap pAb, with a secondary goat anti-rabbit Alexa Flour 568 pAb. Cells were imaged using an Olympus IX51 inverted fluorescence microscope. .... 21
- Figure 2.4 PCV Cap proteins Coomassie staining. Gels represent PCV VLP purification steps using a CsCl gradient and ultracentrifugation. Left gel is from PCV1 VLP purification and right gel is from PCV2 VLP purification. Red circles indicate CsCl purified VLPs as the band corresponds to the expected size of PCV Cap protein

~28 kDa. Lane 2 is supernatant from freeze/thawed Sf9 cells post PCV Cap expression. Lane 3 is supernatant from the discontinuous sucrose gradient. Lane four is supernatant from above the white band observed from CsCl purification of VLPs. Lane 5 is actual PCV Cap protein recovered from a white band formed after CsCl ultracentrifugation. Lanes 6-8 are from MOCK infected Sf9 cells acting as negative controls. Lane 9 and 10 are positive controls with PCV2 rCap from expression in *E. coli* and faint bands can be observed in lane 9 at the expected size. See next figure for PCV2 anti-cap Western Blot results. ....24

Figure 2.5 Western Blot results of duplicate gel run of PCV2 VLP purification from Figure 2.3. Lane 2 is supernatant from freeze/thawed Sf9 cells post PCV Cap expression. Lane 3 is supernatant from the discontinuous sucrose gradient ultracentrifugation. Lane four is supernatant from above the white band observed after CsCl purification of VLPs. Lane 5 is actual PCV Cap protein recovered from a white band formed after CsCl ultracentrifugation. The band observed at ~28 kDa matches the expected band size of PCV2 Cap. Lanes 6-8 are from MOCK infected Sf9 cells acting as negative controls. Lane 9 and 10 are positive controls with PCV2 rCap from expression in *E. coli* showing a protein of ~28 kDa in lane 9. Lane 10 is also recombinant PCV2 Cap but is denatured and in 8M urea post-sonication, causing a change in band migration and fragmentation of PCV2 Cap protein. The second (~18 kDa) and third bands (~10 kDa) seen in lanes 3, 4, and 5 also correspond to the secondary bands observed in lane 10 and is most likely due to fragmentation of the full-length protein. .... 24

Figure 2.6 Example of 37% CsCl purified VLP's. Image taken immediately after 20 hours of centrifugation at 250,000g, 4°C. Note Sf9 cellular debris at the bottom of the tube, and distinct, uniform white band at approximately 1/5 of the total volume. This white band was not observed in negative controls..... 34

Figure 2.7 Transmission electron microscope images of post-CsCl ultracentrifugation purification of PCV VLPs produced by recombinant baculovirus infection of Sf9 cells. Left image A shows PCV1 VLPs at a total magnification of 50,000x. Right image B shows PCV2 VLPs at a total magnification of 40,000x. VLP icosahedral morphology matches 17-20 nm size of PCV2 virions. Negative control of purified Sf9 cells did not show these particles. .... 36

Figure 2.8 Transmission electron microscope image of recombinant baculovirus containing the PCV3 Cap gene at a magnification of 15000x. Viruses generated by reverse genetics in Sf9 cells. This image was taken after density-gradient ultracentrifugation but VLPs are not seen in this image. Viruses identified as baculovirus based on rod-shaped morphology and ~280 x 60 nm size and compared to negative controls. .... 37

Figure 2.9 Example of TUNEL assay images as captured from a Zeiss 780 confocal microscope. Red staining indicates nuclear staining by Hoechst 33342, and green staining indicates TUNEL positive DNA fragmentation. MOCK treated cells are negative control cells treated with only cell culture media as a mock infection. DNase I

treated cells are cells fixed and briefly permeabilized before treatment with DNase I to induce double-stranded breaks as a positive control. 50  $\mu$ M etoposide + PCV2 was used as an additional positive control. PCV1, PCV2, and PCV3 VLPs are samples from PK15 cells treated with each virus Cap VLP. Experiment was run in duplicate with  $n = 2$  for each sample type. .... 40

Figure 2.10 Super-resolution image microscopy (SIM) images of PK15 cells exposed to either infectious PCV2, PCV2 VLPs, or PCV3 VLPs. Left image contains a cell infected with PCV2 with the nuclei in red, and anti-Cap staining in green. Note the presence of PCV2 Cap protein throughout both the cytoplasm and nucleus. Middle image contains PK15 cell nuclei in red and exposed to PCV2 Cap protein in green. Right image contains a PK15 cell nuclei stained in blue, PCV3 Cap protein stained in green and TUNEL positive DNA in red. .... 41

Figure 3.1 PK15 cells exposed for 24 hours to various PCV preparations and controls were stained with Annexin-V FITC and 7-AAD to detect apoptosis. Pre-apoptotic and apoptotic cells were stained by Annexin-V binding to phosphatidylserine residues found on the outer surface of cell membranes. 7-AAD is a DNA intercalating dye which binds to the DNA of cells with compromised cell membranes indicating cell death. In each of the data plots above Q1 represents cells stained only with Annexin-V FITC, Q2 represents cells stained with both Annexin-V FITC and 7-AAD, Q3 represents cells stained by 7-AAD only, and Q4 represents cells which are unstained and viable. 50  $\mu$ M treatment with etoposide acted as a positive control for apoptosis. Heat killing of cells at 60°C for ten minutes acted as a positive control for dead/dying cells. MOCK treated cells were given only media. Dialysis buffer treatment was included to account for any potential effect from dialysis. 1%F PK15 cells represent PK15 cells treated with 1% formaldehyde, dialyzed to remove excess formaldehyde, and lysed by freeze/thaw to account for possible apoptotic effects caused by dead host cells as found in PCV2 virus preps. Sf9 cell lysate and cBac were included to account for any possible apoptotic effect possibly induced by the Sf9 insect cells or the baculovirus without a PCV insert present. Recombinant PCV2 Cap protein expressed and purified from *E. coli* is represented by the rCap graph. 1%F PCV2 represent stock PCV2 virus inactivated by 1% formaldehyde and dialyzed. PCV1 and PCV2 VLPs were both purified by 37% CsCl gradient ultracentrifugation. All quantifiable protein samples were quantified by a Bio-Rad DC protein assay. Each PK15 cell treatment was treated with 100  $\mu$ g of each protein sample or with 200  $\mu$ L of the respective negative control including; media, dialysis buffer, 1% formaldehyde treated PK15 cells, Sf9 cell lysate, or cBac. This raw data is representative of a minimum of two independent experimental replicates for each sample ( $n \geq 2$ ). .... 43

Figure 3.2 PK15 apoptosis was measured by an Annexin-V FITC apoptosis detection kit to determine the total proportion of pre-apoptotic and apoptotic cells in a population after a 24-hour exposure to PCV2 Cap protein. Negative controls of dialysis buffer, MOCK infection, 1% formaldehyde treated PK15 cell lysate, cBac control baculovirus, and Sf9 insect cell lysate were included to establish a grouped baseline level of apoptosis. PCV2 Cap protein produced and purified from *E. coli* (rCap) induced apoptosis in ~28% of PK15 cells exposed for a duration of 24 hours. Stock PCV2 virus

inactivated with 1% formaldehyde induced apoptosis in ~27% of PK15 cells. PCV2 VLPs produced by recombinant baculovirus in Sf9 insect cells and purified by CsCl gradient purification induced apoptosis in ~28% of Pk15 cells exposed for 24 hours. Interestingly, live PCV2 virus at a MOI of ~0.1 was unable to induce apoptosis above negative control baseline apoptosis, indicating possible dose-dependence of PCV2 Cap cytotoxicity or effective regulation of cellular apoptosis by live virus gene products. Treatment of PK15 cells with 50  $\mu$ M etoposide induced apoptosis in ~36% of PK15 cells as a positive control. Error bars represent standard error of the mean over a minimum of two independent experimental replicates for each sample ( $n \geq 2$ ). Significance was established using a Wilcoxon-Mann-Whitney U test between the entire negative control group and individual samples with a p value below 0.05 deemed statistically significant ( $p < 0.05$ ). Statistically significant differences are marked by an asterisk\*.

44

Figure 3.3 TUNEL assay confirmation of flow cytometry results. Negative controls exhibited apoptosis in 12% or less of the total population when exposed to Sf9 insect cell lysate, dialysis buffer, control baculovirus (cBac) or cell culture media (MOCK). Treatment of PK15 cells with 50  $\mu$ M etoposide resulted in approximately 37% of them being driven into apoptosis. Live PCV2 virus once again did not induce apoptosis above negative control results at only 12%. Recombinant PCV2 Cap (rCap) produced in *E. coli*. induced apoptosis in almost 30% of the PK15 cell population in comparison to the 28% measured by Annexin-V apoptosis detection. PCV1 VLPs were able to drive nearly 33% of PK15 cells into apoptosis, while PCV2 VLPs caused nearly 30% apoptosis and PCV3 Cap protein caused 29% apoptosis. These experiments were repeated twice, with the results being non-significant due to low power and replicate number. Error bars represent standard error of the mean over a minimum of two independent experimental replicates for each sample ( $n \geq 2$ ). Significance was established using a Wilcoxon-Mann-Whitney U test between the entire negative control group and individual samples with a p value below 0.05 deemed statistically significant ( $p < 0.05$ ). Statistically significant differences are marked by an asterisk\*.

46

Figure 3.4 A comparison of VLPs from both PCV1 and PCV2. PCV1 is deemed non-pathogenic and does not cause clinical disease in swine, whereas PCV2 is pathogenic and has been etiologically linked to PCVD causing a broad spectrum of disease manifestations in swine. This experiment indicated that both PCV1 and PCV2 Cap protein is cytotoxic to PK15 cells *in vitro* as measured by Annexin-V FITC staining of cells against negative controls and positive control. Treatment of PK15 cells with 50  $\mu$ M etoposide induced apoptosis in ~36% of PK15 cells as a positive control. PCV1 VLPs induced apoptosis in nearly 32% of the total PK15 population after a period of 24 hours compared to the 28% of cells driven into apoptosis by PCV2 VLPs. Sf9 cell lysate and control baculovirus (cBac) negative controls were treated identically to the PCV1 and PCV2 VLP preparations through sonication and CsCl gradient purification, as well as subsequent dialysis. The results indicate PCV VLPs induce apoptosis in PK15 cells higher than all negative controls and similar to inducement of apoptosis by 50  $\mu$ M etoposide. Error bars represent standard error of the mean over a minimum of two independent experimental replicates for each sample ( $n \geq 2$ ). Significance was established using a Wilcoxon-Mann-Whitney U test between the entire negative control

group and individual samples with a p value below 0.05 deemed statistically significant ( $p < 0.05$ ). Statistically significant differences are marked by an asterisk\*. ..... 50

Figure 3.5 TUNEL assay overview graph showing apoptosis of all samples of PK15 cells exposed to various PCV sample preparations with or without caspase-8 and caspase-9 inhibitors. Pre-treatment of PK15 cells for 1 hour with caspase-8 inhibitor II (Z-IE(OMe)TD(OMe), C8i) or caspase-9 inhibitor II (LEHD-CHO, C9i), led to some decreases in apoptosis observed with PK15 cells treated with PCV2 Cap-containing samples. Apoptosis induced by recombinant PCV2 Cap decreased almost 12% when pre-treated with caspase-8 inhibitor II and decreased by 20% when pre-treated with caspase-9 inhibitor II. Apoptosis induced by PCV2 VLPs decreased by 7% when pre-treated with caspase-8 inhibitor II and decreased 14% when pre-treated with caspase-9 inhibitor II. Apoptosis of PK15 cells induced by PCV1 VLPs decreased by approximately 5% when treated with caspase-8 inhibitor II, but slightly increased by nearly 2% when pre-treated with caspase-9 inhibitor II. Apoptosis induced in PK15 by PCV3 Cap protein reached 29%, whereas pre-treatment with caspase-8 inhibitor II resulted in wide variation but an overall slight decrease by almost 2%. Pre-treatment with caspase-9 inhibitor resulted in a 12% decrease in apoptosis observed in PK15 cells exposed to PCV3 Cap protein. Error bars represent standard error of the mean over two independent experimental replicates for each sample ( $n = 2$ ). Significance was established using a Wilcoxon-Mann-Whitney U single-tailed test between the entire negative control group and individual samples with a p value below 0.05 deemed statistically significant ( $p < 0.05$ ). Statistically significant differences are marked by an asterisk\*. .....51

Figure 3.6 Raw flow cytometry data showing the effect of caspase-8 and caspase-9 inhibitors on the apoptotic effect observed by interaction of PCV1 and PCV2 VLPs with PK15 cells. PK15 cells were pre-treated for one hour before exposure to PCV VLPs for 24 hours. This raw data is representative of a minimum of two independent experimental replicates using caspase inhibitors ( $n \geq 2$ ). ..... 53

Figure 3.7 PK15 cells were pre-treated with caspase-8 inhibitor II (Z-IE(OMe)TD(OMe)), or caspase-9 inhibitor II (LEHD-CHO), prior to treatment with negative controls or PCV VLPs to attempt to identify key apoptotic pathways. PCV1 VLP induced apoptosis was not affected by either inhibitor, whereas PCV2 VLP induced apoptosis was reduced by 8% with caspase-8 inhibitor II and 13% by caspase-9 inhibitor II. This result indicates that PCV1 and PCV2 activate apoptosis in PK15 cells by different mechanisms. Error bars represent standard error of the mean over a minimum of two independent experimental replicates for each sample ( $n \geq 2$ ). Significance was established using a Wilcoxon-Mann-Whitney U test between the entire negative control group and individual samples with a p value below 0.05 deemed statistically significant ( $p < 0.05$ ). Statistically significant differences are marked by an asterisk\* .....54

Figure 4.1 Diagram showing the expected cleavage sites of each PCV Cap amino acid sequence showing 99-100% predicted mitochondrial localization sequences (MLS). Sequences are written conventionally with the N-terminus on the left and the C-terminus

to the right of the cut-off point past 100 amino acids. Sequences were predicted by MitoProt prediction software at the following URL: <https://ihg.gsf.de/ihg/mitoprot.html> .. 63

## List of Symbols, Abbreviations and Nomenclature

<b>Symbol/Abbreviation</b>	<b>Definition</b>
<b>μ</b>	Micro (10 <sup>-6</sup> )
<b>°C</b>	Degrees Celsius
<b>aa</b>	Amino acid
<b>AAP</b>	Antarctic alkaline phosphatase
<b>AASV</b>	American Association of Swine Veterinarians
<b>ABTS</b>	2,2'-Azino-bis (3-ethylbenzothiazoline-6-sulphonic acid)
<b>APC</b>	Antigen presenting cell
<b>APS</b>	Ammonium persulfate
<b>BES</b>	Baculovirus expression system
<b>BFDV</b>	Psittacine beak and feather disease virus
<b>BME</b>	2-Mercaptoethanol
<b>bp</b>	Base pair
<b>BSA</b>	Bovine serum albumin
<b>Cap</b>	Capsid protein
<b>cBac</b>	Control baculovirus containing a GUS insert
<b>cm</b>	Centimeter
<b>CO<sub>2</sub></b>	Carbon dioxide
<b>CTL</b>	Cytotoxic T-cells
<b>DAPI</b>	4, 6-Diamidino-2-phenylindole
<b>dH<sub>2</sub>O</b>	Distilled water

<b>DNA</b>	Deoxyribonucleic acid
<b>DPI</b>	Days post infection
<b><i>E. coli</i></b>	<i>Escherichia coli</i>
<b>EDTA</b>	Ethylenediaminetetraacetic acid
<b>eGFP</b>	Enhanced green fluorescent protein
<b>FBS</b>	Fetal bovine serum
<b>FITC</b>	Fluorescein isothiocyanate
<b>g</b>	Gram
<b>GAG</b>	Glycosaminoglycans
<b>GFP</b>	Green fluorescent protein
<b>GUS</b>	B-glucuronidase
<b>h</b>	Hour
<b>His</b>	Histidine
<b>hpi</b>	Hours post infection
<b>HRP</b>	Horseradish peroxidase
<b>HS</b>	Heparan sulfate
<b>IFA</b>	Immunofluorescence assay
<b>IFN-<math>\gamma</math></b>	Interferon gamma
<b>IPTG</b>	Isopropyl $\beta$ -D-1-thiogalactopyranoside
<b>IRES</b>	Internal ribosome entry site
<b>kDa</b>	Kilodalton
<b>LB</b>	Luria broth
<b>M</b>	Molar



<b>mAbs</b>	Monoclonal antibodies
<b>MEM</b>	Minimum essential media
<b>min</b>	Minute
<b>MLS</b>	Mitochondrial Localization Sequence
<b>mL</b>	Milliliter
<b>MOMP</b>	Mitochondrial outer membrane permeabilization
<b>MWCO</b>	Molecular weight cut-off
<b>n</b>	Nano ( $10^{-9}$ )
<b>NA</b>	Neutralizing antibody
<b>NCBI</b>	National center for biotechnology information
<b>Ni</b>	Nickel
<b>NK</b>	Natural killer cells
<b>NLS</b>	Nuclear localization signal
<b>nt</b>	Nucleotides
<b>OD</b>	Optical density
<b>ORF</b>	Open reading frame
<b>Ori</b>	Origin of replication
<b>p</b>	Probability occurring by chance
<b>PAGE</b>	Polyacrylamide gel electrophoresis
<b>PBS</b>	Phosphate buffered saline
<b>PBST</b>	Phosphate buffered saline with Tween-20
<b>PCD</b>	Programmed cell death
<b>PCR</b>	Polymerase chain reaction

<b>PCV</b>	Porcine circovirus
<b>PCVs</b>	Porcine circoviruses
<b>PCV1</b>	Porcine circovirus type 1
<b>PCV2</b>	Porcine circovirus type 2
<b>PCV3</b>	Porcine circovirus type 3
<b>PCVAD</b>	Porcine circovirus associated disease
<b>PDNS</b>	Porcine dermatitis and nephropathy syndrome
<b>PEG</b>	Polyethylene glycol
<b>PFA</b>	Paraformaldehyde
<b>PK15</b>	Porcine kidney epithelial
<b>PMWS</b>	Postweaning multisystemic wasting syndrome
<b>PPV</b>	Porcine parvovirus
<b>PRRSV</b>	Porcine reproductive and respiratory syndrome virus
<b>PVDF</b>	Polyvinylidene fluoride
<b>rCap</b>	Recombinant Cap
<b>RT</b>	Room temperature
<b>SD</b>	Standard deviation
<b>SDS</b>	Sodium dodecyl sulfate
<b>SE</b>	Standard error
<b>SPF</b>	Specific pathogen free
<b>TCID<sub>50</sub>/mL</b>	Tissue culture infectious dose per mL
<b>TEMED</b>	N, N, N', N' - Tetramethylethylenediamine
<b>TEM</b>	Transmission electron microscopy

<b>TUNEL</b>	Terminal deoxynucleotidyl transferase dUTP nick end labeling
<b>UPR</b>	Unfolded protein response
<b>VLP</b>	Virus-like particle

## Chapter One: **Introduction**

### **1.1 Porcine Circoviruses**

Porcine circoviruses are within the family *Circoviridae*, which includes viruses such as psittacine beak & feather disease virus (BFDV), and canine circovirus (CCV). Of the 27-described species of genus *Circovirus* listed by the International Committee on the Taxonomy of Viruses (ICTV) in 2019<sup>1</sup>, at least 11 of them cause disease or are suspected to be the etiological agents of pathology in their hosts<sup>2-11</sup>. Hosts include, swine, dogs, bats, humans, several species of birds, fish, and amphibians<sup>12</sup>. These viruses are icosahedral, non-enveloped, and among the smallest viruses known at approximately 17-20 nm in diameter enclosing a 1.7-2.0 Kb ssDNA circular genome. Despite their diminutive size, pathogenic circoviruses cause major disease through immunosuppression in their respective host species. This is true of porcine circovirus 2 (PCV2) infection of swine because immunosuppression causes a wide range of clinical signs, while allowing secondary opportunistic infections leading to use of the general term porcine circovirus diseases (PCVD)<sup>13</sup>. This places PCV2 as a pathogen of major concern to swine production worldwide. A newly emerging and potentially pathogenic porcine circovirus type 3 (PCV3) has also recently been described as a pathogen of swine in North America<sup>14</sup>, South America<sup>15</sup>, Europe<sup>16-18</sup>, and Asia<sup>14,19</sup>. However, the clinical significance of the emergence of PCV3 has yet to be determined<sup>20</sup>. Within *circoviridae*, porcine circoviruses are most closely related to the pathogenic canine circovirus and mink circovirus, with at least one study showing that mink can be infected with porcine circovirus 2<sup>21</sup> (Figure 1.1).

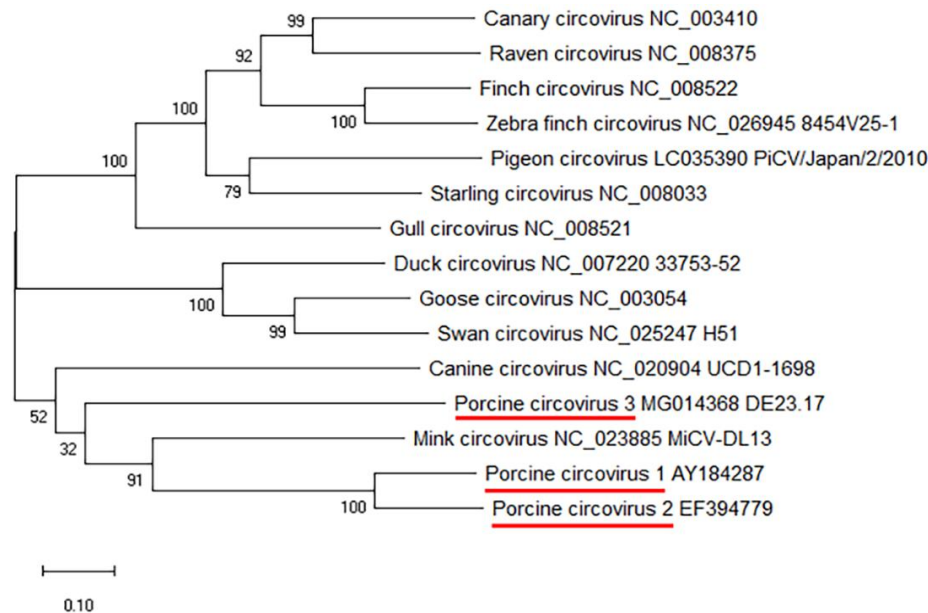


**Figure 1.1** The evolutionary history of pathogenic circoviruses (except non-pathogenic PCV1) was inferred by using the Maximum Likelihood method and Tamura-Nei model<sup>22</sup>. The tree with the highest log likelihood (-30273.32) is shown. The percentage of trees in which the associated taxa clustered together is shown next to the branches. Initial tree(s) for the heuristic search were obtained automatically by applying Neighbor-Join and BioNJ algorithms to a matrix of pairwise distances estimated using the Maximum Composite Likelihood (MCL) approach, and then selecting the topology with superior log likelihood value. The tree is drawn to scale, with branch lengths measured in the number of substitutions per site. This analysis involved 16 nucleotide sequences. Codon positions included were 1st+2nd+3rd+Noncoding. There were a total of 2737 positions in the final dataset. Evolutionary analyses were conducted in MEGA X<sup>23</sup>. Porcine circoviruses are most closely linked to mink (MiCV) and canine circovirus (CCV).

### ***1.1.1 Molecular Biology of Porcine Circoviruses***

Porcine circoviruses are among the smallest autonomously replicating mammalian viruses known with a diameter of 17-20 nm, and a T=1 icosahedral non-enveloped capsid consisting of 60 subunits of Cap protein<sup>24</sup>. The circular single-stranded DNA genome of PCV1 & PCV2 are 1.7 kb in length, while the genome of PCV3 is 2.0 kb in length (Figure 1.2). Two ORFs are critical for virus replication with ORF1 encoding Rep and Rep' (on the reverse sequence) which are necessary for generating the double-stranded DNA intermediate in a replication cycle<sup>25,26</sup>. The second

essential genome component is the ORF2 protein encoding the capsid (Cap) protein which is the only structural protein of the virus and is responsible for encapsidating the progeny virions, for host cellular attachment and entry, as well as its suspected role in activating apoptosis of host cells<sup>25,27-29</sup>. ORF3 regulates host cellular processes by inducing apoptosis but is not an essential gene for replication<sup>30</sup>, while ORF4 antagonizes this action and prevents apoptosis<sup>31,32</sup>. ORF5 of PCV2 has recently been described as dampening host interferon type 1 expression, inducing endoplasmic reticulum stress, and unfolded protein response leading to enhanced viral replication<sup>33,34</sup>.

Porcine circoviruses infect cells by attaching to glycosaminoglycans (GAG) heparin sulphate and chondroitin sulphate B, triggering clathrin-mediated endocytosis (Figure 1.3)<sup>27,35</sup>. Acidification of endosomes and interaction with serine proteases leads to PCV2 to exit the endosomes<sup>36</sup>, and either be localized to the nucleus via the nuclear localization sequence (NLS) or possibly to the mitochondria via the mitochondrial localization sequence (MLS), with both sequences found on the Cap protein. Upon entering the nucleus, the viral genome is converted to a double-stranded intermediate by host DNA polymerases and protein synthesis begins. The Rep and Rep' proteins are imported into the nucleus whereupon they bind to the origin of replication and cleave the double-stranded DNA to initiate rolling circle replication, with each genome being cleaved and packaged individually into a virion in the nucleus<sup>37</sup>. Virus escape is thought to require cell death; although, the mechanism for virus-induced cell death is currently debated<sup>36</sup>. Furthermore, some studies have pointed to the possibility of macrophages and dendritic cells becoming infected and disseminating infectious virus throughout the host lymphatic system which could result from direct infection or through phagocytic removal of apoptotic cells<sup>38,39</sup>.

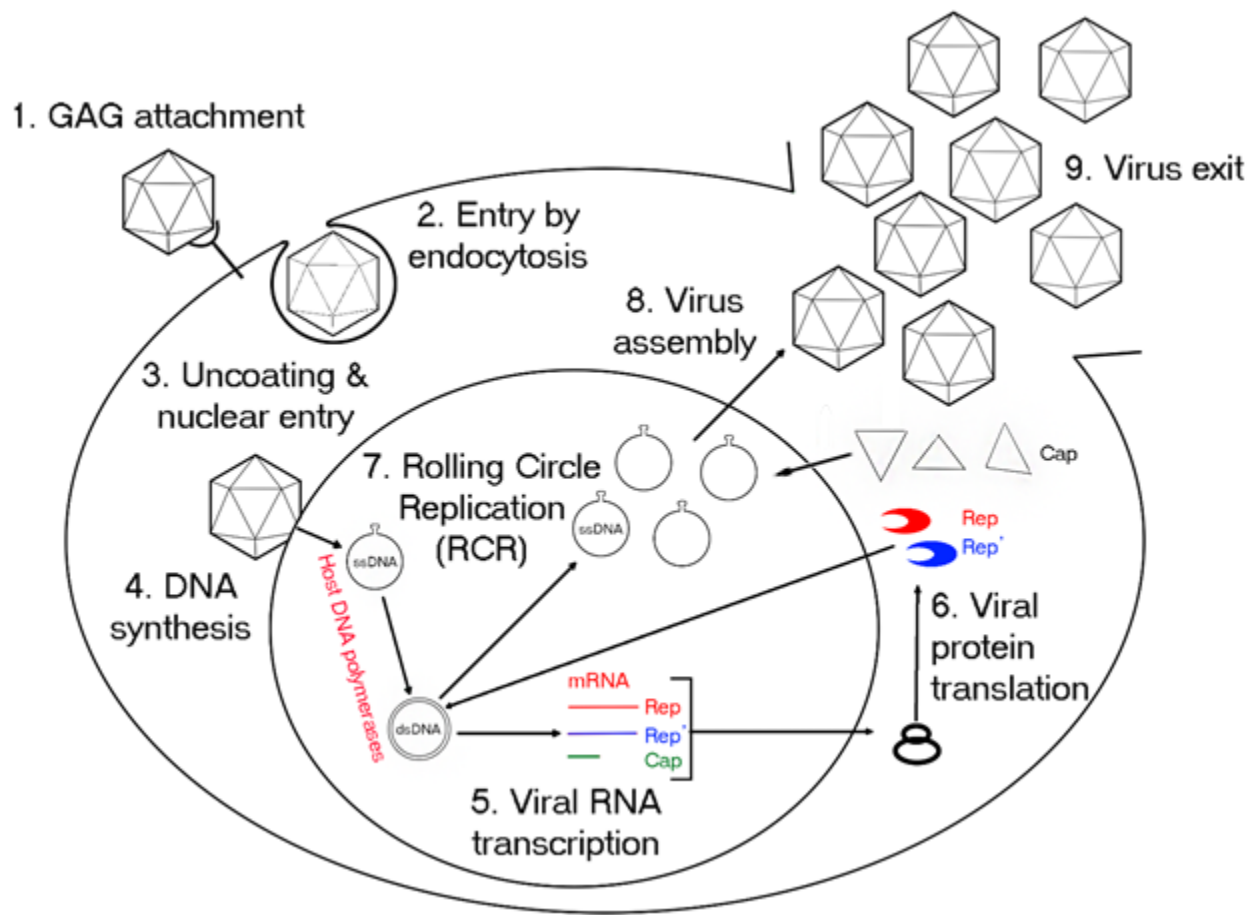


**Figure 1.3** Simplified diagram displaying the viral replication cycle of porcine circoviruses as currently known. Porcine circoviruses attach to the glycosaminoglycans (GAG) heparin sulphate and chondroitin sulphate B leading to clathrin-mediated endocytosis. The mechanism of virus uncoating and entry to the nucleus is unclear but does involve a nuclear localization signal present on Cap protein; however, replication takes place in the nucleus with host DNA replication enzymes. Expressed Rep and Rep' are re-imported into the nucleus to being rolling circle replication of the ssDNA genome before the formation of new virions. Progeny virus then exits the host cell through an unknown mechanism but involves cell death.

### 1.1.2 Porcine Circovirus Type 1

Porcine circovirus type 1 (PCV1) was first discovered as a cell line contaminant in porcine kidney (PK15) ATCC CCL-33 cells in 1976<sup>24</sup>. This virus was determined to be non-pathogenic and of no major concern to swine. The virus was discovered as a contaminant of the human

Rotarix™ vaccine for rotavirus in 2006<sup>40</sup>. One early study suggests that PCV1 may be responsible for fetal piglet stillbirths before they become immunocompetent due to transplacental virus transmission ; however, they found no clinical signs or lesions indicating disease in experimentally infected piglets<sup>41</sup>. PCV1 was isolated up to 9 days post inoculation from a variety of tissues including lymphoid tissues, other quickly growing tissues in the lungs, gastrointestinal linings, and nasal tissues with no evidence of persistent infection observed. This pattern of pleiotropism is an important hallmark in circovirus infection as is the case with pathogenic PCV2<sup>42</sup>. Porcine circoviruses are known to attach to heparin sulphate and chondroitin sulphate B, which are both found ubiquitously on most porcine host cells<sup>27</sup>.

### ***1.1.3 Porcine Circovirus Type 2***

Porcine circovirus type 2 (PCV2) was first described in 1998 and associated with post-weaning multi-systemic wasting syndrome (PMWS) in pigs<sup>43</sup>. PMWS clinical presentation consists of weight loss, wasting, tachypnea, dyspnea, diarrhea, enlarged lymph nodes and jaundice, in addition to interstitial pneumonia, lymphadenopathy, hepatitis, and nephritis<sup>44,45</sup>. Gross and histological lesions observed in infected pigs are found in secondary lymphoid tissues including lymph nodes, spleen, and ileal Peyer's patches, as well as the lungs, liver, reproductive system, and kidneys<sup>13,46,47</sup>. Co-infection of PCV2 commonly occurs with other infectious swine pathogens such as; porcine respiratory and reproductive virus (PRRSV), porcine parvovirus (PPV), porcine epidemic diarrhea virus (PEDV), porcine influenza virus (PIV), encephalomyocarditis virus (EMCV), Aujeszky's disease virus (otherwise known as pseudorabies), *Mycoplasma hyopneumoniae*, *Mycoplasma hyorhinis*, and *Pneumocystis carinii*<sup>48-52,52,53</sup>. As previously mentioned, the wide range of diseases associated with PCV2 infection are termed porcine



circovirus diseases (PCVD)<sup>54</sup>. PCVD has been broken down further into a naming convention which describes porcine circovirus subclinical infection (PCV2-SI); systemic disease (PCV2-SD); respiratory disease (PCV2-LD); proliferative and necrotizing pneumonia (PNP, included in PCV2-LD); enteritis (PCV2-ED); reproductive disease (PCV2-RD); and porcine dermatitis and nephropathy syndrome (PDNS)<sup>13</sup>. This new naming convention recognizes that PCV2 may infect and cause disease in one or more tissues while not affecting others. PCVD was shown to contribute a significant loss to swine production around the world with estimated losses of €5.76 billion in the EU per year alone as of 2009<sup>55</sup>. Canadian studies suggest that between PCV2 and PRRS viruses alone, the pork industry suffers losses in the hundreds of millions of dollars per annum, which led to the creation of the Control of Disease in the Hog Industry (CDHI) initiative by the federal government in 2007<sup>56</sup>. The economic impact of PCVD directed the development of several effective vaccines against the early predominant PCV2a genotype, driving the spread of the PCV2b genotype and the emergence of the more virulent PCV2d genotype<sup>57</sup>.

Current PCV2 vaccines have met with success over the past decade as indicated by field studies which have confirmed efficacy of all currently manufactured vaccines, with proven reduction of PCVD occurrence and severity, reduction in mortality rates, increase in average daily weight gain (ADWG) of nursery and grower pigs, decrease in incidence of co-morbid infections, as well as a significant reduction in viremia, lymphoid lesions, and tissue viral load<sup>50,58–65</sup>. However, recent studies have emerged suggesting that vaccination only reduces viral burden but is unable to elicit an immune response that clears the virus in most infected animals, resulting in subclinical infections and a shift in PCV2 genotypes circulating in swine herds worldwide<sup>66</sup>. Despite the response of both humoral and cellular immunity to PCV2 infection even after vaccination, PCV2 continues to persistently infect and transmit in swine herds worldwide<sup>67</sup>. Piglets

are initially protected from PCV2 after birth by maternally-derived antibodies, but upon weaning after 6-12 weeks they are at their most vulnerable and this is when many of the disease manifestations of PCVD occur<sup>68</sup>. Weaned piglets become highly susceptible to PCV2-SD at this point and begin seroconversion with neutralizing antibodies; although, the development of antibodies does not always confer protection against PCV-SD<sup>69,70</sup>. In recent years the importance of IFN- $\gamma$  secreting cells (IFN- $\gamma$ -SC) during PCV2 infection has been elucidated as evidenced by the inverse correlation with PCV2 viremia<sup>71-73</sup>. Specifically, CD4+ T cells that secrete both IFN- $\gamma$  and TNF- $\alpha$  are implicated in an immune response and potential clearance of PCV2<sup>74</sup>.

#### ***1.1.4 Porcine Circovirus Type 3***

PCV3 was first characterized and described in the US in 2016 and was isolated from pigs exhibiting clinical signs of wasting, weight loss, myocarditis, respiratory disease, dyspnea, neurological disorders, and arteriolitis usually associated with PCVD involving infection with PCV2. Diagnostic tests confirmed the absence of PCV2 and the presence of a novel virus designated PCV3, sharing a Capsid amino acid sequence identity of ~37% with PCV2 Cap<sup>75</sup>. Subsequently, PCV3 was discovered and isolated from pigs showing clinical signs of PDNS characterized by necrotizing vasculitis, glomerulitis, and interstitial nephritis. Aborted fetuses of infected sows displaying PDNS-like clinical signs were also determined to have high viral loads of PCV3 ( $7.57 \times 10^7$  genome copies/mL)<sup>76</sup>. Several countries in the EU<sup>17,18,77</sup> and South America,<sup>15</sup> have also now reported cases of PCV3 indicating a worldwide distribution. PCV3 was also isolated from tissues of neonatal piglets including heart, brain, lungs, and spleen from several herds in southern China; piglets were suffering from congenital tremors resulting in a case fatality rate of 100%<sup>78</sup>. Retrospective studies of archival samples have detected PCV3 in swine from the UK since

at least 2001<sup>20</sup>, and 1996 in Spain<sup>79</sup>. At present the pathogenicity of PCV3 is still debated, requiring more research into elucidating its potential role in the clinical syndromes it has been associated with.

## **1.2 Immunosuppression Caused by PCV2 Infection**

The most pressing concern still existing with PCV2 is the issue of persistent subclinical infection because PCV2 persistently infects a variety of different cell types, leading to continued immunosuppression, shedding, and transmission within swine herds even after successful vaccination<sup>39</sup>. Additionally, it has been shown experimentally that PCV2 capsid (ORF2) protein can cause apoptosis when transiently expressed in porcine kidney cells (PK15) under *in vitro* conditions<sup>28</sup>. The same study showed a significant increase in non-infected bystander cell death 48 hours post infection (hpi) with concurrent exposure to 500U/mL of swine IFN- $\gamma$  ( $p < 0.05$ ). The transient expression effect has not been studied in pig peripheral blood mononuclear cells (PBMCs); although, it has been experimentally shown that non-infected PBMCs exhibit a ~30% apoptosis rate when in the presence of infected cells due to an unconfirmed molecular mechanism, but possibly due to PCV2 capsid protein extracellular exposure (Solis-Worsfold & Waekerlin, personal communication).

Current PCV2 research suggests that PCV2 immunosuppression is multifactorial due to several immune system dysregulations all of which cause lymphocyte depletion. Despite being the smallest mammalian virus known, PCV2 causes major disease or immunosuppressive infection with its 1.7 kB genome, indicating an economy of function within the relatively limited amount of gene products produced upon replication. Encoding only four major open reading frames (11 altogether), PCV2 must be able to do everything required in a viral life cycle while surviving a

complex host immune response. The capsid protein of the virus is only 233 aa long, is responsible for attachment to host receptors and subsequent endocytosis, encapsidating the viral genome, and induces apoptosis when transiently expressed within cells; or induces apoptosis in bystander cells when in the presence of activated and infected cells. This is indicative of an unrecognized cytotoxic motif present within the capsid that is somehow interacting with cellular processes to activate apoptosis even in the absence of infection. What is lacking in the literature is a consensus on the overall method of immunosuppression and why subclinical infection remains of key importance even with development of efficacious vaccines. Research is needed to determine if PCV2 can induce apoptosis in non-infected cells and if this induction is the result of capsid protein.

### ***1.2.1 PCV2 Dysregulates IL-10 Expression***

PCV2 infection of swine is known to significantly alter cytokine expression profiles contributing to immunosuppression. The most critical cytokine observed to be dysregulated by increase in expression during infection is interleukin-10 (IL-10). IL-10 is an immunosuppressive cytokine responsible for controlling and decreasing the immune response as an infection wanes through several mechanisms. IL-10 reduces proliferation of lymphocytes, leading to reduced T and B cell production and responses during an infection. IL-10 can also induce apoptosis in monocytes through up-regulating the cell surface expression of CD95/APO-1/Fas<sup>80</sup>; additionally, IL-10 can also up-regulate the cell-membrane bound expression of TNF- $\alpha$  in subsets of T<sub>reg</sub> cells, thereby activating apoptosis and causing immune dysregulation<sup>81</sup>. T<sub>H1</sub>, macrophages, and NK cells are all inhibited by IL-10 expression, yet these cells are critical for pathogen clearance. IL-10 expression also leads to the inhibition of IFN- $\gamma$ , IFN- $\alpha$ , and IL-12 during PCV2 infection, all of which are critical for producing an immune anti-viral state<sup>82</sup>. Elevated IL-10 expression has been

associated with PCV-SD and positively correlates with lymphocyte depletion in the lymphoid organs such as the thymus<sup>83</sup>. PCV2 viremia also positively correlates with the amount of circulating IL-10 levels<sup>84</sup>. Of interesting note, some studies have shown that PCV1 does not induce the upregulation of IL-10 expression<sup>82,83</sup>. Although IL-10 is a potent immunosuppressive cytokine, the mechanism behind its upregulation is not known during PCV2 infection but could be a direct result of capsid protein interaction. This mechanism of apoptosis is unlikely the main cause of apoptosis in PK15 cells *in vitro*, as these cells do not produce IL-10 near the levels produced by T<sub>H</sub>1 cells *in vivo*.

### ***1.2.2 PCV2 Upregulates Expression of Programmed Death-1 Receptor (PD-1)***

Other researchers observed that PCV2 upregulates the programmed death-1 (PD-1) receptor response through upregulation and overexpression of its ligands PD-L1 (CD274) or PD-L2 (CD273) present on antigen presenting cells (APCs) after infection with PCV2 leading to T cell exhaustion, as well as inhibition of activation and proliferation<sup>85</sup>. In a healthy immune response to infection, PD-1 and its ligands are a component of negative host immunomodulation by down-regulating T cell responses and promoting self-tolerance during pathogen clearance<sup>86,87</sup>. Additionally, PD-1 is known to promote apoptosis of lymphocytes<sup>88</sup>, thus an overexpression of ligands during PCV2 infection could create an important mechanism for causing immunosuppression as observed in lymphocyte depletion of lymphoid tissues.

### ***1.2.3 PCV2 Upregulates Expression of Fas/FasL Activation-Induced Cell Death***

Another apoptotic pathway associated with immunosuppression caused by PCV2 infection is Fas/Fas-L activation-induced cell death (AICD). One study was able to show that PCV2

infection causes the upregulation of Fas on lymphocytes and increased FasL expression on splenic macrophages (SMs), which in turn led to significantly higher rates of lymphocyte apoptosis when both cell types were co-cultured compared to Mock-exposed cells<sup>89</sup>. This effect was then amplified upon co-infection with PRRSV, strengthening the argument of Fas/Fas-L being a contributing factor of lymphocyte depletion observed in PCVD; however, it is unknown how PCV2 causes this upregulation.

#### ***1.2.4 PCV2 Cap Protein Drives Cellular Apoptosis Regardless of Subcellular Localization***

The virulence of PCV2 has been shown to be different in viruses having minimal mutations within the Cap gene such as the removal of a 9-nt sequence or the deletion of 1-2 amino acids<sup>90-93</sup>. This difference in cytotoxicity observed by mutation of PCV2 Cap was followed up with a study involving transient expression of PCV2 Cap by a lentiviral system in PK15, and 293T cells. This study determined that Cap protein drives apoptosis of PK15 cells only (and not 293T cells) regardless of the subcellular location whether the Cap protein was present in either the cytoplasm or the nucleus<sup>28</sup>. This study also suggested that PCV2 Cap may activate more than one independent mechanisms of programmed cell death. Taken together with the observation that a proportion of non-infected bystander cells are driven into apoptosis<sup>28</sup>, this suggests that PCV2 Cap protein is a major determinant of virulence.

### **1.3 Mechanisms of Cell Death**

The Nomenclature Committee on Cell Death describes at least 12 unique mechanisms for programmed cell death (PCD) such as; anoikis, apoptosis, autophagy, cornification, excitotoxicity, oncosis, necrosis/necroptosis, mitotic catastrophe, paraptosis, pyronecrosis, and pyroptosis<sup>94</sup>. The

major characteristics of apoptosis include; rounding of the cell and loss of cell volume (pyknosis), condensation and fragmentation of nuclei (karyorrhexis), and phosphatidylserine (PS) exposure onto the outer surface of the plasma membrane during early apoptosis. Apoptosis has several different pathways which can be extrinsically or intrinsically activated and may involve a variety of apoptosis-inducing signalling molecules such as cathepsins, calpains, caspases, apoptosis-inducing-factor (AIF), endonuclease G, and may or may not require the involvement of the mitochondria<sup>95</sup>. Research into the apoptotic mechanism of PCV2 has pointed to mitochondrial driven apoptosis using caspase-3 and caspase-9 through the activation of mitochondrial membrane polarization (MMP) driven by  $\text{Ca}^{2+}$ , reactive oxygen species (ROS) generation, and the release of cytochrome c<sup>29,96</sup>. This study aims to further elucidate the mechanisms driving PCV2-induced apoptosis in comparison to PCV1 and provide initial observations of the cytotoxicity of PCV3.

#### **1.4 Hypothesis and Objectives of the Study**

This study's main goal was to determine the role of PCV2 Cap protein as a causation of bystander cell death observed during infections with PCV2 because the main question still unanswered regarding PCV2 is how it causes lymphocyte depletion and thus immunosuppression of the host. The null hypothesis is that there is no difference in apoptosis between populations of PK15 cells exposed to PCV2 Cap protein and those exposed to negative controls. The alternative hypothesis is that PCV2 Cap is interacting with and directly or indirectly activating one (or more) of the extrinsic or intrinsic apoptosis activation pathways in non-infected cells. To this end the following objectives were determined for this study;

**Objective 1.** Determine the cytotoxicity of recombinant PCV2 Cap expressed in and purified from *E. coli* in a monomeric/denatured form. This protein was denatured using 8M urea and sonication, and then purified using a His tag.

**Objective 2.** Determine whether inactivated PCV2 would be cytotoxic to PK15 cells when externally exposed. Formaldehyde inactivated virus would retain conformational epitopes and a “native” form which could then interact with the host cell without causing infection.

**Objective 3.** Determine whether PCV2 VLPs would be cytotoxic to PK15 cells *in vitro* when externally exposed. VLPs would ensure no other viral proteins or genomic components would be present and allow for a natural interaction with host cells in that the VLPs would be able to undergo conformational changes and dissociate.

**Objective 4.** Compare PCV1 VLPs, PCV2 VLPs, and PCV3 VLPs to determine if there is a difference in cytotoxicity between the viruses which could account for the difference in pathogenicity observed between these closely related viruses.

**Objective 5.** Experiment to uncover the key apoptotic pathways triggered by PCV Cap by pre-treating PK15 cells with either caspase-8 or caspase-9 inhibitors before exposure to VLPs. Caspase-8 is a key intermediary protein in the apoptotic cascade due to extrinsic activation of cellular apoptosis, whereas caspase-9 is a critical mediator of intrinsically activated apoptosis.



## Chapter Two: **Materials and Methods**

### **2.1 Cell Culture**

The PK15 cell line used in this study was provided by Dr. Carl A. Gagnon from the Faculty of Veterinary Medicine at the University of Montreal, Quebec. The PK15 cell line has been immortalized by the addition of SV40 T antigen<sup>97</sup>. The cell stock was confirmed to be absent of PCV2 and *Mycoplasma sp.* infection.

PK15 cells were cultured *in vitro* in Dulbecco's Minimum Essential Media (DMEM) (Gibco) and supplemented with 10% heat-inactivated fetal bovine serum (FBS) (Gibco), 1% penicillin-streptomycin antibiotic solution (Sigma-Aldrich), 1% non-essential amino acids (Sigma-Aldrich), and 1% sodium pyruvate (Gibco). PK15 cells were seeded and grown in T25 or T75 tissue culture flasks (Falcon) at 37°C with 5% CO<sub>2</sub> in a non-humidified Hera Cell 150i incubator. Passaging of cells was carried out by removing media, washing cells with phosphate buffered saline solution (1x PBS), and incubating with trypsin-EDTA (0.25%) (Invitrogen) for 5-7 minutes at 37°C to detach cells. Upon detachment, 5 mL of cell culture media was added to neutralize trypsin, and all cells were collected for centrifugation at 200g for 5 minutes. The supernatant was removed, and cells were re-suspended in cell culture media to perform a cell count for further passaging or for use in experiments.

#### ***2.1.1 Hemocytometer Cell Counting***

To estimate the number of cells in suspension, a cell suspension aliquot was taken and diluted 1:2 in 0.4% Trypan Blue (Gibco) viability exclusion dye and loaded into both wells of a hemocytometer (Hausser Scientific). Unstained cells in the four corner squares of each well were

counted to obtain an average cell count per section, and total cells per mL were calculated as follows:

$$\text{Total Cells/mL} = \frac{\text{Total Cells Counted}}{\text{Number of Squares}} \times \text{Dilution Factor} \times 10^4 \text{ nL/1mL}$$

## **2.2 PCV2 Virus Stock Production**

PCV2b strain 05-32650 (GenBank Accession: EF394779) was initially produced using reverse genetics by cloning two full-length PCV2 genome copies into plasmid pJ201 and subsequently transforming competent *E. coli* to generate DNA clones for extraction and transfection of PK15 cells. PK15 cells were transfected using Lipofectamine 2000 (Invitrogen) and OptiMEM (Gibco). Cells were collected after four passages, frozen and thawed three times sonicated at 80% power (QSonica, 125-Watt, 20 kHz) for 1 minute before centrifugation at 500g for 10 minutes to collect the supernatant containing infectious PCV2 particles. This supernatant was then used to infect PK15 cells with an additional four rounds of super-infection upon passaging. The supernatant was then collected and aliquoted for storage at -80°C and subsequently titered using the Reed-Muench 50% end-point titration. The reverse genetics and viral amplification were carried out by previous members of Dr. Czub's lab. Infectivity of the live PCV2 virus was confirmed prior to further experimentation using an immunofluorescence assay (Figure 2.1).

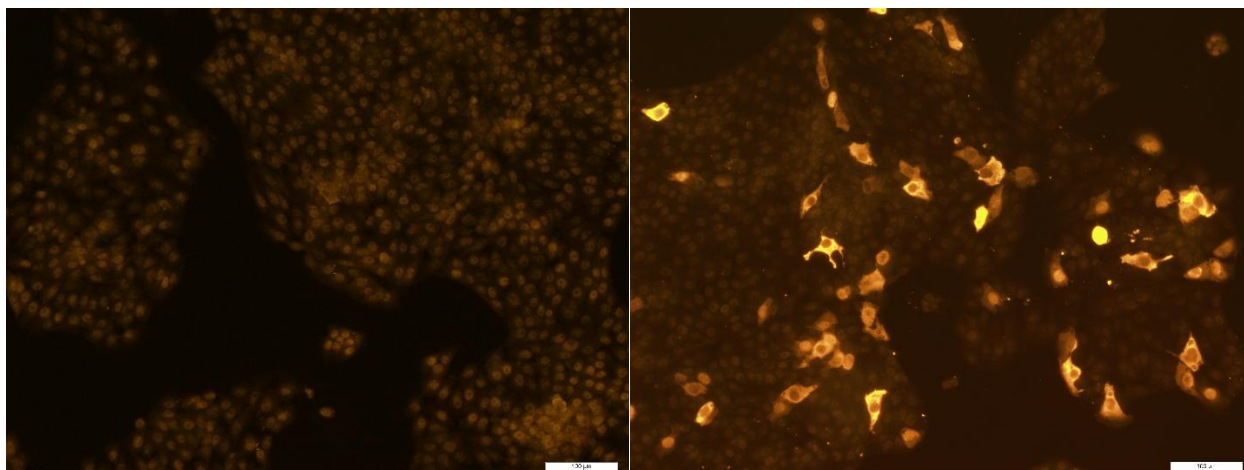


**Figure 2.1** Immunofluorescence assay image for detection of stock PCV2 virus infection of PK15 cells at 48 hpi. Antibody staining is against PCV2 Cap protein. Left image contains MOCK infected PK15 cells with the absence of fluorescence signals indicating no active PCV2 infection versus the right image showing numerous infected PK15 cells. Note both cytoplasmic and nuclear staining of PK15 cells infected with PCV2. Cells were imaged using an Olympus IX51 inverted fluorescence microscope.

### ***2.2.1 Stock PCV2 Virus Precipitation and Purification***

A total volume of 200 ml of PCV2 stock virus ( $TCID_{50}$   $3.16 \times 10^4$ /mL) was first precipitated by the addition of PEG 8000 and 0.5M sodium chloride (NaCl) with gentle agitation overnight at 4°C. The following day, precipitated virus was pelleted by centrifugation at 15,000g for 30 minutes at 4°C. The supernatant was discarded, and the viral pellet was then re-dissolved in TNE buffer (10mM Tris, 150mM NaCl, and 2mM EDTA). This solution was then overlaid onto a discontinuous sucrose gradient consisting of 35% sucrose and 65% sucrose in a 3.3 mL ultracentrifuge tube (Beckman-Coulter). Samples were spun at 185,000g for 3 hours using a Beckman-Coulter MLS 50 rotor, whereupon a whitish band was observed between the interface of the 35% and 65% sucrose layers. Each fraction of the ultracentrifuge tube was then collected and analyzed by Coomassie staining and Western Blot for the presence of PCV2 Cap. Semi-purified PCV2 was isolated from the bottom 65% sucrose fraction for subsequent experiments.

### **2.3 PCV2 Capsid Protein Production in Rosetta Blue BL21(DE3) *Escherichia coli***

Sequences for PCV1 capsid protein and PCV2 capsid protein were PCR amplified from plasmid constructs pJ201 AY184287 and pJ201 EF394779 respectively. The sequence for enhanced green fluorescent protein (eGFP) was PCR amplified from plasmid construct pEGFP-N1 CVU7762. The PCV1 sequence were amplified with a 5' NdeI restriction site and a 3' BamHI restriction site. The PCV2 capsid sequence was amplified with a 5' XhoI restriction site and a 3' NdeI restriction site. The eGFP sequence was amplified with a 5' XbaI restriction site and a 3' XhoI restriction site. Plasmid vector pET28a (+) containing a kanamycin resistance gene was digested with the respective restriction enzymes above for 60 minutes at 37°C before subsequent treatment with Antarctic alkaline phosphatase for an additional 30-minute incubation period at 37°C. PCR amplified gene sequences were also digested with each respective restriction enzyme pair to generate compatible sticky ends for ligation reactions. After gel purification of the products, vector plasmid and insert were combined in a 1:5 vector-insert ratio with the addition of T4 ligase and T4 ligase buffer for 15 minutes at room temperature. T4 ligase was heat inactivated by incubating the samples at 65°C for 20 minutes. Each ligation product was then transformed into competent DH5 $\alpha$  cells to measure successful cloning. After 1 hour of outgrowth in SOC media at 37°C with shaking in a bacterial culture incubator (Innova) at 225 rpm, 100  $\mu$ L of each transformation was plated onto fresh 100 x 15mm LB-agar petri dishes (Falcon) containing 50  $\mu$ g/mL kanamycin. The following day, colonies were picked for PCR analysis to find positive clones for successive plasmid purification and sequencing. Once the appropriate plasmid clones were obtained, these were transformed into competent Rosetta Blue BL21 (DE3) cells for protein expression. Colonies were picked and grown up in 3 mL of LB-broth containing 50  $\mu$ g/mL

kanamycin overnight and then inoculated into 400 mL of fresh Terrific Broth. Once optical density at 600nm (OD<sub>600</sub>) of 0.4-0.6 was reached, induction of protein production under control of a lac operon was induced with 1mM of IPTG for 4 hours at 37°C with shaking.

### ***2.3.1 PCV2 Capsid Protein Purification from BL21(DE3) E. coli***

After overnight induction of capsid expression, bacterial cultures were pelleted for 20 minutes at 4°C and 3000g. Supernatants were discarded, and pellets were re-suspended in imidazole lysis buffer and incubated overnight at 4°C with shaking. The following day, cell lysates were sonicated using an amplitude setting of 60%, with 30 second intervals of sonication followed by 30 seconds off for a total of five minutes. Cell lysates were then centrifuged at 3000g for 20 minutes at 4°C. Pellets were stored at -20°C, and the supernatants were added to equilibrated Ni-NTA (Qiagen) agarose beads in a 15 ml polypropylene column tube containing a frit to prevent beads from being lost. Samples were incubated with the beads for 1 hour with rocking at room temperature. The first flow through was collected and additional lysis buffer was added to the columns as a second wash. The samples were then washed with a pH 6.3 wash buffer for 20 minutes with shaking at room temperature. This was repeated twice before final elution of the his-tagged protein using an imidazole elution buffer. All samples were then analyzed by SDS-PAGE via colloidal Coomassie blue staining and Western blot.

## **2.4 Colony PCR**

Colony PCR analysis was carried out to determine clones positive for gene insert. Freshly transformed colonies were picked, lightly touched to an appropriate antibiotic-containing, labelled LB-agar “patch” plate, and then added to 50 µL of PCR mix containing:

- 10 µL of Phusion HF 5x buffer

- 34.5  $\mu$ L of Ultrapure distilled H<sub>2</sub>O
- 2.5  $\mu$ L of 10 mM forward primer
- 2.5  $\mu$ L of 10 mM reverse primer
- 0.5  $\mu$ L of Phusion High-fidelity polymerase

Immediately after addition of the colonies, PCR tubes were loaded into a pre-heated Eppendorf AG Thermocycler with the following program cycle:

- 1) 10 minutes @ 97°C
- 2) 30 seconds @ 97°C
- 3) 25 seconds @ 55°C
- 4) 30 seconds @ 72°C
- 5) Repeat cycles 2-4 x34
- 6) 5 minutes @ 72°C

Forward and reverse primers used were either specific primers flanking the cloning region or chosen from the insert itself. Positive colonies could be discerned from negative colonies by an expected band size difference between positive and negative colonies (Figure 2.2).

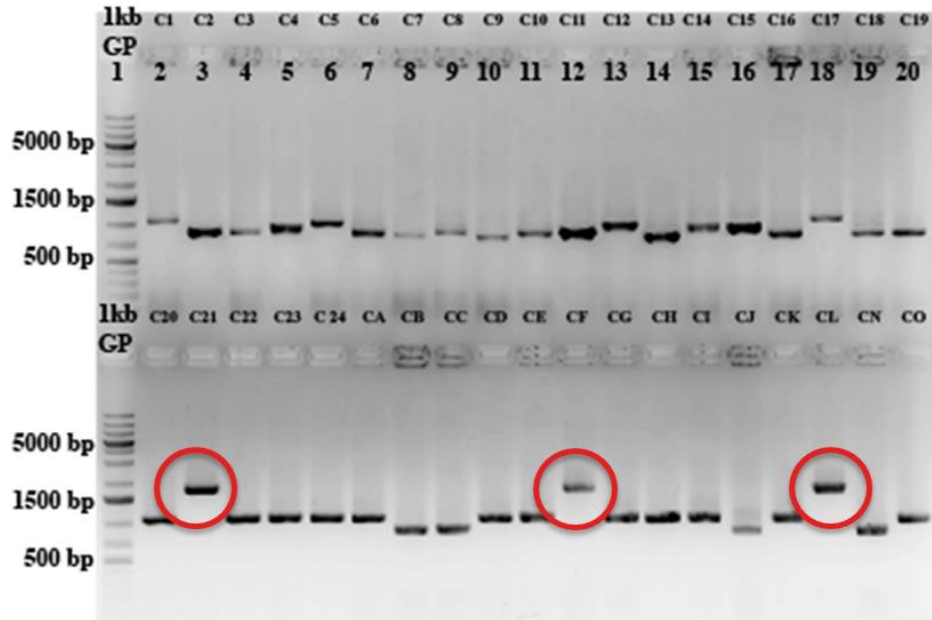


**Figure 2.2** Colony PCR agarose gel electrophoresis to detect colonies positive for PCV Cap insert into pFastBac plasmid. Positive colonies are denoted by a red circle and indicate an amplicon of expected band size of ~1600 bp which include full-length PCV Cap, WSSV IRES, and eGFP. These colonies were subsequently grown, and plasmids were extracted for sequence confirmation. Sequences confirmed for PCV1, PCV2, and PCV3 Cap were then transposed into parent bacmids by transforming DH10Bac *E. coli* with the confirmed pFastBac plasmids.

## 2.5 Virus Inactivation with 1% Formaldehyde Solution

Both stock and semi-purified PCV2 virus was inactivated by combining volumes of 4% formaldehyde in a 1:4 ratio for a final concentration of 1% formaldehyde and incubated at 37°C for 48 hours. PK15 cell lysate (freeze/thawed/sonicated) was also included as a negative control to account for possible formaldehyde contamination after dialysis. Untreated stock and semi-purified PCV2 virus were included as a positive control to ensure infectivity after 37°C incubation and subsequent dialysis. Samples were then dialyzed together using Slide-A-Lyzer (Thermo Scientific) dialysis cassettes in 1x PBS for 48 hours at 4°C and 200-fold total dilution after 3 buffer exchanges. After dialysis was completed, virus titration using the Reed-Münch method was

carried out with each dialyzed sample using PK15 cells to confirm presence or absence of infectivity. All virus samples treated with formaldehyde showed no infectivity versus positive controls when exposed to PK15 cells in tissue culture plates after 24 hpi as confirmed by immunofluorescence assay (Figure 2.3).

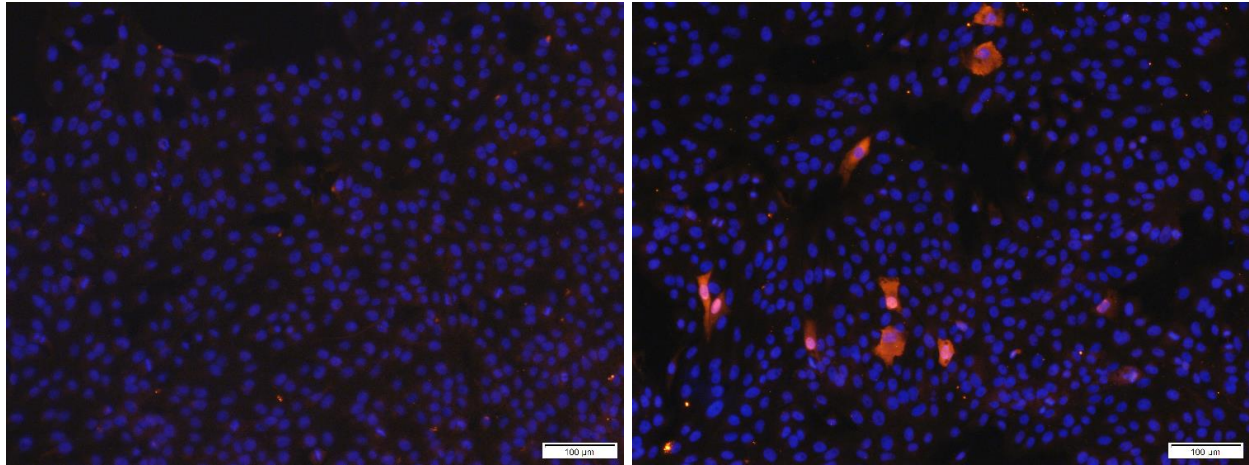


**Figure 2.3** Immunofluorescence assay to confirm PCV2 infection absence in PK15 cells infected 24 hours after dialysis. Left Image A represents PK15 cells treated with 1% formaldehyde inactivated stock PCV2 virus post-dialysis. Right Image B represents PK15 cells treated with stock PCV2 virus post-dialysis to confirm absence of infectivity was not due to dialysis treatment. Nuclei are stained blue with Hoescht 33342 and PCV2 Cap is stained with a primary rabbit anti-cap pAb, with a secondary goat anti-rabbit Alexa Flour 568 pAb. Cells were imaged using an Olympus IX51 inverted fluorescence microscope.

## **2.6 Dialysis of Purified PCV2 Cap, Inactivated PCV2 Virus, and all PCV VLP Preparations**

Each sample was loaded into an appropriate size Slide-A-Lyzer (Thermo Scientific) dialysis cassette with a MWCO of 10 kDa as per the manufacturer's instructions. Cassettes were then loaded into a 4L bucket filled with sterilized 1x PBS and incubated at 4°C using a magnetic stirrer (Thermo Scientific Isotemp Ceramic Stirrer) for 2 hours after which the buffer was exchanged, and samples continued to be incubated overnight. The total buffer volume used was at least 200x the total volume of samples dialyzed. Samples were collected and analyzed by



Coomassie staining and Western blot for the presence of PCV Cap protein. In addition, negative controls were also subjected to dialysis including formaldehyde treated PK15 cell lysate, control baculovirus infected Sf9 cells, and Sf9 cell lysate. A positive control of live PCV2 virus was also included to show that viral inactivation was not the result of dialysis treatment.

## **2.7 PCV Cap Protein Detection and Confirmation**

Several techniques were used to detect the presence of PCV Cap during recombinant production including; Sodium dodecyl sulfate polyacrylamide gel electrophoresis (SDS-PAGE) and subsequent Coomassie staining in conjunction with Western blotting, immunofluorescence assay (IFA), transmission electron microscopy (TEM), and approximate quantification using a Bio-Rad DC protein assay. Indirect PCV Cap production confirmation from recombinant baculovirus infection of Sf9 insect cells was carried out using a bicistronic gene cassette consisting of PCV Cap protein followed by an internal ribosome entry site (IRES) from White Spot Syndrome Virus (WSSV), and finally with an enhanced green fluorescent protein (eGFP).

### ***2.7.1 SDS-PAGE, Coomassie Staining and Western Blot for PCV Cap Proteins***

Each sample to be analyzed was mixed with 4x SDS sample buffer containing SDS (Sigma-Aldrich) and 2-Mercaptoethanol (BME). Samples were heated at 99°C for 20 minutes in a Thermomixer (Eppendorf), then briefly vortexed and centrifuged before loading onto a 12% polyacrylamide denaturing gel. Electrophoresis of each gel was carried out in a Bio-Rad Mini-Protean Tetra System for 2 hours at 100V in 1x SDS running buffer. Samples were run on 2 gels in parallel so that one gel could be transferred to Coomassie blue staining solution and the other could then be transferred onto a polyvinylidene difluoride (PVDF) membrane (GE Healthcare)

using a Bio-Rad semi-dry transfer apparatus for 50 minutes at 25V. Coomassie stained gels were incubated in Coomassie colloidal blue (Sigma) for 30 minutes at room temperature and subsequently incubated in Coomassie de-staining solution (40% glacial acetic acid, 40% methanol) overnight at 4°C with rocking. PVDF membranes were incubated in 5% skim milk (Mead & Johnson) in 1x PBST (0.1%) blocking buffer for 60 minutes at room temperature before the addition of primary rabbit anti-Cap antibody (1:2000) or swine serum (1:100) overnight at 4°C with rocking. The PVDF membrane was then washed three times with 1x PBST (0.3%) and then incubated in blocking buffer containing secondary goat anti-rabbit or mouse anti-swine antibodies conjugated to horseradish peroxidase (HRP) at 1:8000 dilution for 90 minutes at RT with rocking. The PVDF membrane was then washed three times with 1x PBST (0.3%) before incubation with Illuminata (GE Healthcare) chemiluminescent substrate for 10 minutes at RT. Developed PVDF membrane was then visualized and analyzed using a Bio-Rad VersaDoc 5000 MP imaging system and Quantity-one software (Bio-Rad) (Figures 2.4, 2.5).

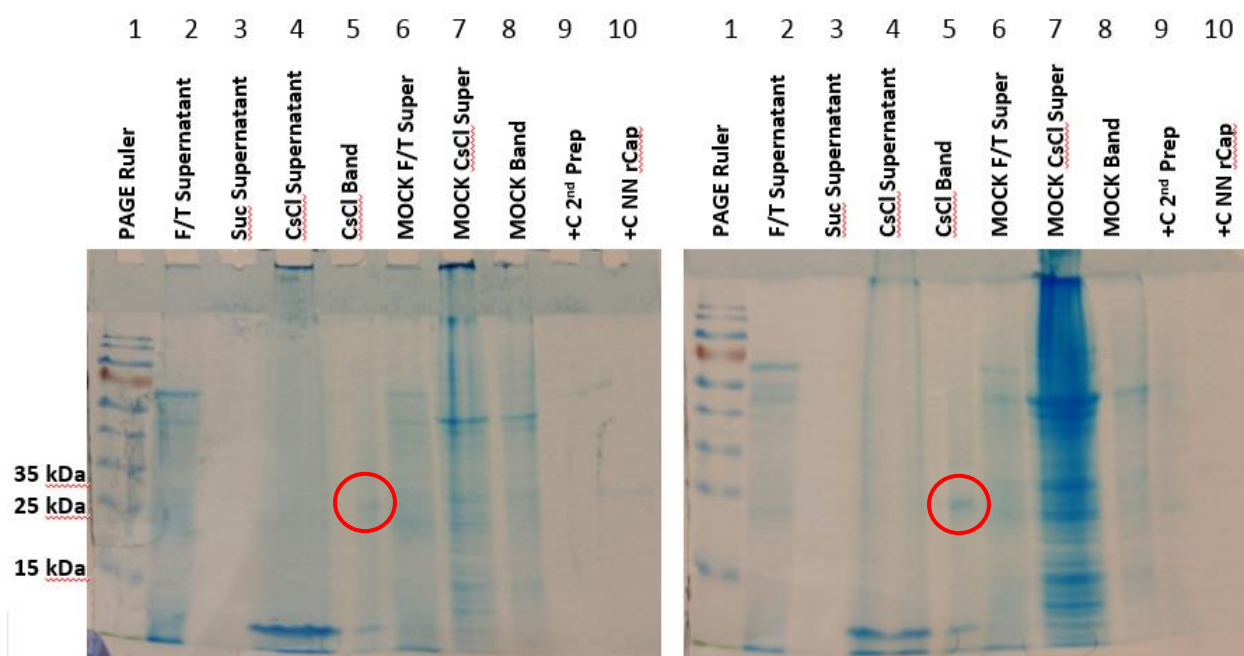


**Figure 2.4** PCV Cap proteins Coomassie staining. Gels represent PCV VLP purification steps using a CsCl gradient and ultracentrifugation. Left gel is from PCV1 VLP purification and right gel is from PCV2 VLP purification. Red circles indicate CsCl purified VLPs as the band corresponds to the expected size of PCV Cap protein ~28 kDa. Lane 2 is supernatant from freeze/thawed Sf9 cells post PCV Cap expression. Lane 3 is supernatant from the discontinuous sucrose gradient. Lane four is supernatant from above the white band observed from CsCl purification of VLPs. Lane 5 is actual PCV Cap protein recovered from a white band formed after CsCl ultracentrifugation. Lanes 6-8 are from MOCK infected Sf9 cells acting as negative controls. Lane 9 and 10 are positive controls with PCV2 rCap from expression in *E. coli* and faint bands can be observed in lane 9 at the expected size. See next figure for PCV2 anti-cap Western Blot results.

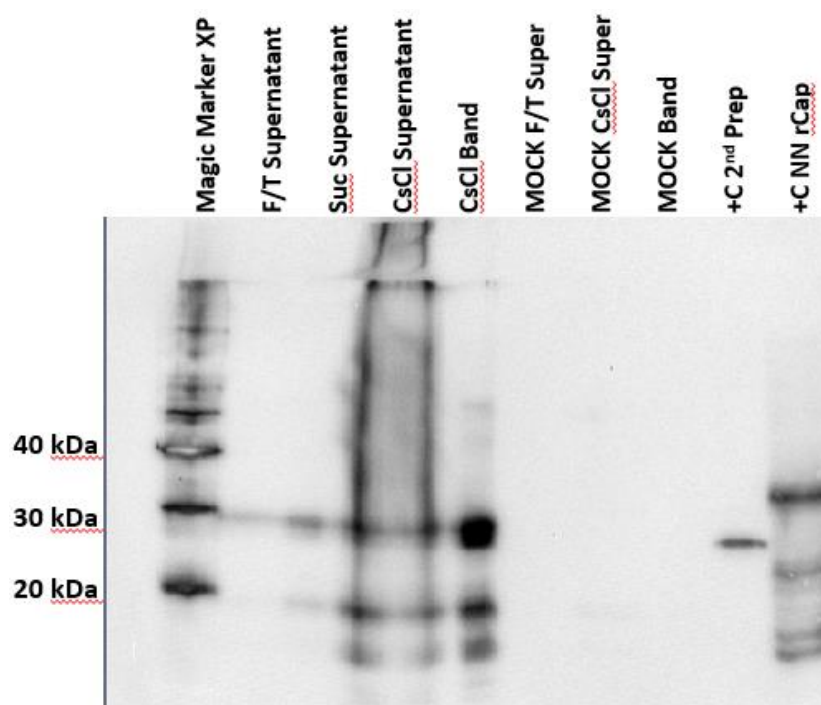


**Figure 2.5** Western Blot results of duplicate gel run of PCV2 VLP purification from Figure 2.3. Lane 2 is supernatant from freeze/thawed Sf9 cells post PCV Cap expression. Lane 3 is supernatant from the discontinuous sucrose gradient ultracentrifugation. Lane four is supernatant from above the white band observed after CsCl purification of VLPs. Lane 5 is actual PCV Cap protein recovered from a white band formed after CsCl ultracentrifugation. The band observed at ~28 kDa matches the expected band size of PCV2 Cap. Lanes 6-8 are from MOCK infected Sf9 cells acting as negative controls. Lane 9 and 10 are positive controls with PCV2 rCap from expression in *E. coli* showing a protein of ~28 kDa in lane 9. Lane 10 is also recombinant PCV2 Cap but is denatured and in 8M urea post-sonication, causing a change in band migration and fragmentation of PCV2 Cap protein. The second (~18 kDa) and third bands (~10 kDa) seen in lanes 3, 4, and 5 also correspond to the secondary bands observed in lane 10 and is most likely due to fragmentation of the full-length protein.

### ***2.7.2 Immunofluorescence Assay (IFA) for Detection of PCV2 Infection***

Three 96-well plates were seeded with  $\sim 15 \times 10^4$  PK15 cells/well to attain  $\sim 50\%$  confluency after cells were allowed to attach for 2 hours before infection with stock PCV2 virus, post-dialysis treated virus, and 1% formaldehyde treated virus. Equivalent volumes of 100  $\mu\text{L}$  of each virus prep were inoculated into the wells in quadruplicate, including a MOCK infection using only cell culture media. Exposed cells were then incubated for 24 hours at  $37^\circ\text{C}$ ,  $5\% \text{ CO}_2$  in a Heracell 150i incubator. At 24 hpi, media was removed, and cells were washed twice with sterile 1x PBS prior to fixation using 4% formaldehyde solution in 1x PBS (pH 7.0) for 20 min at RT. After fixation, formaldehyde was removed, and each well was washed twice again in 1x PBS. Each well was then incubated in permeabilization buffer including a primary rabbit anti-PCV2 Cap antibody at 1:400 dilution for 90 minutes at  $37^\circ\text{C}$ . After incubation with primary antibody, wells were washed three times with PBST (0.1%). Sample wells were then incubated for an additional 90 minutes at  $37^\circ\text{C}$  with secondary goat anti-rabbit HRP antibody at 1:200 dilution. Wells were then washed twice with PBST (0.1%) and then incubated with Hoechst 33342 (Hoechst AG) for 5 min at RT. Wells were then washed 3 more times with 1x PBS before visualization under an Olympus IX51 inverted fluorescence microscope. Infected wells were deemed positive if any cells expressed PCV2 capsid protein either in the nuclei, cytoplasm, or both (Figure 2.1).

### **2.8 Virus Stock Titration by the Reed-Müench Method**

PCV2 virus and recombinant baculovirus stocks were titered using the Reed-Müench 50% end-point dilution method by using 5-fold serial dilutions of the virus on PK15 cells (PCV2) or 10-fold serial dilutions of recombinant baculovirus on Sf9 cells in a 96-well plate. A 96-well tissue culture plate (Corning) was seeded with  $10^4$  PK15 (or Sf9) cells/well and allowed to grow to 50%

confluency. PCV2 stock virus was prepared in 5-fold serial dilutions from  $10^0$  to  $10^{-7}$ , and baculovirus stock was prepared in 10-fold serial dilutions from  $10^0$  to  $10^{-8}$ . Each virus stock dilution was inoculated onto the appropriate host cell in replicates of 8 per dilution. PK15 cells infected with PCV2 were incubated for 24 hours at 37°C, 5% CO<sub>2</sub> in a Heracell 150i incubator. At 24 hpi, media was removed, and cells were washed twice with sterile 1x PBS prior to fixation using 4% formaldehyde solution in 1x PBS (pH 7.0) for 20 min at RT. See above immunofluorescence assay for staining method. Sf9 cells infected with recombinant baculoviruses were incubated for 12 days at 28°C, 0.1% CO<sub>2</sub> in a Heracell 150i incubator. Media was then removed from the Sf9 cells and then a 25:75 mixture of 0.4% Trypan Blue (Gibco) and 1x PBS was added to each well to assess Sf9 cell viability. Infected wells contained mostly dead cells (>90% cell death) and were marked as positive for baculovirus using the Reed-Muench method<sup>98</sup> (Figure 2.6).

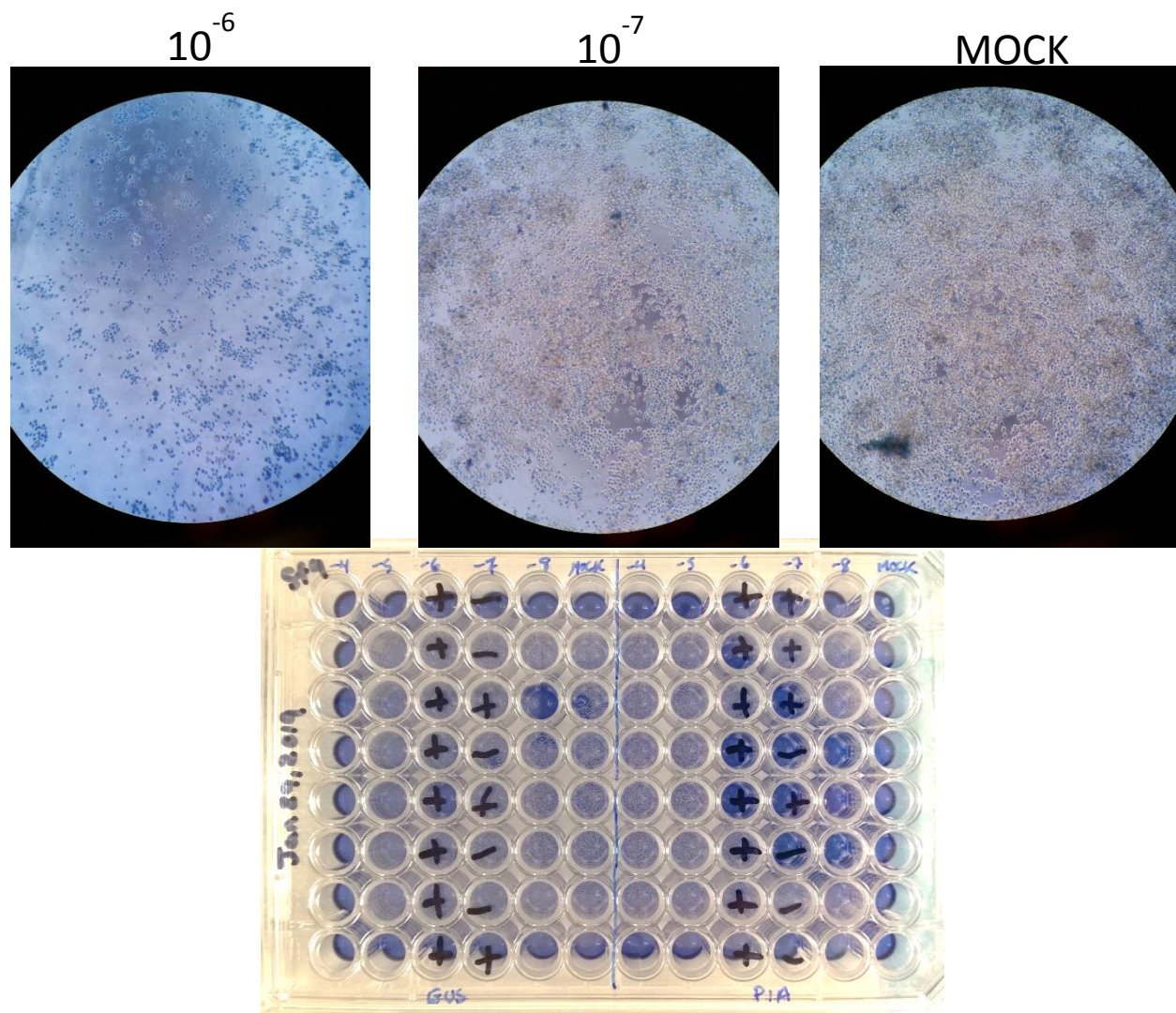


**Figure 2.6** Example of baculovirus titration using the 50% endpoint dilution method developed by Reed-Müench. Wells infected with recombinant baculovirus displayed nearly 100% cytopathic effect and mortality rate as observed in the leftmost image panel representing virus stock diluted by  $10^{-6}$ . Trypan blue dye was used to assess the viability of the cells as cells with compromised cellular membranes will stain blue, while viable cells remain unstained as seen in the center  $10^{-7}$  dilution image. MOCK infected cells remain viable and are used to differentiate infected versus non-infected wells as shown in the bottom image to calculate the titer of the virus stock. PCV2 titrations were carried out using immunofluorescence detection of PCV2 Cap protein after 48 hpi.

The TCID<sub>50</sub>/mL of the stock PCV2 virus was determined to be  $\sim 3.4 \times 10^4$ /mL.

The TCID<sub>50</sub>/mL of the semi-purified PCV2 virus was determined to be  $\sim 4.6 \times 10^5$ /mL.

The TCID<sub>50</sub>/mL of the PCV1 PIG recombinant baculovirus was determined to be  $\sim 1.0 \times 10^8$ /mL.

The TCID<sub>50</sub>/mL of the PCV2 PIG recombinant baculovirus was determined to be  $\sim 3.9 \times 10^7$ /mL.

The TCID<sub>50</sub>/mL of the PCV3 PIG recombinant baculovirus was determined to be  $\sim 6.5 \times 10^7$ /mL.

## **2.9 PCV1 & PCV2 Capsid Proteins Restriction Enzyme Cloning into pFastBac Vector**

The PCV1 capsid gene was PCR amplified from plasmid construct pJ201 containing PCV1 strain AY184287 using primers containing a 5' BamHI restriction site and a 3' SpeI restriction site in addition to an inserted 5' Kozak sequence "GCCACC" prior to each start codon. The PCV2 capsid gene was PCR amplified from plasmid construct pJ201 containing PCV2 strain EF394779 using primers also containing a 5' BamHI restriction site with the addition of a Kozak sequence, and a 3' SpeI restriction site. An internal ribosome entry site (IRES) sequence from white-spot syndrome virus (WSSV) was synthetically ordered in two fragments which were then spliced together using sequence overlap extension PCR. This IRES sequence contained a 5' SpeI restriction site and a 3' EcoRI restriction site. An enhanced green-fluorescent protein (eGFP) sequence was PCR amplified from plasmid pEGFP-C1 using primers containing a 5' EcoRI restriction site and a 3' PstI restriction site. PCR cleanup of the IRES and eGFP amplicons was carried out and then spliced together using sequence overlap extension PCR with overlapping primers. The resulting product was then agarose gel purified and the band of the expected size was excised for further purification. 1  $\mu$ g of this purified product was then restriction enzyme digested with SpeI-HF and PstI-HF for 30 minutes at 37°C. 1  $\mu$ g of PCV capsid amplicons and 1  $\mu$ g of pFastBac (Invitrogen) plasmid were restriction enzyme digested in separate reactions with BamHI-HF and SpeI-HF (or PstI-HF for the pFastBac plasmid) for 30 minutes at 37°C. Digested pFastBac



plasmid was then treated with Antarctic alkaline phosphatase (New England Biolabs) for an additional 30 minutes at 37°C. All enzyme reactions were stopped by incubation at 80°C for 20 minutes. Cut pFastBac plasmid samples were then run on a 1% agarose gel to obtain pure DNA band size of ~4800 bp. Bands were then excised using a sterile razor blade and weighed prior to gel extraction. Gel extraction of the band was carried out using a Qiagen gel extraction kit.

Four different ligation reactions were prepared based on the previous restriction enzyme digests. BamHI-HF and SpeI-HF digested PCV1 or PCV2 capsid gene and pFastBac plasmid were combined for the first two ligation reactions. The second two ligation reactions were prepared as multi-way ligations containing BamHI-HF and SpeI-HF digested PCV1 or PCV2 capsid gene with SpeI-HF and PstI-HF digested IRES-eGFP and pFastBac plasmid. A vector to insert ratio of 1:5 was used for all ligation reactions. Ligation reactions were carried out with T4 ligase (NEB) and T4 ligase buffer in 20 µL volumes for 20 min at room temperature. T4 ligase was heat inactivated by incubating the samples at 65°C for 20 minutes. Ligation products were then transformed into DH5α cells by adding 5 µL of each ligation product to 50 µL of competent DH5α cells on ice and incubated for 30 minutes. After 1 hour of outgrowth in SOC media at 37°C with shaking at 225 rpm, 250 µL of each transformation was plated onto fresh LB-agar 100 x 15mm petri dishes (Falcon) containing 100 µg/mL ampicillin. The following day, colonies were picked for colony PCR analysis to find positive clones for successive plasmid purification and sequencing. The positive sequences were labelled PCV1 Cap, PCV1 PIG (PCV Cap/IRES/eGFP), PCV2 Cap, or PCV2 PIG.



### **2.9.1 PCV3 Capsid Gibson Cloning into pFastBac Vector**

Previously generated PCV1 PIG pFastBac vector was double-digested with restriction enzymes BamHI-HF and SpeI-HF to remove the PCV1 Cap sequence. Digestion was carried out using CutSmart buffer (NEB) at 37°C for 30 minutes before the addition of Antarctic alkaline phosphatase (AAP) for an additional 30 minutes at 37°C. Vector was then purified using a Qiagen PCR cleanup kit to remove enzymes and buffers before running the sample on an agarose gel for 45 min at 100V to determine restriction enzyme cut efficiency and correct cut vector size. Vector concentration was determined using a Nanodrop 1000 spectrophotometer (Thermo Scientific). PCV3 Cap insert was designed from strain DE23.17 (GenBank Accession: MG014368) and included 5' Kozak sequence "GCCACC" prior to the start codon. Gibson assembly of the PCV3 Cap insert was carried out using a SGI-DNA BioXp 3200 Synthetic DNA System as recommended by the manufacturer's protocols. Linearized vector and synthesized insert were combined in equimolar amounts before addition of Gibson Cloning Master Mix to a total volume of 20 µL. This mixture was then incubated in an Eppendorf AG Thermocycler for 1 hour at 50°C. Subsequent reaction mixture was then used to transform DH5α *E. coli* as previously described. Colony PCR was then used to determine positive clones for production of recombinant bacmids.

### **2.10 Recombinant Bacmids Production**

After sequence confirmation of cloned pFastBac plasmids containing either PCV capsid or PCV capsid and IRES/eGFP, plasmids were then transformed into DH10Bac competent cells containing a parent bacmid conferring Kanamycin resistance and helper plasmid containing tetracycline resistance and enabling transposition of the pFastBac gene cassette into the bacmid. Transformants were selected on LB-agar plates containing 7 µg/mL gentamycin, 10 µg/mL

tetracycline, 50 µg/mL of kanamycin, and 50 µg/mL of blue-gal. Positive white colonies were picked after a 72-hour incubation period and inoculated into 4 mL of SOC media at 37°C with shaking at 225 rpm overnight. The following morning the recombinant bacmids were extracted using a Hi-Pure Plasmid Extraction kit (Invitrogen).

### ***2.10.1 Reverse Genetics Production of Recombinant Baculoviruses***

The extracted recombinant bacmids were transfected into ~50% confluent Sf9 cells using Cellfectin II reagent (Gibco). DNA-lipid complexes in unsupplemented Grace's media were left on the Sf9 cells overnight and media was then replaced with 25% serum-supplemented TNMFH and 75% Sf-900 III SFM the following day. Evidence of infection appeared approximately 5 days after the initial transfection took place. Recombinant baculovirus-infected Sf9 cells containing eGFP showed fluorescent under an Olympus IX51 inverted fluorescence microscope within 72 hours in isolated patches. Recombinant baculovirus was first collected in the supernatants at 4- and 5-days post-transfection. These samples were centrifuged at 10,000g for 15 minutes at room temperature to separate cellular debris from supernatant and labelled accordingly. Cells and supernatants were also collected at 7 days post-transfection for analysis by western blot for the presence of PCV capsid protein. Upon Coomassie staining and western blot analysis, PCV2 capsid was found in the cellular component of the P0.5 sample using a rabbit anti-capsid primary antibody at a ratio of 1:2000 and a secondary goat anti-rabbit HRP antibody at a ratio of 1:5000. There was evidence of mild cross-reactivity of the PCV2 primary antibody to the PCV1 P0.5 sample showing a band of expected size at ~28 kDa. Both PCV1 & PCV2 capsid producing recombinant bacmids were then amplified for further protein production.

## **2.11 PCV Capsid Protein Expression via Recombinant Bacmid Infection of Sf9 Cells**

Sf9 cells were first adapted to suspension growth in 250 mL PETG (Corning) shaker flasks using the following protocol. Three T-75 flasks with confluent Sf9 cells in monolayer were passaged via sloughing and a cell count was performed. These cells were placed into a 250 mL PETG shaker flask in 50 mL of 25% supplemented TNMFH and 75% SFM-III 900 serum-free media at a cell density of approximately  $6 \times 10^5$  cells/mL. This shaker flask was then placed into an Innova shaker incubator and incubated at 28°C with 100 rpm shaking speed. The rpm of the culture was increased by 5 rpm each day after cell count and cell viability determination until the rpm reached 140 rpm. Doubling time of Sf9 cells in suspension was determined to be approximately 72 hours.

Four 150 mL PETG flasks were seeded with 70 mL containing  $\sim 1.5 \times 10^6$  Sf9 cells/mL. MOCK infected cells were inoculated with 700  $\mu$ L of Sf900-III serum free media, a second control consisting of unmodified/no-insert baculovirus was inoculated into a second flask at a MOI of 0.1. A third flask was inoculated with PCV1 Cap-containing recombinant baculovirus, a fourth flask was inoculated with PCV2 Cap-containing recombinant baculovirus, and a fifth flask was inoculated with PCV3 Cap-containing recombinant baculovirus. Sf9 cell count and viability was determined every day until day five when cell viability of each infected cell culture was less than or equal to 5%. At this time point the cell cultures were harvested into 50 mL centrifuge tubes and centrifuged at 2000g for 20 minutes at 4°C. Supernatants were collected and stored at 4°C or frozen at -20°C with the addition of 2.5% glycerol. Cell pellets were resuspended in 3 mL 1x PBS containing 5 IU of DNase I and cOmplete protease inhibitor (Sigma). Samples were briefly vortexed and incubated on ice for 30 minutes. After incubation, each sample was centrifuged again at 2500g for 20 minutes at 4°C. Supernatants were once again removed and stored at 4°C or frozen

with glycerol. Pellets were then resuspended in 1.5 mL of RIPA buffer (10 mM Tris-HCl, 1 mM EDTA, 140 mM NaCl, 1% Triton X-100, 0.1% sodium deoxycholate, pH 8.0) and vortexed vigorously for 30 seconds. Each sample was then sonicated using a QSonica 125-Watt, 20 kHz sonicator at 30% amplitude for 10 cycles of 10 seconds on, 20 seconds off while incubating the samples in ice. Samples taken before RIPA buffer and sonication were compared to samples afterwards by placing 5  $\mu$ L of each sample on a microscope slide and visualizing at 40x magnification for the presence of inclusion bodies not seen in the negative control samples.

#### ***2.11.1 PCV Cap Inclusion Bodies & Virus-Like Particles (VLPs) Purification***

Each Sf9 lysate sample after treatment with detergent and sonication was then overlaid on top of 60% w/v sucrose and spun at 3000g for 30 minutes at 4°C. The density of PCV particles is estimated to be approximately 1.35 g/cm<sup>3</sup>, whereas the density of 60% w/v sucrose is approximately 1.28 g/cm<sup>3</sup>. The supernatant above the sucrose layer and sucrose layer were removed and stored at -20°C for later analysis. The remaining bottom fraction was then overlaid atop a 37% CsCl solution in 3.3 mL (Beckman-Coulter) ultracentrifuge tubes. Ultracentrifugation of these sample fractions were carried out at 250,000g for 20 hours at 4°C using an MLS 50 rotor. The CsCl supernatant was removed by pipette and frozen at -20°C for later analysis. A distinct band was formed in all samples except controls at approximately 1/5 of the totally volume (Figure 2.6). This band was recovered using a pipette and transferred to a Slide-A-Lyzer (Thermo Scientific) dialysis cassette for dialysis to remove the remaining CsCl. All samples were dialyzed in a 250x volume of 1x PBS at 4°C over a period of 24 hours with one buffer exchange after 2 hours. Samples were also analyzed by Coomassie and Western Blot.

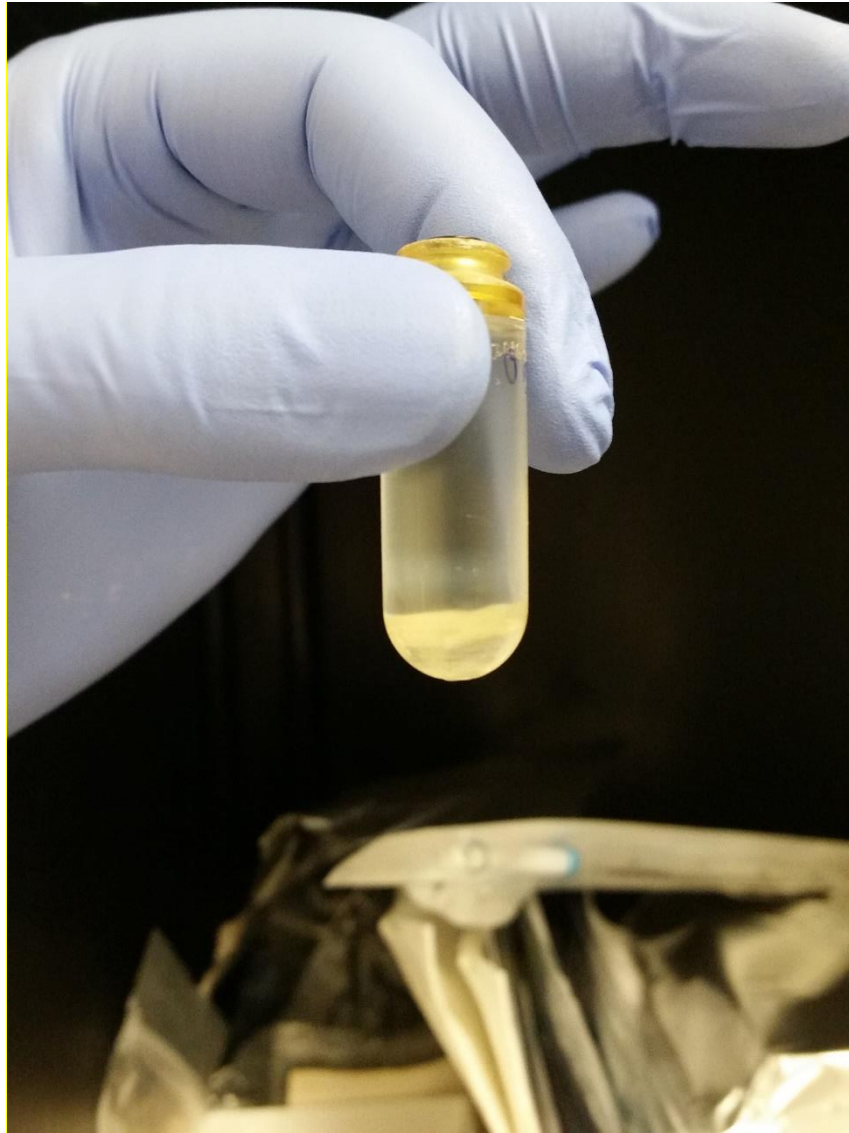


**Figure 2.6** Example of 37% CsCl purified VLP's. Image taken immediately after 20 hours of centrifugation at 250,000g, 4°C. Note Sf9 cellular debris at the bottom of the tube, and distinct, uniform white band at approximately 1/5 of the total volume. This white band was not observed in negative controls.

#### ***2.11.2 Protein Quantification using Bio-Rad DC Protein Assay Kit***

Bovine serum albumin (BSA) protein standard was prepared in the following concentrations to estimate sample quantities: 1.41 mg/mL, 1.0 mg/mL, 0.75 mg/mL, 0.5 mg/mL,

0.25 mg/mL, and 0.1 mg/mL. To 2mL of Bio-Rad solution A, 100  $\mu$ L of Bio-Rad solution S was mixed to produce solution A'. In a 96-well plate, 5  $\mu$ L of each protein standard including samples were added in triplicate or quadruplicate. In each well containing sample, 25  $\mu$ L of Bio-Rad solution A' was added as well as 200  $\mu$ L of Bio-Rad solution B. The plate was then incubated in the dark for 15 minutes. The 96-well plate was then analyzed using a Bio-Rad iMark microplate reader at a wavelength of 750 nm. A standard curve was generated, and sample quantities were analyzed from the linear regression equation determined from the standard curve.

### ***2.11.3 PCV Virus-Like Particles and Recombinant Baculoviruses Transmission Electron Microscopy***

Samples suspected of containing PCV VLPs were analyzed at the Microscopy and Imaging Facility at the University of Calgary using a Hitachi 7650 TEM at 80kV. Samples were prepared by placing 30  $\mu$ L of each sample onto parafilm and placing carbon-coated TEM copper grids onto each sample for 5 minutes. Excess fluid was removed from the grids using filter paper, then each grid was incubated for 30 seconds in 2% uranyl acetate (negative stain) and dried once again with filter paper to remove excess fluid. Images were captured of VLPs at a magnification of 40000-50000x and identified as PCV1 or PCV2 VLPs based on morphology and size compared to a negative control (Figure 2.7). Recombinant baculovirus images were captured at 15000x total magnification and identified as baculovirus based on morphology and size compared to a negative control (Figure 2.8).

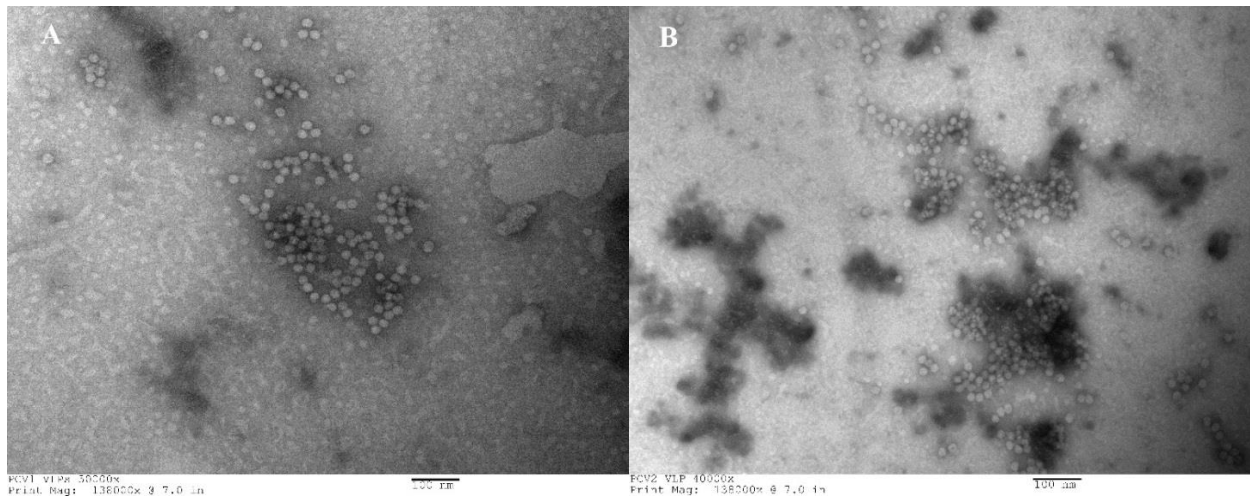


**Figure 2.7** Transmission electron microscope images of post-CsCl ultracentrifugation purification of PCV VLPs produced by recombinant baculovirus infection of Sf9 cells. Left image A shows PCV1 VLPs at a total magnification of 50,000x. Right image B shows PCV2 VLPs at a total magnification of 40,000x. VLP icosahedral morphology matches 17-20 nm size of PCV2 virions. Negative control of purified Sf9 cells did not show these particles.

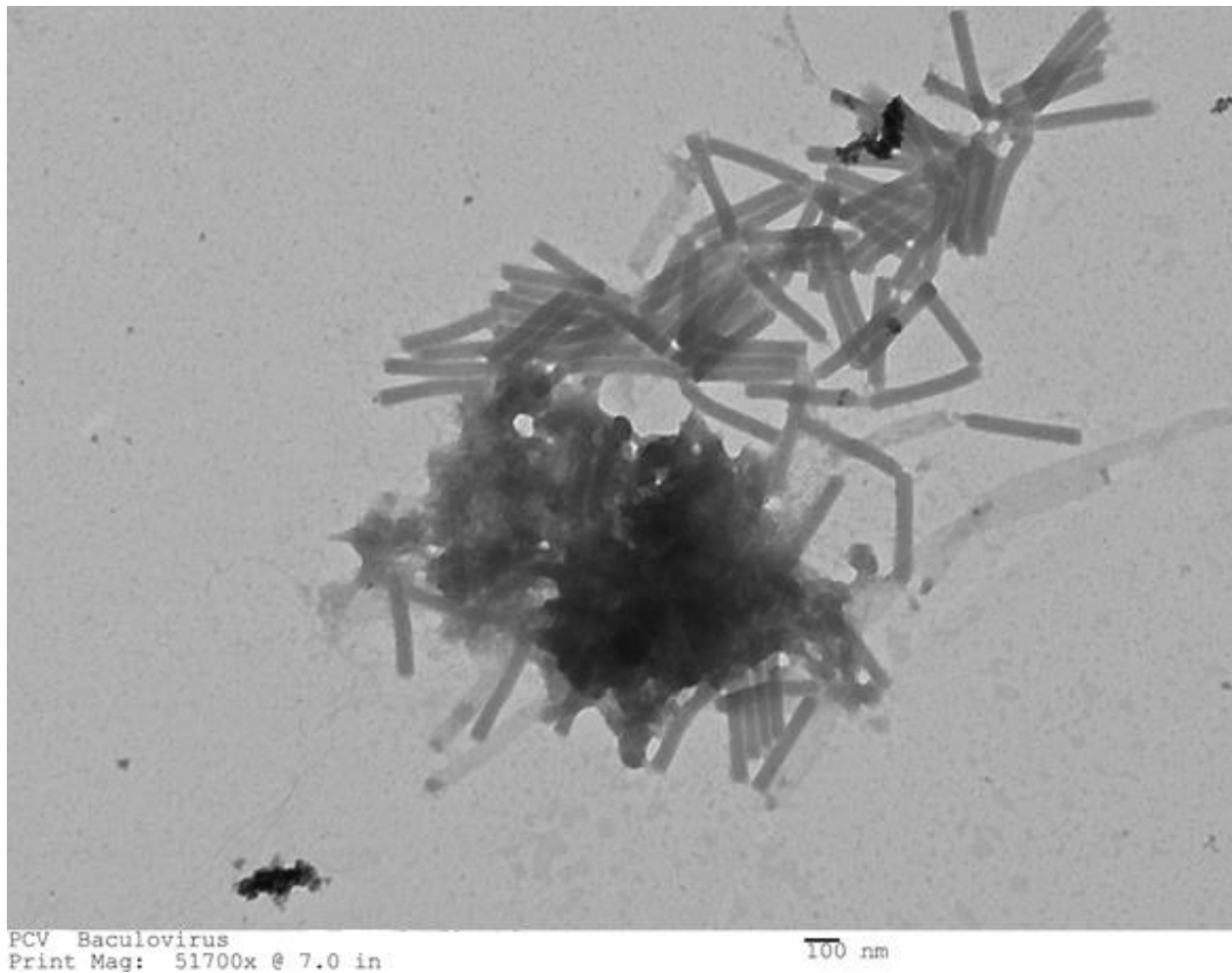


**Figure 2.8** Transmission electron microscope image of recombinant baculovirus containing the PCV3 Cap gene at a magnification of 15000x. Viruses generated by reverse genetics in Sf9 cells. This image was taken after density-gradient ultracentrifugation but VLPs are not seen in this image. Viruses identified as baculovirus based on rod-shaped morphology and ~280 x 60 nm size and compared to negative controls.

## 2.12 Cellular Apoptosis Assay Using Flow Cytometry

PK15 cells were seeded at a density of  $5 \times 10^5$  cells/well in 6-well cell culture plates (Corning) in a total volume of 2 mL of Dulbecco's Modified Enhanced Media containing 10% fetal bovine serum (FBS), 5% penicillin/streptomycin antibiotic, 5% sodium pyruvate, and 5% non-essential amino acids (NEAA). Attached cells were treated with various reagents and sample



preps while at ~60% confluency including pre-treatment with or without pre-treatment using 10  $\mu$ M caspase-8 inhibitor II (Z-IE(OMe)TD(OMe)-FMK/Granzyme B Inhibitor III, EMD Millipore), 10  $\mu$ M caspase-9 inhibitor II (LEHD-CHO, EMD Millipore), or 50  $\mu$ M etoposide treatment. 10  $\mu$ M of each inhibitor was used as recommended for a working concentration for each inhibitor. Treatments included: No treatment, 2  $\mu$ L of 50mM etoposide, dialysis buffer, 1% formaldehyde treated PK15 cells post-dialysis, 1% formaldehyde inactivated stock PCV2, 1% formaldehyde inactivated semi-purified PCV2, recombinant PCV2 capsid protein expressed from bacteria, PCV2 MOCK infection, Sf9 cell lysate post-cesium chloride ultracentrifugation and dialysis, control (cBac) baculovirus post-cesium chloride ultracentrifugation and dialysis, PCV1 VLPs, PCV2 VLPs, and PCV3 VLP preps. Treated PK15 cells were incubated for 24 hours at 37°C, 5% CO<sub>2</sub> in a Heracell 150i incubator. The 24-hour timepoint was chosen because the measured effect on bystander effect has been observed within 24 hours of exposure in past studies, thus the bystander death effect could not be attributed to completion of the viral life cycles of porcine circoviruses. After this, the same time-point was kept consistent although apoptosis could be triggered much earlier and measured by mitochondrial membrane polarization. 100  $\mu$ g of each virus Cap protein preparation as measured by the Bio-Rad DC protein quantification assay was used for each experimental replicate and thereafter kept consistent.

At 24 hours post treatment, all supernatants were collected, and each well was washed with sterile 1x PBS which was also collected. Each well was then treated with 0.25% trypsin/EDTA for 6 minutes at 37°C. Cells were detached and added to the previously collected supernatants and washes in 15 mL Falcon centrifuge tubes. Samples were then centrifuged at 300g for 10 minutes at room temperature (RT). Supernatants were carefully aspirated, and the cell pellets were resuspended in 2 mL of 1x PBS for washing. Each tube was centrifuged again at 300g for 10

minutes at RT. Supernatants were aspirated once again and then the cell pellets were resuspended in 1x Annexin V binding buffer. Heat-killed positive control samples were incubated in an Eppendorf Thermomixer at 60°C for 10 minutes to provide a positive control for 7-AAD staining. 50 µL of each sample was pipetted into a 1.5 mL Eppendorf tube at a cell concentration of  $\sim 1 \times 10^5$ . Each sample was then treated with 5 µL of Annexin V-FITC and 1 µL of 7-AAD (Except for the no treatment and single stain controls) and mixed gently before spinning down on a benchtop microfuge (VWR). Samples were then incubated in the dark at RT for 30 minutes. After 30 minutes, 450 µL of 1x Annexin V binding buffer was added to each sample. Samples were then immediately analyzed by an Attune Violet Flow Cytometer. Lasers BL1 (FITC) and BL3 (7-AAD) were used to for data collection from the samples. Each sample was then analyzed using FlowJo v 10.5.3.

### **2.13 PCV-Induced Apoptosis TUNEL Assay Detection**

A 24-well cell culture plate (Falcon) was seeded with  $7.5 \times 10^4$  cells/well containing a round 18mm round coverslip (VWR, 1.0 refractive index). Cells were allowed to grow to approximately 60% confluency before pre-treatment with 10 µM caspase-8 inhibitor II (Z-IE(OMe)TD(OMe)-FMK/Granzyme B Inhibitor III, EMD Millipore), 10 µM caspase-9 inhibitor II (LEHD-CHO, EMD Millipore), or 50 µM etoposide treatment with various PCV preparations including controls. At 24 hours post-exposure supernatants were removed, and cells were fixed using 4% formaldehyde for 30 min at RT. After formaldehyde was removed, cells were permeabilized for 3 minutes at 4°C using 0.1% Triton X-100 (Sigma) in 0.1% sodium citrate. Each well was then prepared for TUNEL assay using the Roche *in situ* Cell Death Detection Kit with TMR red according to the manufacturer's protocols. Coverslips were then mounted to microscope

slides using ProLong™ diamond antifade mountant (Invitrogen) and visualized using a Zeiss LSM 780 confocal microscope. Danielle Grant assisted in using and taking images with the confocal microscope. Images were analyzed for TUNEL positive cells using ImageJ software version 1.51. (Figure 2.9, 2.10).

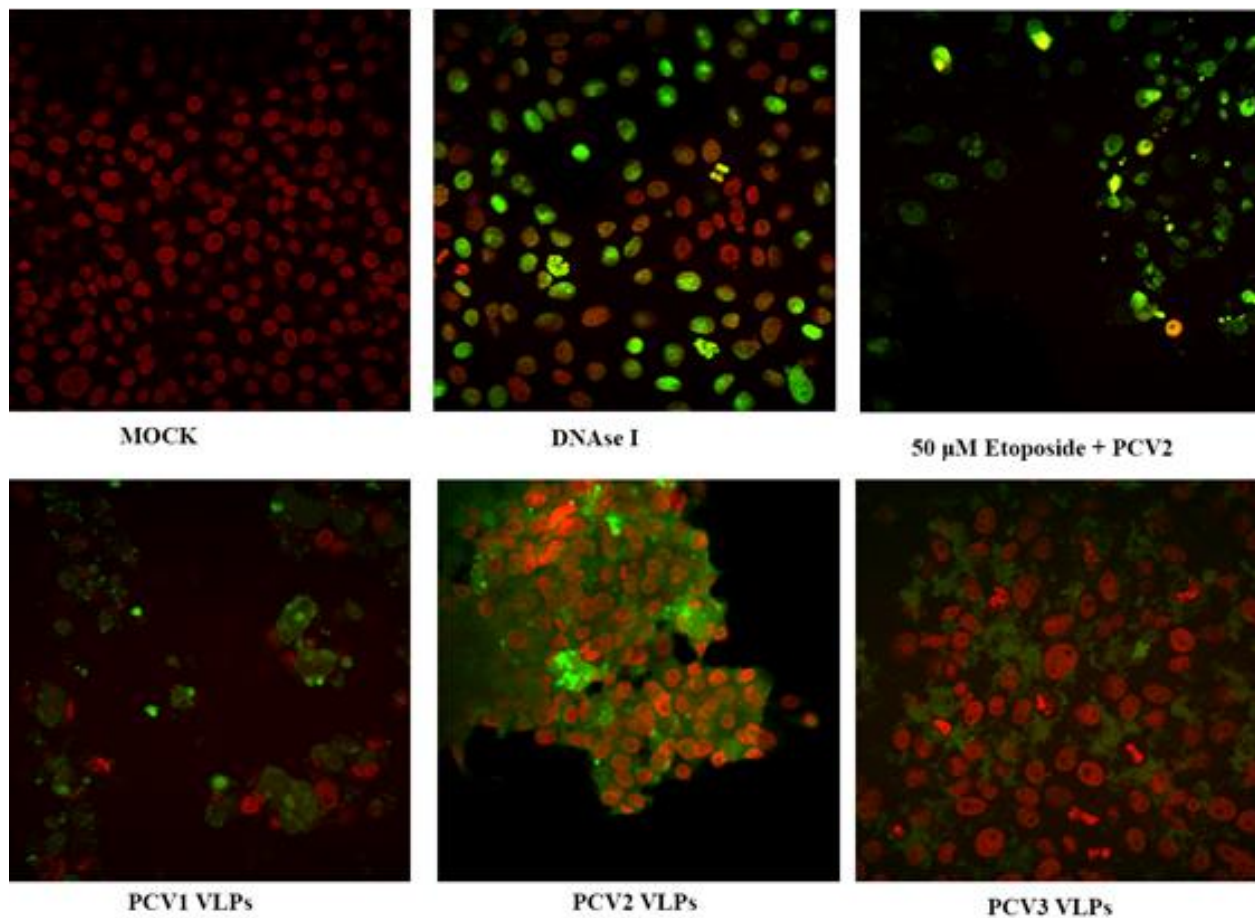


**Figure 2.9** Example of TUNEL assay images as captured from a Zeiss 780 confocal microscope. Red staining indicates nuclear staining by Hoechst 33342, and green staining indicates TUNEL positive DNA fragmentation. MOCK treated cells are negative control cells treated with only cell culture media as a mock infection. DNase I treated cells are cells fixed and briefly permeabilized before treatment with DNase I to induce double-stranded breaks as a positive control. 50 µM etoposide + PCV2 was used as an additional positive control. PCV1, PCV2, and PCV3 VLPs are samples from PK15 cells treated with each virus Cap VLP. Experiment was run in duplicate with  $n = 2$  for each sample type.

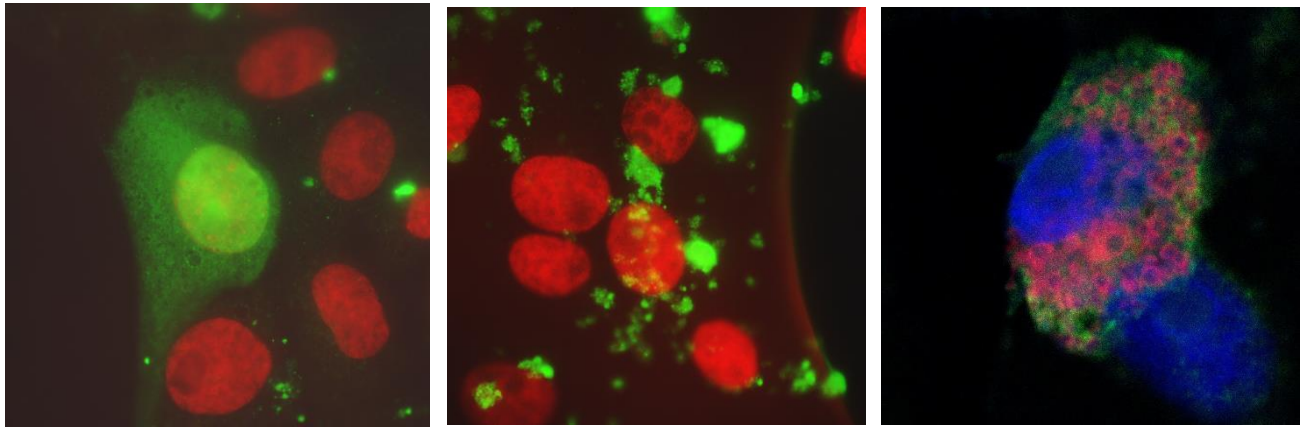


**Figure 2.10** Super-resolution image microscopy (SIM) images of PK15 cells exposed to either infectious PCV2, PCV2 VLPs, or PCV3 VLPs. Left image contains a cell infected with PCV2 with the nuclei in red, and anti-Cap staining in green. Note the presence of PCV2 Cap protein throughout both the cytoplasm and nucleus. Middle image contains PK15 cell nuclei in red and exposed to PCV2 Cap protein in green. Right image contains a PK15 cell nuclei stained in blue, PCV3 Cap protein stained in green and TUNEL positive DNA in red.

## Chapter Three: Results

### 3.1 Porcine Circovirus 2 Cap Protein Recombinantly Expressed in *E. coli* is Cytotoxic to PK15 Cells *in vitro*, Causing Apoptosis

Previous research has shown that recombinant PCV2 capsid protein expressed in PK15 cytoplasm or nuclei was able to induce an apoptotic response<sup>28</sup>. One of the objectives of this research was to examine if recombinant PCV2 capsid protein would be able to induce apoptosis when exposed to PK15 cells extracellularly. To determine this PK15 cells were exposed to approximately 100 µg of recombinant purified PCV2 capsid. Cap induced apoptosis was measured at 24 hours post-exposure through both flow cytometry using an Annexin-V Apoptosis detection kit (Sigma) and TUNEL assay (Roche). PCV2 Cap protein induced apoptosis in PK15 cells by 24 hours post exposure. Exposure to PCV2 Cap protein for 24 hours resulted in an average of 28% of PK15 cells being positive for Annexin V, similar to the 32% average of cells positive when exposed to 50 µM etoposide, a potent inducer of cellular apoptosis through inhibiting the p53 apoptotic pathway. Negative controls exhibited cellular apoptosis in approximately 8-17% of the total cell population (Figures 3.1, 3.2, Table 1.1). Recombinant PCV2 Cap protein significantly increased the level of apoptosis induction as determined by a single-tailed Wilcoxon-Mann-Whitney U test comparing the grouped negative controls against individual sample treatments ( $p < 0.05$ ).

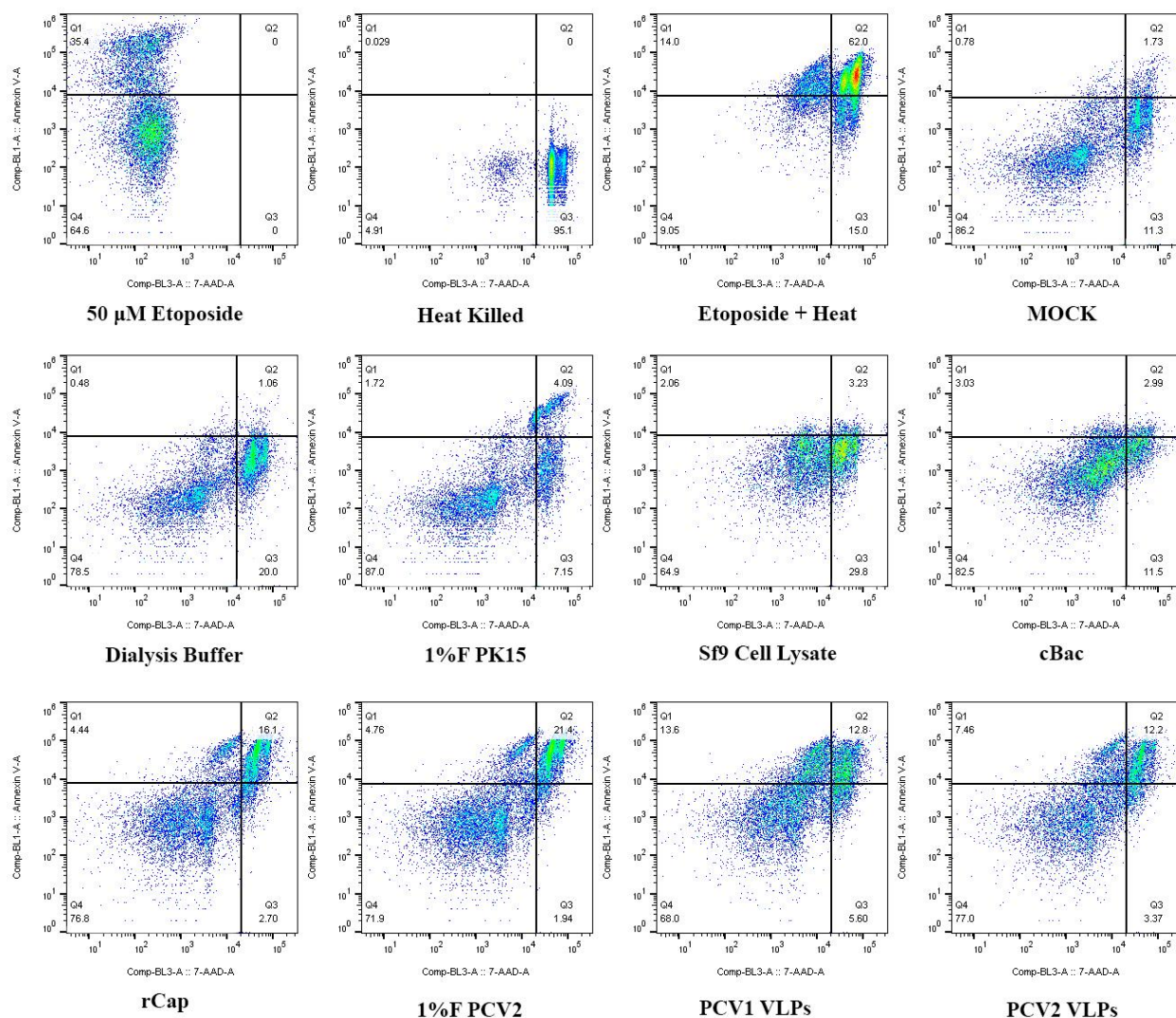


**Figure 3.1** PK15 cells exposed for 24 hours to various PCV preparations and controls were stained with Annexin-V FITC and 7-AAD to detect apoptosis. Pre-apoptotic and apoptotic cells were stained by Annexin-V binding to phosphatidylserine residues found on the outer surface of cell membranes. 7-AAD is a DNA intercalating dye which binds to the DNA of cells with compromised cell membranes indicating cell death. In each of the data plots above Q1 represents cells stained only with Annexin-V FITC, Q2 represents cells stained with both Annexin-V FITC and 7-AAD, Q3 represents cells stained by 7-AAD only, and Q4 represents cells which are unstained and viable. 50  $\mu$ M treatment with etoposide acted as a positive control for apoptosis. Heat killing of cells at 60°C for ten minutes acted as a positive control for dead/dying cells. MOCK treated cells were given only media. Dialysis buffer treatment was included to account for any potential effect from dialysis. 1%F PK15 cells represent PK15 cells treated with 1% formaldehyde, dialyzed to remove excess formaldehyde, and lysed by freeze/thaw to account for possible apoptotic effects caused by dead host cells as found in PCV2 virus preps. Sf9 cell lysate and cBac were



included to account for any possible apoptotic effect possibly induced by the Sf9 insect cells or the baculovirus without a PCV2 insert present. Recombinant PCV2 Cap protein expressed and purified from *E. coli* is represented by the rCap graph. 1%F PCV2 represent stock PCV2 virus inactivated by 1% formaldehyde and dialyzed. PCV1 and PCV2 VLPs were both purified by 37% CsCl gradient ultracentrifugation. All quantifiable protein samples were quantified by a Bio-Rad DC protein assay. Each PK15 cell treatment was treated with 100 µg of each protein sample or with 200 µL of the respective negative control including; media, dialysis buffer, 1% formaldehyde treated PK15 cells, Sf9 cell lysate, or cBac. This raw data is representative of a minimum of two independent experimental replicates for each sample (n ≥ 2).

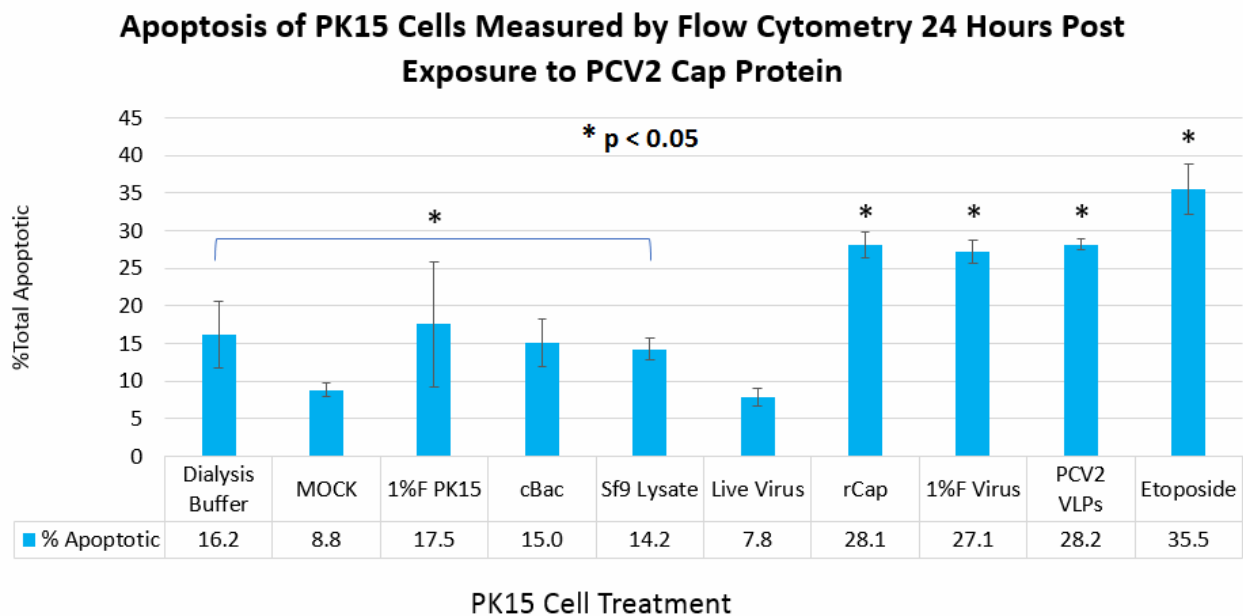


**Figure 3.2** PK15 apoptosis was measured by an Annexin-V FITC apoptosis detection kit to determine the total proportion of pre-apoptotic and apoptotic cells in a population after a 24-hour exposure to PCV2 Cap protein. Negative controls of dialysis buffer, MOCK infection, 1% formaldehyde treated PK15 cell lysate, cBac control baculovirus, and Sf9 insect cell lysate were included to establish a grouped baseline level of apoptosis. PCV2 Cap protein produced and purified from *E. coli* (rCap) induced apoptosis in ~28% of PK15 cells exposed for a duration of 24 hours. Stock PCV2 virus inactivated with 1% formaldehyde induced apoptosis in ~27% of PK15 cells. PCV2 VLPs produced by recombinant baculovirus in Sf9 insect cells and purified by CsCl gradient purification induced apoptosis in ~28% of PK15 cells exposed for 24 hours. Interestingly, live PCV2 virus at a MOI of ~0.1 was unable to induce apoptosis above negative control baseline apoptosis, indicating possible dose-dependence of PCV2 Cap cytotoxicity or effective regulation of cellular apoptosis by live virus gene products. Treatment of PK15 cells with 50 µM etoposide

**induced apoptosis in ~36% of PK15 cells as a positive control. Error bars represent standard error of the mean over a minimum of two independent experimental replicates for each sample ( $n \geq 2$ ). Significance was established using a Wilcoxon-Mann-Whitney U test between the entire negative control group and individual samples with a p value below 0.05 deemed statistically significant ( $p < 0.05$ ). Statistically significant differences are marked by an asterisk\*.**

Recombinant PCV2 Cap protein was shown to cause apoptosis using a TUNEL assay with an average proportion of TUNEL positive cells at ~29% (Fig 3.3). This was similar to the 37% apoptosis seen in the positive control using 50  $\mu$ M etoposide. Apoptosis due to recombinant Cap was higher than observed in the negative controls with the highest proportion of apoptotic cells being 12% in PK15 cells treated with Sf9 cell lysate. This recombinant PCV2 Cap preparation was previously denatured and linearized for purification resulting in a homogenous monomeric Cap protein for the experiment. Induced apoptosis in PK15 cells with linearized PCV2 Cap protein prompted the next question of whether retaining conformational epitopes of the PCV2 Cap protein would cause a similar result.



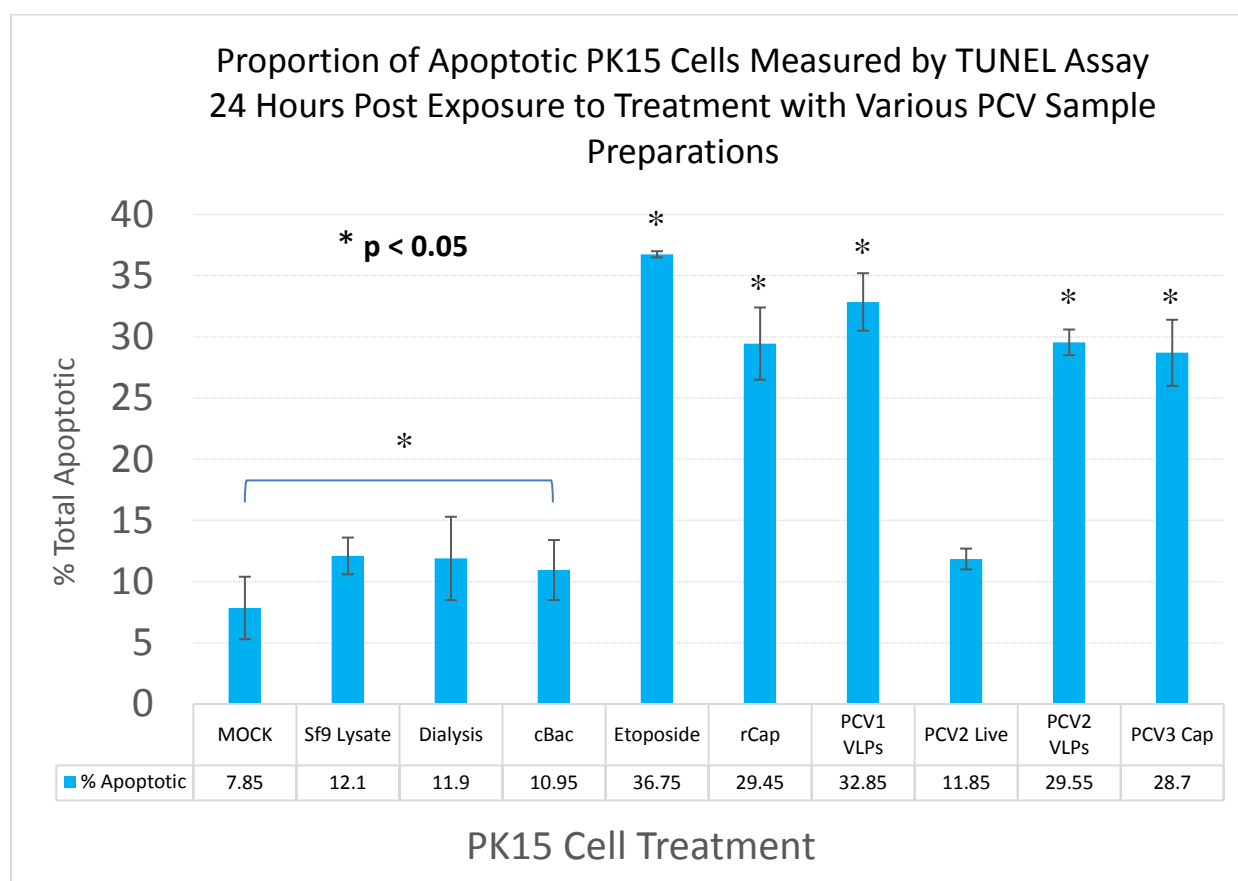


**Figure 3.3 TUNEL assay confirmation of flow cytometry results. Negative controls exhibited apoptosis in 12% or less of the total population when exposed to Sf9 insect cell lysate, dialysis buffer, control baculovirus (cBac) or cell culture media (MOCK). Treatment of PK15 cells with 50  $\mu$ M etoposide resulted in approximately 37% of them being driven into apoptosis. Live PCV2 virus once again did not induce apoptosis above negative control results at only 12%. Recombinant PCV2 Cap (rCap) produced in *E. coli*. induced apoptosis in almost 30% of the PK15 cell population in comparison to the 28% measured by Annexin-V apoptosis detection. PCV1 VLPs were able to drive nearly 33% of PK15 cells into apoptosis, while PCV2 VLPs caused nearly 30% apoptosis and PCV3 Cap protein caused 29% apoptosis. These experiments were repeated twice, with the results being non-significant due to low power and replicate number. Error bars represent standard error of the mean over a minimum of two independent experimental replicates for each sample ( $n \geq 2$ ). Significance was established using a Wilcoxon-Mann-Whitney U test between the entire negative control group and individual samples with a p value below 0.05 deemed statistically significant ( $p < 0.05$ ). Statistically significant differences are marked by an asterisk\*.**

### **3.2 Porcine Circovirus 2 Inactivated with 1% Formaldehyde is Cytotoxic to PK15 Cells *in vitro***

Live and infectious stock PCV2 virus treated with 1% formaldehyde for 48 hours and then dialyzed to remove excess formaldehyde was shown to be non-infectious by means of an immunofluorescence assay (Figure 2.3). Treated virus was shown next to untreated, dialyzed virus to show absence of infection from treated virus after 24 hours. PK15 cells *in vitro* were then exposed to approximately 100 µg of inactivated virus prep for 24 hours and then assessed for cell death via flow cytometry using Annexin V staining. Inactivated stock PCV2 induced cell death in approximately 27% of PK15 cells exposed, similar to the 32% average caused by 50 µM etoposide, and higher than in all negative controls. This result shows that inactivated virus is still capable of significantly inducing an apoptotic response in PK15 cells ( $p < 0.05$ ) (Figure 3.2).

### **3.3 Live PCV2 Virus Does Not Cause Apoptosis of PK15 Cells at Low MOI**

One of the more interesting results of this study suggests that live virus inhibits apoptotic responses in host cells early during infection, at least at a low MOI (0.1). Several replicates of low infectious MOI revealed that PK15 cells exhibited no difference in apoptosis at 24 hours post infection as compared to negative controls. Only 8% of cells in this group showed signs of apoptosis after several replicates. To further confirm this result, additional negative controls were added to try and account for the difference between live virus and inactivated stock virus, because the inactivated virus came from the original stock virus. Dialysis buffer was added as a negative control to ensure that apoptosis was not due to contamination from formaldehyde during the inactivation process. Formaldehyde treated PK15 cell lysate was also included to account for any possible host cell effect on PK15 apoptosis. Despite these controls, live virus was not seen to

activate apoptosis in PK15 cells 24 hours post-infection at a MOI of 0.1, and yet the same amount of inactivated virus was able to induce apoptosis in PK15 cells at nearly 27% at 24 hours post-infection. This data suggests that PCV2 effectively controls host cell processes very quickly after initial infection, or that PCV2 Cap cytotoxicity is dose-dependant. The caveat to this result is that infection of PK15 cells was not confirmed during each individual experimental replicate; although, live PCV2 virus was confirmed to be infectious prior to experimentation via immunofluorescence assay against PCV2 Cap protein (Figure 2.1).

### **3.4 Porcine Circovirus 2 Virus-like Particles are Cytotoxic to PK15 Cells *in vitro***

With the knowledge that PCV2 Cap protein is able to induce apoptosis in PK15 cells both as a monomeric protein and as a conformationally-locked inactive particle, this raised the question of whether virus-like-particles (VLPs) of PCV2 might also be able to induce an apoptotic response in PK15 cells. VLPs consist of only the Cap protein of the virus without the addition of any other proteins or viral genome present and allow for a flexible and more natural interaction with host cells. Conformational epitopes of the virus would be conserved and the VLPs could also change conformation upon interaction with host cellular processes including attachment, entry, and cellular trafficking. PK15 cells were exposed for 24 hours to 100 µg of PCV2 VLPs produced and purified from recombinant baculovirus infection of Sf9 insect cells. VLPs were confirmed through transmission electron microscopy. Flow cytometry analysis revealed that PCV2 VLPs caused 28% of PK15 cells to be apoptotic at 24 hours post exposure, which was significantly higher than all negative controls including a control baculovirus and lysed insect cells (Figure 3.2). This result was additionally confirmed via TUNEL assay, which showed 29% of PK15 cells to be apoptotic after a 24-hour exposure (Figure 3.3). Both PCV1 and PCV2 VLPs were determined to

significantly induce apoptosis versus grouped negative controls in PK15 cells by Wilcoxon-Mann-Whitney U test statistical analysis of the means ( $p < 0.05$ ). This finding further reinforces that PCV2 Cap protein is a potent inducer of cellular apoptosis regardless of linear versus conformational epitopes of Cap protein, but also shows PCV1 Cap protein as an equally potent inducer of apoptosis in PK15 cells.

### **3.5 Porcine Circovirus 1 Virus-like Particles are Cytotoxic to PK15 Cells *in vitro***

The results indicating PCV2 Cap protein as cytotoxic led to the question of whether the Cap proteins of both PCV1 and PCV3 might also exhibit similar cytotoxicity. PCV1 has been determined to be non-pathogenic and the pathogenicity of PCV3 has not been definitively proven yet. VLPs of PCV1 were concurrently generated with PCV2 VLPs and then exposed to PK15 cells for 24 hours as described above for PCV2. PCV1 VLPs were able to cause approximately 32% of PK15 cells to become apoptotic which was significant compared to the MOCK negative control as determined by a Wilcoxon-Mann-Whitney U test ( $p < 0.05$ ) (Figure 3.2, 3.3, 3.4). This result was also comparable to apoptosis induced by 50  $\mu$ M etoposide as a positive control. Past research pointed towards PCV1 having a more potent ORF3 protein than PCV2 causing apoptosis in host cells, with this result also indicating that PCV1 Cap has a similar ability to PCV2 Cap in inducing apoptosis in host cells.

### Apoptosis of PK15 Cells Measured by Flow Cytometry 24 Hours Post Exposure to Treatment with PCV1 & PCV2 VLPs

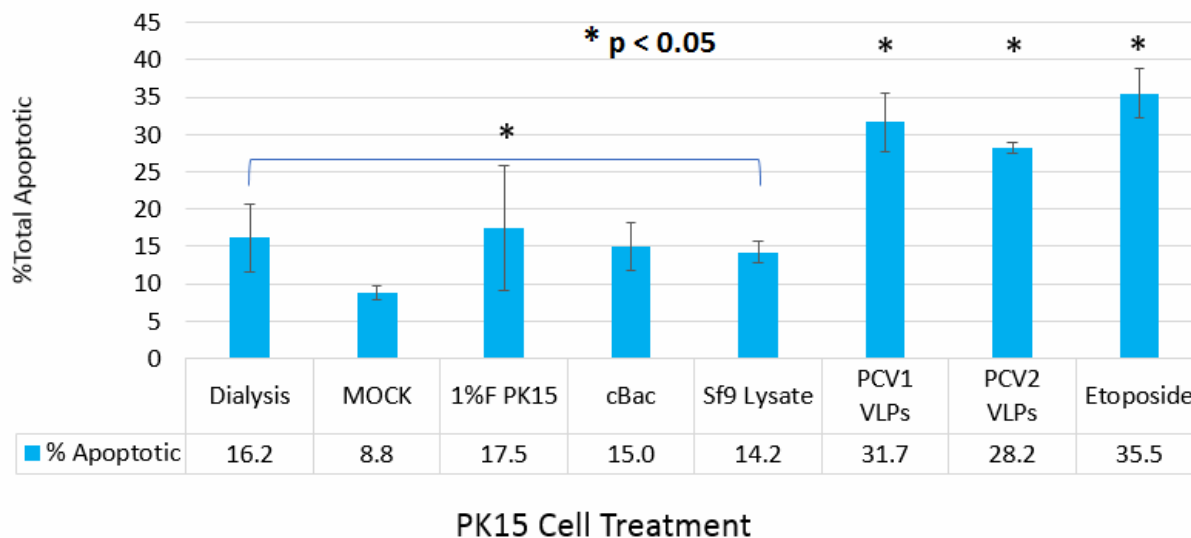


**Figure 3.4** A comparison of VLPs from both PCV1 and PCV2. PCV1 is deemed non-pathogenic and does not cause clinical disease in swine, whereas PCV2 is pathogenic and has been etiologically linked to PCVD causing a broad spectrum of disease manifestations in swine. This experiment indicated that both PCV1 and PCV2 Cap protein is cytotoxic to PK15 cells *in vitro* as measured by Annexin-V FITC staining of cells against negative controls and positive control. Treatment of PK15 cells with 50  $\mu$ M etoposide induced apoptosis in ~36% of PK15 cells as a positive control. PCV1 VLPs induced apoptosis in nearly 32% of the total PK15 population after a period of 24 hours compared to the 28% of cells driven into apoptosis by PCV2 VLPs. Sf9 cell lysate and control baculovirus (cBac) negative controls were treated identically to the PCV1 and PCV2 VLP preparations through sonication and CsCl gradient purification, as well as subsequent dialysis. The results indicate PCV VLPs induce apoptosis in PK15 cells higher than all negative controls and similar to inducement of apoptosis by 50  $\mu$ M etoposide. Error bars represent standard error of the mean over a minimum of two independent experimental replicates for each sample ( $n \geq 2$ ). Significance was established using a Wilcoxon-Mann-Whitney U test between the entire negative control group and individual samples with a p value below 0.05 deemed statistically significant ( $p < 0.05$ ). Statistically significant differences are marked by an asterisk\*.

### 3.6 Porcine Circovirus 3 Virus-like Particles are Cytotoxic to PK15 Cells *in vitro*

Preliminary results suggest that PCV3 Cap protein is cytotoxic to PK15 cells as indicated by TUNEL assay. After two experimental replicates of TUNEL assay, PCV3 Cap protein was able to significantly induce apoptosis in 28% of PK15 cells exposed for 24 hours ( $p < 0.05$ ) (Figure 3.3, 3.5). In comparison, negative controls as a group were only observed to undergo 12% or less apoptosis in the total cell population. These differences were deemed to be significant a one-tailed Wilcoxon-Mann-Whitney U test statistical analysis of the means ( $p < 0.05$ ). These initial results indicate a significant increase of approximately 16% in cellular apoptosis due to the presence of PCV3 Cap protein; although, these results should be interpreted with caution as only two-independent experimental replicates were carried out leading to lower statistical power.

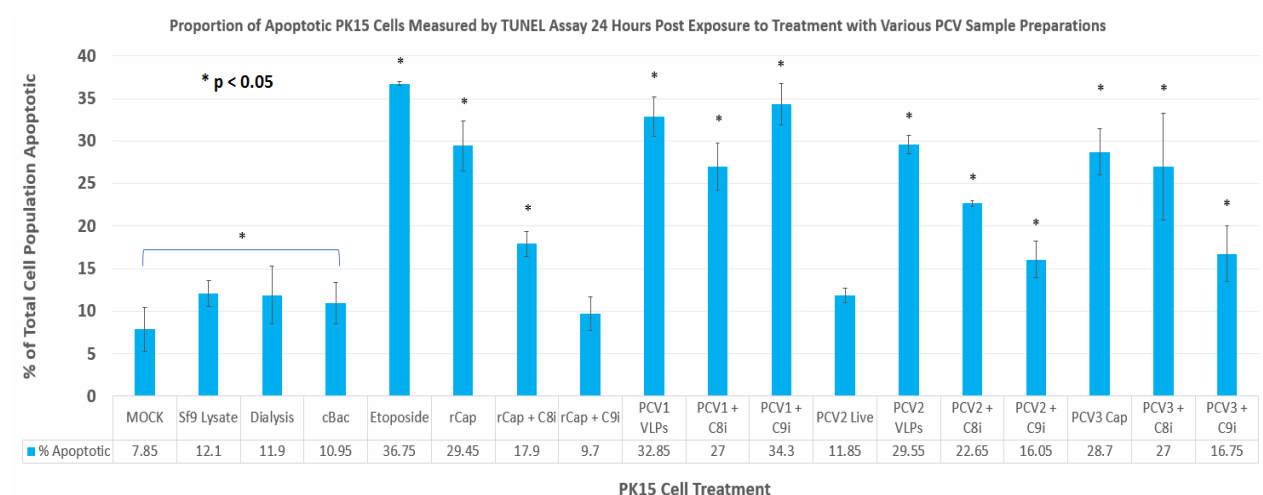


**Figure 3.5** TUNEL assay overview graph showing apoptosis of all samples of PK15 cells exposed to various PCV sample preparations with or without caspase-8 and caspase-9 inhibitors. Pre-treatment of PK15 cells for 1 hour with caspase-8 inhibitor II (Z-IE(OMe)TD(OMe), C8i) or caspase-9 inhibitor II (LEHD-CHO, C9i), led to some decreases in apoptosis observed with PK15 cells treated with PCV2 Cap-containing samples. Apoptosis induced by recombinant PCV2 Cap decreased almost 12% when pre-treated with caspase-8 inhibitor II and decreased by 20% when pre-treated with caspase-9 inhibitor II. Apoptosis induced by PCV2 VLPs decreased by 7% when pre-treated with caspase-8 inhibitor II and decreased 14% when pre-treated with caspase-9 inhibitor II. Apoptosis of PK15 cells induced

by PCV1 VLPs decreased by approximately 5% when treated with caspase-8 inhibitor II, but slightly increased by nearly 2% when pre-treated with caspase-9 inhibitor II. Apoptosis induced in PK15 by PCV3 Cap protein reached 29%, whereas pre-treatment with caspase-8 inhibitor II resulted in wide variation but an overall slight decrease by almost 2%. Pre-treatment with caspase-9 inhibitor resulted in a 12% decrease in apoptosis observed in PK15 cells exposed to PCV3 Cap protein. Error bars represent standard error of the mean over two independent experimental replicates for each sample ( $n = 2$ ). Significance was established using a Wilcoxon-Mann-Whitney U single-tailed test between the entire negative control group and individual samples with a  $p$  value below 0.05 deemed statistically significant ( $p < 0.05$ ). Statistically significant differences are marked by an asterisk\*.

### **3.7 PK15 Cell Apoptosis Caused by Porcine Circovirus 2 Cap is Reduced by Pre-treatment with Caspase-8 Inhibitor**

There are numerous cellular pathways which lead to activation of the apoptosis cascade with several pathways leading through the bottleneck of caspase-8 activation from extrinsically activated receptors including TNF- $\alpha$ , TRAIL-R, and FasR. To narrow down the apoptotic pathways activated by PCV2 Cap protein PK15 cells were pre-treated for 1 hour with 10  $\mu$ M caspase-8 inhibitor II (Z-IE(OMe)TD(OMe)-FMK/Granzyme B Inhibitor III, EMD Millipore) before exposure to Cap protein for 24 hours. PK15 cells were then analyzed by flow cytometry with Annexin-V staining for apoptotic cells and also with a TUNEL assay. Pre-treatment with caspase-8 inhibitor led to a 7% average decrease in apoptotic cells which was still considered to be statistically significant compared to the negative control group according to a single-tail Wilcoxon-Mann-Whitney U test ( $p < 0.05$ ) (Figures 3.3, 3.6, 3.7). Interpreting this result leads to the conclusion that caspase-8 mediated apoptosis is not the only apoptotic pathway used by PCV2 to induce apoptosis in PK15 cells.

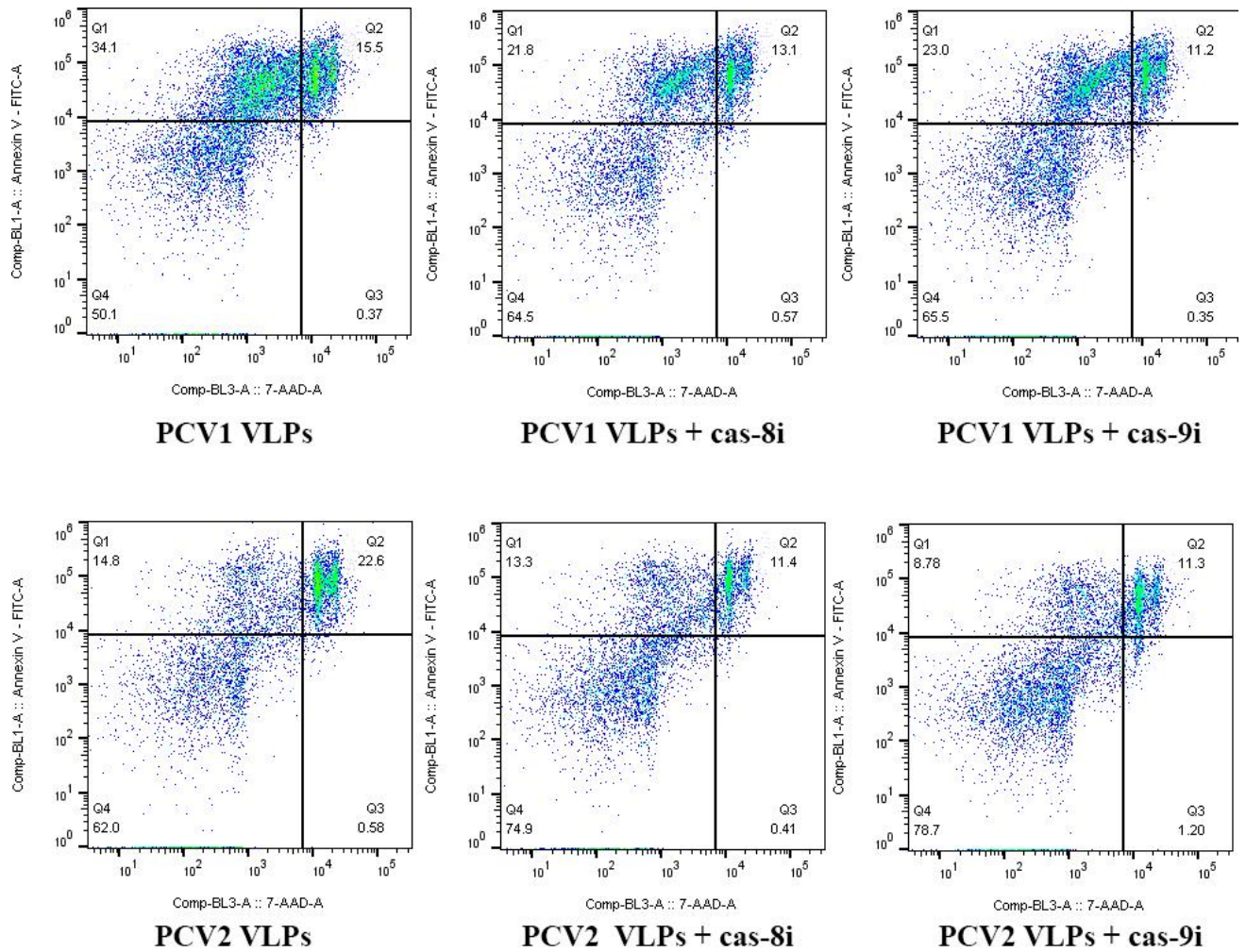


**Figure 3.6** Raw flow cytometry data showing the effect of caspase-8 and caspase-9 inhibitors on the apoptotic effect observed by interaction of PCV1 and PCV2 VLPs with PK15 cells. PK15 cells were pre-treated for one hour before exposure to PCV VLPs for 24 hours. This raw data is representative of a minimum of two independent experimental replicates using caspase inhibitors ( $n \geq 2$ ).



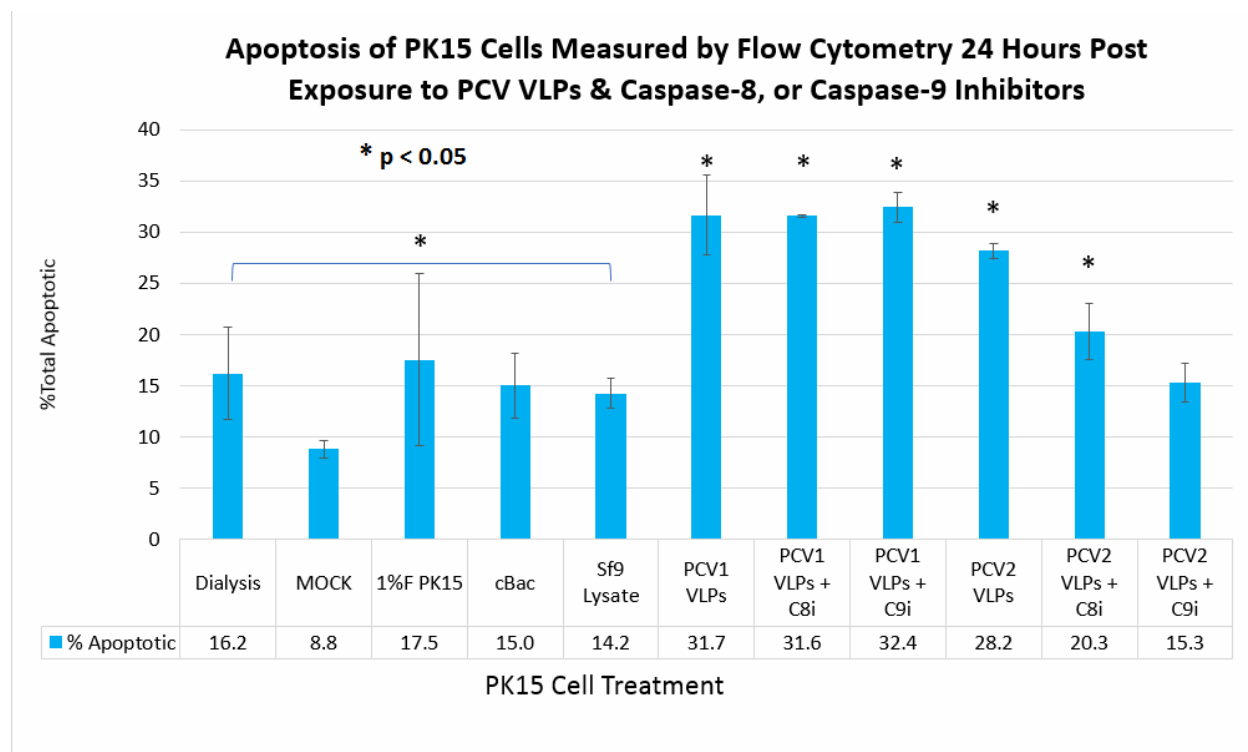


**Figure 3.7** PK15 cells were pre-treated with caspase-8 inhibitor II (Z-IE(OMe)TD(OMe)), or caspase-9 inhibitor II (LEHD-CHO), prior to treatment with negative controls or PCV VLPs to attempt to identify key apoptotic pathways. PCV1 VLP induced apoptosis was not affected by either inhibitor, whereas PCV2 VLP induced apoptosis was reduced by 8% with caspase-8 inhibitor II and 13% by caspase-9 inhibitor II. This result indicates that PCV1 and PCV2 activate apoptosis in PK15 cells by different mechanisms. Error bars represent standard error of the mean over a minimum of two independent experimental replicates for each sample ( $n \geq 2$ ). Significance was established using a Wilcoxon-Mann-Whitney U test between the entire negative control group and individual samples with a p value below 0.05 deemed statistically significant ( $p < 0.05$ ). Statistically significant differences are marked by an asterisk\*.

### 3.8 PK15 Cell Apoptosis Caused by Porcine Circovirus 2 Cap and Porcine Circovirus 3 Cap is Reduced by Treatment with Caspase-9 Inhibitor

The other major apoptotic pathway bottleneck is through caspase-9, which is activated by intrinsic cellular mechanisms. To test whether PCV2 Cap activates apoptosis mediated through caspase 9, PK15 cells were pre-treated for 1 hour with 10  $\mu$ M caspase-9 inhibitor II (LEHD-CHO,

EMD Millipore) before exposure to 100 µg of PCV2 VLPs for 24 hours. Flow cytometry analysis indicated a ~13% reduction of total apoptotic cells. However, of interesting note when both the caspase-8 and caspase-9 inhibitory effects are added together the total reduction in total apoptosis observed drops to negative control levels, indicating that both pathways are activated and critical to apoptosis driven by PCV2 Cap protein (Figures 3.5, 3.7). Caspase-8 and caspase-9 inhibitors were not tested together in a single sample.

PK15 cells pre-treated for 1 hour with 10 µM caspase-9 inhibitor II (LEHD-CHO, EMD Millipore) before exposure to 100 µg of PCV3 Cap for 24 hours also showed a reduction in apoptosis induction by approximately 11% using a TUNEL assay. This reduction in apoptotic cells was shown to be not significantly different from the negative controls as shown by a single-tailed Wilcoxon-Mann-Whitney U test indicating a major role for caspase-9 in the activation of apoptosis caused by PCV3 Cap protein (Figure 3.5, 3.7).

### **3.9 Statistical Analysis**

A minimum of two experimental replicates ( $n \geq 2$ ) was performed for each flow cytometric and TUNEL sample acquired. Data was considered non-parametric due to the low replicate number resulting in low statistical power for subsequent analysis. Kruskal-Wallis statistical analysis was performed on all independent samples followed by Dunn's post hoc test analysis to assess the significance of differences observed between individual apoptosis sample results. Grouping of negative controls analyzed against individual treatment samples were performed using a single-tailed Wilcoxon-Mann-Whitney U test to detect statistically significant increases in apoptosis. A p value of  $< 0.05$  was deemed significant. Analysis was performed using R software (V 3.6.0).

**Table 1.1 Table overview summary of flow cytometric and TUNEL assay results.** Live PCV2 Virus is unmodified stock virus exposed to cells at a MOI of 0.1. MOCK Infection samples were PK15 cells treated with only cell culture media and no additional treatments. Dialysis Buffer samples were collected after the last round of dialysis after formaldehyde treatments of stock virus and lysed PK15 cells. 1%F PK15 sample are cells lysed, treated with 1% formaldehyde, and then dialyzed to remove excess formaldehyde. The cBac sample is baculovirus containing a GUS insert and used as a wild-type control. Etoposide is a potent inducer of mammalian cell apoptosis at a final concentration of 50  $\mu$ M. 1%F PCV2 virus is 1% formaldehyde treated live virus post-dialysis. PCV VLPs represent virus-like-particles of each respective virus. C8i and C9i represent caspase-8 inhibitor II (Z-IE(OMe)TD(OMe)-FMK) and caspase-9 inhibitor II (LEHD-CHO), respectively. Recombinant and purified monomeric PCV2 cap is represented by rCap.

<b>Flow Cytometry Dataset</b>			
<b>Sample</b>	<b>% Apoptotic (Mean)</b>	<b>Sample</b>	<b>% Apoptotic (Mean)</b>
Live PCV2 Virus	7.8	PCV1 VLPs	31.7
MOCK Infection (-C)	8.8	PCV1 VLPs + C8i	31.6
Dialysis Buffer (-C)	12.8	PCV1 VLPs + C9i	32.4
1%F PK15 (-C)	14.2	PCV2 VLPs	28.2
Sf9 Lysate (-C)	14.2	PCV2 VLPs + C8i	20.3
cBac (-C)	15.0	PCV2 VLPs + C9i	15.3
Etoposide (+C)	35.5	rCap	28.1
1%F PCV2 Virus	27.1	rCap + C8i	27.5
		rCap + C9i	28.6
<b>TUNEL Assay Dataset</b>			
Live PCV2 Virus	11.9	PCV1 VLPs	32.9
MOCK Infection (-C)	7.9	PCV1 VLPs + C8i	27
Dialysis Buffer (-C)	11.9	PCV1 VLPs + C9i	34.3
Sf9 Lysate (-C)	12.1	PCV2 VLPs	29.6
cBac (-C)	11.0	PCV2 VLPs + C8i	22.7
Etoposide (+C)	36.7	PCV2 VLPs + C9i	16.1
PCV3 Cap	28.7	rCap	29.5
PCV3 + C8i	27	rCap + C8i	17.9
PCV3 + C9i	16.8	rCap + C9i	9.7

## Chapter Four: **DISCUSSION**

### **4.1 PCV2 Effectively Regulates Host Cell Processes to Control Host Apoptosis and PCV2 Cap is a Major Cytotoxic Mediator**

For any virus to successfully infect and productively replicate within a host cell, it must become an efficient regulator of host cellular processes. This includes successfully evading the initial host cell innate immune response. The virus must also prevent the cell from undergoing apoptosis at least before the completion of a replication cycle, and then must find a way to exit the host cell to infect subsequent cells. Despite being one of the tiniest autonomously replicating mammalian viruses known at 17 nm diameter with a 1.7 kb genome, PCV2 accomplishes all the above host-pathogen interactions in order to successfully replicate and transmit itself to other hosts. In doing so, PCV2 causes PCVD consisting of immunosuppression via lymphocyte depletion and wasting of infected animals in addition to the plethora of other clinical signs of disease in conjunction with other infectious pathogens of swine<sup>99</sup>. Thus, PCV2 represents a prime example of the virology concept of genomic economy in that within its 1.7 kb genome it must encode factors for cellular attachment and entry, host immune evasion, replication, cell cycle modification, virion production/encapsidation, and cellular death signalling.

The PCV2 Cap protein from ORF2 is the only structural protein of the virus and has been shown to be cytotoxic after intracellular expression and in the absence of the apoptotic ORF3 gene<sup>28,29</sup>. This study was undertaken to ask how the cytotoxicity of the PCV2 Cap protein by itself with no other viral components present may be responsible for the proportion of cell death observed during infections both *in vitro* and *in vivo*. Previous studies have shown how either knocking out 9 nucleotides<sup>92</sup>, or two amino acids within the Cap protein itself could abrogate the virulence of the virus<sup>90</sup>, supporting the critical role of Cap protein in causing disease.

The first question asked in this study was whether recombinantly expressed monomeric PCV2 Cap protein produced in *E. coli* could drive swine PK15 cells into apoptosis when externally exposed to a linearized/denatured form of the protein. Observations of PK15 cells after exposure for 24 hours to recombinant Cap showed a marked increase in apoptosis compared to negative controls, indicating that Cap protein by itself is indeed cytotoxic to swine cells, driving nearly 30% of them into apoptosis after only 24 hours. This result indicates that monomeric and denatured PCV2 Cap protein is cytotoxic and does not require a conformational motif in order to activate mitochondrial apoptosis.

Similar apoptotic results were observed when PK15 cells were exposed to formaldehyde inactivated PCV2 virus, where the virus particles were cross-linked by formaldehyde to prevent any conformational changes to the viral capsid but could still interact with host cells. After a 24-hour exposure to inactivated virus, nearly 30% of PK15 cells were driven into apoptosis. This indicates that the cytotoxic motif present on PCV Cap is present and still active despite being conformationally locked by formaldehyde.

To further prove the point, VLPs of PCV2 were produced to mimic infectious virions with no additional genome or gene products present using a recombinant baculovirus expression system. This system was chosen to ensure eukaryotic post-translational modification and conformational epitopes of the PCV2 Cap protein as opposed to the prokaryotic post-translational modifications and linear epitopes when producing PCV2 Cap in *E. coli*. Once again, exposure of PCV2 VLPs to PK15 cells for 24-hours resulted in nearly 30% of the cellular population to exhibit characteristics of apoptosis through the presence of either phosphatidylserine (PS) residues or double stranded DNA breakage as indicated by Annexin-V staining or TUNEL assay respectively.

In conclusion, PCV2 Cap is cytotoxic and initiates apoptosis in the absence of infection regardless of its amino acid structure other than the primary sequence itself.

#### **4.2 PCV2 Cap Driven Apoptosis is Linked to Caspase-8 and Caspase-9 Dependant Pathways**

Other research into PCV2-induced apoptosis of PK15 cells have shown that PCV2 causes apoptosis through caspase-3 and caspase-9 dependant pathways<sup>29,96,100</sup>. Additionally, upregulation of several cytokines and cell-death signalling receptors have been reported in the literature<sup>83-85,101,102</sup>. Pre-treating PK15 cells with caspase-8 inhibitor II (Z-IE(OMe)TD(OMe)) or the caspase-9 inhibitor II (LEHD-CHO) led to the result that PCV1-driven apoptosis is not regulated through the caspase-8 or caspase-9 mediated apoptotic pathways, but that PCV2-driven apoptosis is regulated through these two pathways. This is indicative of PCV2 having evolved different mechanism(s) of apoptosis in order to infect and successfully replicate within host cells. PCV1 Cap and PCV2 Cap share 68% nucleotide sequence identity and 67% amino acid sequence identity. PCV2 Cap protein was also recently implicated in dysregulating cytoplasmic  $\text{Ca}^{2+}$  and ROS production leading to apoptosis via the PERK-pathway including caspase-3 and caspase-9<sup>29</sup>. This pathway is indicative of ER-stress leading to the unfolded-protein response (UPR) of the host cell which leads to mitochondrial outer membrane permeabilization (MOMP) and subsequent apoptosis<sup>103</sup>. What this could also potentially mean is that cells exposed to PCV2 Cap upregulate cell-death receptors such as Fas, TNF-R, or TRAIL-R, which then cause these cells that are non-infected to be targeted and cleared by the host immune response. In the absence of host lymphocytes, activation of caspase-9 dependant apoptosis would still drive cell death as observed *in vitro*.

#### **4.3 Preliminary Results Indicate PCV1 and 3 Cap are also Cytotoxic**

PCV2 has been etiologically associated with PCVD since it was described in 1997 by Harding and Clark and dating back to observed clinical signs in swine farms in Western Canada<sup>44–46</sup>. The most major hallmark of PCV2 infection is the depletion of lymphoid cells causing lymphopenia and immunosuppression of infected animals, allowing for the variety of secondary co-infections and disease manifestations seen with PCVD. The overall aim of this work was to further tease out the molecular mechanism of virulence that PCV2 uses to accomplish immunosuppression, especially since it is so similar to the non-pathogenic PCV1 virus. PCV1 was discovered as a contaminant in a cell line<sup>24</sup>, and was subsequently identified in swine herds, but to no detriment or association with disease; PCV1 was deemed non-pathogenic and of no concern. Additionally, research has begun to determine the pathogenicity of PCV3 with the appearance of this novel virus panzootically spreading worldwide and its association with clinical syndromes<sup>20,75,78</sup>.

Previous research led to the understanding that PCV1 possessed an ORF3 protein which was more potently apoptotic than the ORF3 protein of PCV2<sup>30</sup>. In this study, PCV1 Cap protein was similarly apoptotic compared to PCV2 Cap protein, driving nearly 30% of PK15 cells into apoptosis within a 24-hour time period. The discovery that PCV1 Cap was also clearly cytotoxic was surprising and means that the mechanism which drives the cytotoxicity of both viruses must be regulated differently by the host immune response in order to cause such a clear distinction in pathogenicity between the two viruses. One possibility is that PCV1 induces greater inflammation during initial infection which leads to a more robust initial immune response which is subsequently cleared by the immune system and leads to an effective memory response. Another suggestion is that because PCV2 upregulates the expression of immunosuppressive cytokine IL-10, the swine

immune system *in vivo* is unable to properly respond to infection with PCV2 in a way that successfully clears the virus.

Preliminary results of this study also indicate that PCV3 cap protein is also cytotoxic and drives PK15 cells into apoptosis and that this effect may also be at least partially mediated by caspase-9 activation. Under these experimental conditions, PCV3 Cap protein was able to cause apoptosis in ~29% of cells within a 24-hour period via TUNEL assay. As the pathogenicity of PCV3 has yet to be definitively determined, the cytotoxicity seen by PCV3 Cap may be indicative of enough virulence to cause similar PCVD to that seen in PCV2 clinical syndromes such as PDNS or PCV2 reproductive disease (PCV2-RD).

#### ***4.3.1 PCV1 Activates Apoptosis Through a Caspase-Independent Mechanism***

It is still unclear as to why PCV1 is non-pathogenic as compared to the closely related PCV2. The results of this study point to PCV1 Cap being similarly apoptotic to PCV2 Cap, yet through a caspase-independent mechanism, rather than the caspase-dependant mechanism of PK15 cell apoptosis observed when exposed to PCV2 Cap. Since the Annexin-V FITC and TUNEL assays were both able to detect apoptosis of PK15 cells by PCV1 Cap within 24 hours, this suggests alternative apoptotic pathways potentially activated by cathepsins, calpains, AIF, granzyme A, or endonuclease G mediated mechanisms of caspase-independent apoptosis. There are numerous ways for this to occur, but taken together with the following subsection involving mitochondrial localization of PCV Cap proteins it is reasonable to assume that caspase-independent apoptosis is the result of loss of mitochondrial function<sup>104</sup>.



#### **4.4 PCV1, PCV2, and PCV3 Capsid Proteins all Contain Mitochondrial Localization Sequences**

A key question of this study was to discover what host cellular mechanisms porcine circoviruses utilize to activate apoptosis. PCV2 activates apoptosis in host cells to cause immunosuppression, which supports past indications that PCV2 Cap protein activates apoptosis through both extrinsic and intrinsically activated, caspase-dependant mechanisms of apoptosis<sup>28,105</sup>. What is novel to this study is that three separate preparations of PCV2 Cap protein were used to check for the possible contributions of linear vs. conformational epitopes to apoptosis. Other studies have used virus-knock out clones or lentiviral expressed proteins to produce PCV2 Cap protein, whereas this study utilized three different methods of isolating PCV2 Cap protein. Recombinant denatured and therefore linearized Cap protein; 1% formaldehyde inactivated virus; and virus-like particles of PCV2 Cap all produced similar apoptosis of PK15 cells within a 24-hour time period indicating that the epitopes required to induce apoptosis are active regardless of Cap amino acid sequence tertiary structure. Of interesting note, by running all three full-length Cap proteins from PCV1, PCV2, and PCV3 through the MitoProt mitochondrial localization sequence (MLS) prediction software, the N-terminal region of all three Cap proteins have a 99-100% predicted MLS sequence in addition to a nuclear localization sequence<sup>106,107</sup> (Figure 4.1). This finding corresponds to previous studies describing the association of PCV2 virus particles/inclusion bodies with the mitochondria of infected swine cells<sup>108</sup>. Also, the confocal images of this study each show the localization of VLP's to the perinuclear region of each cell nuclei which was also shown by another study to be associated with the mitochondria<sup>108</sup>. Therefore, each virus localizes to the mitochondria at an early point during infection, and initiates apoptosis through either caspase-dependant or caspase-independent mechanisms leading to cell

death. Yet PCV1 does not cause clinical disease in infected pigs, while PCV2 causes disease via immunosuppression. The altered cytokine profiles observed in PCVD indicate PCV2 is able to cause host immunosuppression via upregulation of IL-10<sup>84</sup>, Fas/FasL<sup>89</sup>, TNF- $\alpha$ <sup>109,110</sup>, and down-regulation of suppressor of cytokine signalling molecule 3(SOCS)<sup>111</sup>. It is unknown if PCV1 or PCV3 causes any of the same changes in host cytokine signalling. Since PCV2 Cap induces activation of both caspase-8 and caspase-9, Cap must initiate both extrinsic and intrinsic pathways of apoptosis in contrast with PCV1 and PCV3. PCV1 and PCV3 activated apoptosis was not observed to be diminished through the caspase-8 dependant pathways indicating that both viruses are unable to activate apoptosis through extrinsic pathways. PCV3 activated apoptosis was reduced using caspase-9 inhibitors indicating the involvement of the intrinsic caspase-9 dependant apoptosis activation pathway. This critical difference in apoptosis activation pathways could be an explanation for the difference in pathogenicity observed between all three viruses, with PCV1 being non-pathogenic, PCV3 being associated with clinical syndromes in the field, but neither virus appears to exhibit the level of virulence and immunosuppression observed with PCV2 infections.

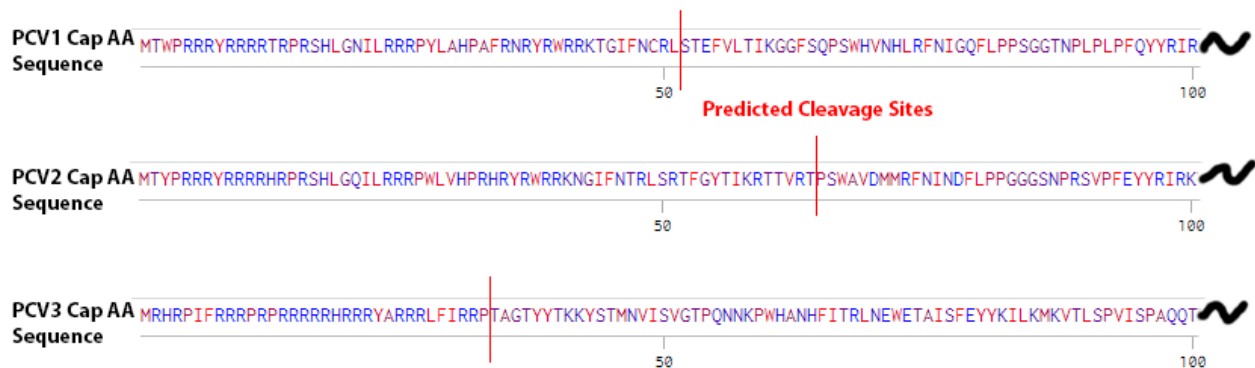


**Figure 4.1** Diagram showing the expected cleavage sites of each PCV Cap amino acid sequence showing 99-100% predicted mitochondrial localization sequences (MLS). Sequences are written conventionally with the N-terminus on the left and the C-terminus to

the right of the cut-off point past 100 amino acids. Sequences were predicted by MitoProt prediction software at the following URL: <https://ihg.gsf.de/ihg/mitoprot.html>

#### **4.5 Live PCV2 Virus at a low MOI Does Not Cause Apoptosis in PK15 Cells**

Another result of this study which was somewhat surprising was that live PCV2 virus at a low MOI of 0.1, did not produce any change in the proportion of apoptotic cells as compared to the negative controls. This is interesting because the 1% formaldehyde inactivated PCV2 virus preparation was made from the same stock virus and PK15 cells were treated with similar volumes of either live virus or inactivated virus. The result clearly showed that 1% formaldehyde inactivated virus was still able to drive nearly 30% of cells into apoptosis, but the live virus did not. Subsequent experiments included dialysis buffer to control for the possible presence of remaining formaldehyde, yet the dialysis negative control also showed a negligible apoptotic response. This brings up two key possibilities. The first obvious question would be what the infectious particle to particle ratio of PCV2 would be in a given infection as a productive infection would produce a certain proportion of infectious versus replication defective progeny virions. If a majority of particles in a given viral prep are infectious and yet only 5-10% of cells are infected regardless of MOI, perhaps a large proportion of infectious virions are localized to the host-cell mitochondria rather than the nucleus which is required for productive infection/replication. This effect would then be dose-dependant depending on the amount of Cap protein produced during a productive infection. The second major point is that the ORF4 protein of PCV2 has been described as being anti-apoptotic by several researchers<sup>31,32,100</sup>, and could play a key role in determining the balance of apoptotic vs. anti-apoptotic signals produced in the cell during a full replication cycle. Once the virus has produced a higher proportion of Cap protein to ORF4 protein, the cell is finally driven into cell death for release of the viral progeny. Another possibility is that PK15 cells do not

respond to apoptotic signals the same way as lymphocytes because previous research carried out on activated PBMCs showed apoptosis in ~30% of these cell populations, but specifically in activated cells while another study showed enhanced bystander cell death in PK15 cells only after treatment with IFN- $\gamma$ . These results suggest that the PCV2 Cap protein is most likely the main cause of apoptosis in non-infected bystander cells leading to the clinical signs of wasting and immunosuppression observed in PCV2 infected swine. This could be either through direct interaction with cellular apoptotic pathways or possibly through upregulation of extrinsic apoptotic pathway receptors and secretion of cellular death signals. During an infection, PCV Cap is produced at high enough levels to produce intracellular inclusion bodies, and thus upon cell death Cap protein could be released from dying/lytic cells which could then interact with bystander cells and cause additional apoptosis without directly infecting neighbouring cells.

#### **4.6 Unanswered Questions and Future Directions**

The exact molecular mechanism(s) of apoptosis caused by PCV remains to be discovered. This study indicates that each virus may activate completely different pathways which could account for the difference in pathogenicity between the viruses while also considering that PCV3 has yet to be definitively linked to clinical disease. Knowing that each virus capsid has a cytotoxic component implies several different ideas. It is reasonable to assume that PCV1 may cause greater inflammation in infected animals leading to an effective immune response which is able to control and clear the virus. In contrast, PCV2 seems to have evolved a way to kill bystander cells and effectively evade the immune response through apoptotic pathways which reduce local inflammation due to infection. This has several implications for subclinical infections observed on farms despite the robust protection conferred by vaccines against PCV2 infection. What has been

consistently shown is that vaccines against PCV2 are effective at preventing clinical signs of disease yet are unable to prevent subclinical infection<sup>67</sup>. One way to test this hypothesis would be to infect multiple cohorts of snatch-farrow or specific-pathogen free (SPF) swine with either PCV1, PCV2, PCV3, or multiple viruses concurrently and including a negative control group to observe the cytokine profiles of the animals in relation to viremia and clinical signs of disease. PCVD is typically not seen in PCV2 infected animals without coinfections; however, the swine immune response to infection from each virus could still be monitored to tease out critical differences including the relative levels of inflammatory cytokines.

A limitation of this study was that it targeted the responses of PK15 cells and no other swine cell lines. PK15 cells are immortalized with an SV40 T antigen which has effects on cellular apoptosis that could create different results in primary cell lines or *in vivo*. Previous work showed a similar bystander death effect in PBMCs (Solis-Worsfold & Waekerlin, personal communication), as well as PK15 cells activated by IFN- $\gamma$  when PCV2 Cap was transiently expressed using a lentiviral vector<sup>28</sup>. Experiments done *in vitro* are inherently limited for ease of experimental protocols but may not be indicative of the complexity of the infection/disease progression *in vivo*. The above experiments could be carried out further using other swine cell lines such VR1BL or perhaps primary hepatocyte cells could prove the point. With enough resources, *in vivo* experiments could be undertaken to see if PCV VLPs could have detrimental effects on primary cell lines derived *ex vivo* or directly from exposing pigs to VLPs and determining the immune response of the animals.

Further understanding the role of the mitochondrial localization sequence (MLS) sequence in all three Cap sequences is crucial to understanding the role of the mitochondria during PCV infections. Previous work showed that the removal of the nuclear localization sequence (NLS)

sequence caused apoptosis of transfected cells regardless of location in the nucleus or cytoplasm<sup>28</sup>; however, this study did not take into account the full-length predicted sequence of MLS predicted for each Cap protein individually. Truncation of each Cap protein to remove the MLS sequences and then repeating the above experiments could further shed light on the direct action of Cap protein on mitochondrial destabilization/loss-of-function.

Initial results on PCV3 Cap protein suggest that it is still cytotoxic and may also utilize caspase-9 mediated mechanism of apoptosis. What needs to be further determined is whether PCV3 definitively causes clinical disease. Typically, a pathogen is defined by meeting Koch's postulates<sup>112</sup>, or more modernly molecular Koch's postulates<sup>113</sup>; however, PCV2 and possibly PCV3 seem to also require co-infection for the manifestation of PCVD which makes associating PCV3 with disease somewhat more difficult even though it has been isolated from clinically diseased animals and stillborn piglets in the absence of other known swine pathogens<sup>76</sup>. In order to ascertain the pathogenicity of PCV3, experiments should be carried out in a similar vein to past experiments establishing PCV2 as the etiological agent of PCVD including *in vivo* infection studies with immune stimulants.

## REFERENCES

1. Genus: Circovirus - Circoviridae - ssDNA Viruses - International Committee on Taxonomy of Viruses (ICTV). *International Committee on Taxonomy of Viruses (ICTV)* Available at: [https://talk.ictvonline.org/ictv-reports/ictv\\_online\\_report/ssdna-viruses/w/circoviridae/659/genus-circovirus](https://talk.ictvonline.org/ictv-reports/ictv_online_report/ssdna-viruses/w/circoviridae/659/genus-circovirus). (Accessed: 8th January 2018)
2. Raue, R. *et al.* A disease complex associated with pigeon circovirus infection, young pigeon disease syndrome. *Avian Pathol.* **34**, 418–425 (2005).
3. Zhang, X. *et al.* An investigation of duck circovirus and co-infection in Cherry Valley ducks in Shandong Province, China. *Vet. Microbiol.* **133**, 252–256 (2009).
4. Rampin, T., Manarolla, G., Pisoni, G., Recordati, C. & Sironi, G. Circovirus inclusion bodies in intestinal muscle cells of a canary. *Avian Pathol.* **35**, 277–279 (2006).
5. Twentyman, C. M., Alley, M. R., Meers, J., Cooke, M. M. & Duignan, P. J. Circovirus-like infection in a southern black-backed gull (*Larus dominicanus*). *Avian Pathol.* **28**, 513–516 (1999).
6. Halami, M. Y., Nieper, H., Müller, H. & Johne, R. Detection of a novel circovirus in mute swans (*Cygnus olor*) by using nested broad-spectrum PCR. *Virus Res.* **132**, 208–212 (2008).
7. Stewart, M. E., Perry, R. & Raidal, S. R. Identification of a novel circovirus in Australian ravens (*Corvus coronoides*) with feather disease. *Avian Pathol.* **35**, 86–92 (2006).
8. Rinder, M. *et al.* Molecular characterization of a recently identified circovirus in zebra finches (*Taeniopygia guttata*) associated with immunosuppression and opportunistic infections. *Avian Pathol.* **46**, 106–116 (2017).
9. Abadie, J. *et al.* Pigeon circovirus infection: Pathological observations and suggested pathogenesis. *Avian Pathol.* **30**, 149–158 (2001).

10. Guo, J. *et al.* Pathological observations of an experimental infection of geese with goose circovirus. *Avian Pathol.* **40**, 55–61 (2011).
11. Shivaprasad, H. L., Hill, D., Todd, D. & Smyth, J. A. Circovirus infection in a Gouldian finch (*Chloebia gouldiae*). *Avian Pathol.* **33**, 525–529 (2004).
12. Tarján, Z., Péntzes, J., Tóth, R. & Benkő, M. First detection of circovirus-like sequences in amphibians and novel putative circoviruses in fishes. *Acta Vet. Hung.* **62**, 134–144 (2013).
13. Segalés, J. Porcine circovirus type 2 (PCV2) infections: Clinical signs, pathology and laboratory diagnosis. *Virus Res.* **164**, 10–19 (2012).
14. Zhai, S.-L. *et al.* Comparative epidemiology of porcine circovirus type 3 in pigs with different clinical presentations. *Virol. J.* **14**, (2017).
15. Tochetto, C. *et al.* Full-Genome Sequence of Porcine Circovirus type 3 recovered from serum of sows with stillbirths in Brazil. *Transbound. Emerg. Dis.* n/a-n/a  
doi:10.1111/tbed.12735
16. Collins, P. J., McKillen, J. & Allan, G. Porcine circovirus type 3 in the UK. *Vet. Rec.* **181**, 599–599 (2017).
17. Stadejek, T., Woźniak, A., Miłek, D. & Biernacka, K. First detection of porcine circovirus type 3 on commercial pig farms in Poland. *Transbound. Emerg. Dis.* **64**, 1350–1353 (2017).
18. Faccini, S. *et al.* Detection and genetic characterization of Porcine circovirus type 3 in Italy. *Transbound. Emerg. Dis.* **64**, 1661–1664 (2017).
19. Wen, S. *et al.* The detection of porcine circovirus 3 in Guangxi, China. *Transbound. Emerg. Dis.* n/a-n/a doi:10.1111/tbed.12754
20. Li, X. & Tian, K. Porcine circovirus type 3: a threat to the pig industry? *Vet. Rec.* **181**, 659–660 (2017).



21. Wang, G. *et al.* Genetic analysis of porcine circovirus type 2 from dead minks. *J. Gen. Virol.* **97**, 2316–2322 (2016).
22. Tamura, K. & Nei, M. Estimation of the number of nucleotide substitutions in the control region of mitochondrial DNA in humans and chimpanzees. *Mol. Biol. Evol.* **10**, 512–526 (1993).
23. Kumar, S., Stecher, G., Li, M., Knyaz, C. & Tamura, K. MEGA X: Molecular Evolutionary Genetics Analysis across Computing Platforms. *Mol. Biol. Evol.* **35**, 1547–1549 (2018).
24. Tischer, I., Gelderblom, H., Vettermann, W. & Koch, M. A. A very small porcine virus with circular single-stranded DNA. *Nature* **295**, 64–66 (1982).
25. Mankertz, A. *et al.* Molecular biology of Porcine circovirus: analyses of gene expression and viral replication. *Vet. Microbiol.* **98**, 81–88 (2004).
26. Mankertz, A., Persson, F., Mankertz, J., Blaess, G. & Buhk, H. J. Mapping and characterization of the origin of DNA replication of porcine circovirus. *J. Virol.* **71**, 2562–2566 (1997).
27. Misinzo, G., Delputte, P. L., Meerts, P., Lefebvre, D. J. & Nauwynck, H. J. Porcine circovirus 2 uses heparan sulfate and chondroitin sulfate B glycosaminoglycans as receptors for its attachment to host cells. *J. Virol.* **80**, 3487–3494 (2006).
28. Walia, R., Dardari, R., Chaiyakul, M. & Czub, M. Porcine circovirus-2 capsid protein induces cell death in PK15 cells. *Virology* **468–470**, 126–132 (2014).
29. Zhang, Y. *et al.* Porcine Circovirus Type 2 Induces ORF3-Independent Mitochondrial Apoptosis via PERK Activation and Elevation of Cytosolic Calcium. *J. Virol.* **93**, e01784-18 (2019).

30. Chaiyakul, M., Hsu, K., Dardari, R., Marshall, F. & Czub, M. Cytotoxicity of ORF3 Proteins from a Nonpathogenic and a Pathogenic Porcine Circovirus. *J. Virol.* **84**, 11440–11447 (2010).
31. He, J. *et al.* Identification and Functional Analysis of the Novel ORF4 Protein Encoded by Porcine Circovirus Type 2. *J. Virol.* **87**, 1420–1429 (2013).
32. Lv, Q., Guo, K., Zhang, G. & Zhang, Y. The ORF4 protein of porcine circovirus type 2 antagonizes apoptosis by stabilizing the concentration of ferritin heavy chain through physical interaction. *J. Gen. Virol.* **97**, 1636–1646 (2016).
33. Choi, C.-Y. *et al.* The ORF5 protein of porcine circovirus type 2 enhances viral replication by dampening type I interferon expression in porcine epithelial cells. *Vet. Microbiol.* **226**, 50–58 (2018).
34. Ouyang, Y. *et al.* Porcine circovirus type 2 ORF5 protein induces endoplasmic reticulum stress and unfolded protein response in porcine alveolar macrophages. *Arch. Virol.* **164**, 1323–1334 (2019).
35. Misinzo, G., Delputte, P. L., Lefebvre, D. J. & Nauwynck, H. J. Porcine circovirus 2 infection of epithelial cells is clathrin-, caveolae- and dynamin-independent, actin and Rho-GTPase-mediated, and enhanced by cholesterol depletion. *Virus Res.* **139**, 1–9 (2009).
36. Finsterbusch, T. & Mankertz, A. Porcine circoviruses—Small but powerful. *Virus Res.* **143**, 177–183 (2009).
37. Cheung, A. K. Porcine circovirus: Transcription and DNA replication. *Virus Res.* **164**, 46–53 (2012).

38. Yang, N. *et al.* Change in the immune function of porcine iliac artery endothelial cells infected with porcine circovirus type 2 and its inhibition on monocyte derived dendritic cells maturation. *PLOS ONE* **12**, e0186775 (2017).
39. Kekarainen, T. *et al.* Immune responses and vaccine-induced immunity against Porcine circovirus type 2. *Vet. Immunol. Immunopathol.* **136**, 185–193 (2010).
40. Baylis, S. A., Finsterbusch, T., Bannert, N., Blümel, J. & Mankertz, A. Analysis of porcine circovirus type 1 detected in Rotarix vaccine. *Vaccine* **29**, 690–697 (2011).
41. Allan, G. M. *et al.* Pathogenesis of porcine circovirus; experimental infections of colostrum deprived piglets and examination of pig foetal material. *Vet. Microbiol.* **44**, 49–64 (1995).
42. Steiner, E., Balmelli, C., Herrmann, B., Summerfield, A. & McCullough, K. Porcine circovirus type 2 displays pluripotency in cell targeting. *Virology* **378**, 311–322 (2008).
43. Meehan, B. M. *et al.* Characterization of novel circovirus DNAs associated with wasting syndromes in pigs. *J. Gen. Virol.* **79**, 2171–2179 (1998).
44. Harding, J. C. & Clark, E. G. Recognizing and diagnosing postweaning multisystemic wasting syndrome (PMWS). *J. Swine Health Prod.* **5**, 201–203 (1997).
45. Harding, J. C. S. Postweaning multisystemic wasting syndrome: Epidemiology and clinical presentation. *J. Swine Health Prod.* **6**, 249–254 (1998).
46. Ellis, J. *et al.* Isolation of circovirus from lesions of pigs with postweaning multisystemic wasting syndrome. *Can. Vet. J.* **39**, 44 (1998).
47. Tummaruk, P. & Pearodwong, P. Expression of PCV2 antigen in the ovarian tissues of gilts. *J. Vet. Med. Sci.* **78**, 457–461 (2016).
48. Allan, G. M. *et al.* PMWS: experimental model and co-infections. *Vet. Microbiol.* **98**, 165–168 (2004).

49. Hirai, T., Nunoya, T., Ihara, T., Kusanagi, K. & Shibuya, K. Dual infection with PCV-2 and porcine epidemic diarrhoea virus in neonatal piglets. *Vet. Rec.* **148**, 482–484 (2001).
50. Kixmüller, M. *et al.* Reduction of PMWS-associated clinical signs and co-infections by vaccination against PCV2. *Vaccine* **26**, 3443–3451 (2008).
51. Rodriguez-Arrioja, G. M. *et al.* Aujeszky's disease virus infection concurrent with postweaning multisystemic wasting syndrome in pigs. *Vet. Rec.* **144**, 152–153 (1999).
52. Harms, P. A. *et al.* Experimental Reproduction of Severe Disease in CD/CD Pigs Concurrently Infected with Type 2 Porcine Circovirus and Porcine Reproductive and Respiratory Syndrome Virus. *Vet. Pathol. Online* **38**, 528–539 (2001).
53. Dorr, P. M., Baker, R. B., Almond, G. W., Wayne, S. R. & Gebreyes, W. A. Epidemiologic assessment of porcine circovirus type 2 coinfection with other pathogens in swine. *J. Am. Vet. Med. Assoc.* **230**, 244–250 (2007).
54. Opriessnig, T. & Halbur, P. G. Concurrent infections are important for expression of porcine circovirus associated disease. *Virus Res.* **164**, 20–32 (2012).
55. Burch, D. Ten years of PCV2 in the UK. *Pig Prog.* **25**, 21 (2009).
56. Government of Canada, S. C. The changing face of the Canadian hog industry. (2014). Available at: <http://www.statcan.gc.ca/pub/96-325-x/2014001/article/14027-eng.htm>. (Accessed: 9th January 2018)
57. Ramamoorthy, S. & Meng, X.-J. Porcine circoviruses: a minuscule yet mammoth paradox. *Anim. Health Res. Rev.* **10**, 1–20 (2009).
58. Martelli, P. *et al.* One dose of a porcine circovirus 2 subunit vaccine induces humoral and cell-mediated immunity and protects against porcine circovirus-associated disease under field conditions. *Vet. Microbiol.* **149**, 339–351 (2011).

59. Martelli, P. *et al.* Concurrent vaccinations against PCV2 and PRRSV: Study on the specific immunity and clinical protection in naturally infected pigs. *Vet. Microbiol.* **162**, 558–571 (2013).
60. Pejsak, Z., Podgórska, K., Truszczyński, M., Karbowiak, P. & Stadejek, T. Efficacy of different protocols of vaccination against porcine circovirus type 2 (PCV2) in a farm affected by postweaning multisystemic wasting syndrome (PMWS). *Comp. Immunol. Microbiol. Infect. Dis.* **33**, e1–e5 (2010).
61. Cline, G., Wilt, V., Diaz, E. & Edler, R. Efficacy of immunising pigs against porcine circovirus type 2 at three or six weeks of age. *Vet. Rec.* **163**, 737–740 (2008).
62. Fachinger, V., Bischoff, R., Jedidia, S. B., Saalmüller, A. & Elbers, K. The effect of vaccination against porcine circovirus type 2 in pigs suffering from porcine respiratory disease complex. *Vaccine* **26**, 1488–1499 (2008).
63. Horlen, K. P. *et al.* A field evaluation of mortality rate and growth performance in pigs vaccinated against porcine circovirus type 2. *J. Am. Vet. Med. Assoc.* **232**, 906–912 (2008).
64. Desrosiers, R., Clark, E., Tremblay, D., Tremblay, R. & Polson, D. Use of a one-dose subunit vaccine to prevent losses associated with porcine circovirus type 2. *J. Swine Health Prod.* **17**, 148–154 (2009).
65. Segalés, J. *et al.* A genetically engineered chimeric vaccine against porcine circovirus type 2 (PCV2) improves clinical, pathological and virological outcomes in postweaning multisystemic wasting syndrome affected farms. *Vaccine* **27**, 7313–7321 (2009).
66. Karuppannan, A. K. & Opriessnig, T. Porcine Circovirus Type 2 (PCV2) Vaccines in the Context of Current Molecular Epidemiology. *Viruses* **9**, (2017).

67. Afghah, Z., Webb, B., Meng, X.-J. & Ramamoorthy, S. Ten years of PCV2 vaccines and vaccination: Is eradication a possibility? *Vet. Microbiol.* **206**, 21–28 (2017).
68. Martelli, P. *et al.* Impact of maternally derived immunity on piglets' immune response and protection against porcine circovirus type 2 (PCV2) after vaccination against PCV2 at different age. *BMC Vet. Res.* **12**, (2016).
69. Rodríguez-Arrioja, G. M. *et al.* Dynamics of porcine circovirus type 2 infection in a herd of pigs with postweaning multisystemic wasting syndrome. *Am. J. Vet. Res.* **63**, 354–357 (2002).
70. Sibila, M. *et al.* Use of a polymerase chain reaction assay and an ELISA to monitor porcine circovirus type 2 infection in pigs from farms with and without postweaning multisystemic wasting syndrome. *Am. J. Vet. Res.* **65**, 88–92 (2004).
71. Fort, M., Olvera, A., Sibila, M., Segalés, J. & Mateu, E. Detection of neutralizing antibodies in postweaning multisystemic wasting syndrome (PMWS)-affected and non-PMWS-affected pigs. *Vet. Microbiol.* **125**, 244–255 (2007).
72. Fort, M. *et al.* Porcine circovirus type 2 (PCV2) vaccination of conventional pigs prevents viremia against PCV2 isolates of different genotypes and geographic origins. *Vaccine* **26**, 1063–1071 (2008).
73. Meerts, P., Gucht, S. V., Cox, E., Vandebosch, A. & Nauwynck, H. j. Correlation Between Type of Adaptive Immune Response Against Porcine Circovirus Type 2 and Level of Virus Replication. *Viral Immunol.* **18**, 333–341 (2005).
74. Koinig, H. C. *et al.* PCV2 vaccination induces IFN- $\gamma$ /TNF- $\alpha$  co-producing T cells with a potential role in protection. *Vet. Res.* **46**, (2015).

75. Phan, T. G. *et al.* Detection of a novel circovirus PCV3 in pigs with cardiac and multi-systemic inflammation. *Viol. J.* **13**, 184 (2016).
76. Palinski, R. *et al.* A Novel Porcine Circovirus Distantly Related to Known Circoviruses Is Associated with Porcine Dermatitis and Nephropathy Syndrome and Reproductive Failure. *J. Virol.* **91**, UNSP e01879-16 (2017).
77. Franzo, G. *et al.* Full-genome sequencing of porcine circovirus 3 field strains from Denmark, Italy and Spain demonstrates a high within-Europe genetic heterogeneity. *Transbound. Emerg. Dis.* **65**, 602–606 (2018).
78. Chen, G. H. *et al.* Detection and genome sequencing of porcine circovirus 3 in neonatal pigs with congenital tremors in South China. *Transbound. Emerg. Dis.* **64**, 1650–1654 (2017).
79. Klaumann, F. *et al.* Retrospective detection of Porcine circovirus 3 (PCV-3) in pig serum samples from Spain. *Transbound. Emerg. Dis.* **65**, 1290–1296 (2018).
80. Schmidt, M. *et al.* IL-10 induces apoptosis in human monocytes involving the CD95 receptor/ligand pathway. *Eur. J. Immunol.* **30**, 1769–1777 (2000).
81. Marra, L. E. *et al.* IL-10 Induces Regulatory T Cell Apoptosis by Up-Regulation of the Membrane Form of TNF- $\alpha$ . *J. Immunol.* **172**, 1028–1035 (2004).
82. Kekarainen, T., Montoya, M., Dominguez, J., Mateu, E. & Segalés, J. Porcine circovirus type 2 (PCV2) viral components immunomodulate recall antigen responses. *Vet. Immunol. Immunopathol.* **124**, 41–49 (2008).
83. Darwich, L. *et al.* Cytokine mRNA expression profiles in lymphoid tissues of pigs naturally affected by postweaning multisystemic wasting syndrome. *J. Gen. Virol.* **84**, 2117–2125 (2003).

84. Darwich, L. *et al.* Transient correlation between viremia levels and IL-10 expression in pigs subclinically infected with porcine circovirus type 2 (PCV2). *Res. Vet. Sci.* **84**, 194–198 (2008).
85. Yue, F. *et al.* Overexpression of Programmed Death Ligands in Naturally Occurring Postweaning Multisystemic Wasting Syndrome. *Viral Immunol.* **28**, 101–106 (2015).
86. Keir, M. E., Butte, M. J., Freeman, G. J. & Sharpe, A. H. PD-1 and its ligands in tolerance and immunity. *Annu Rev Immunol* **26**, 677–704 (2008).
87. Jin, H.-T., Ahmed, R. & Okazaki, T. Role of PD-1 in Regulating T-Cell Immunity. in *Negative Co-Receptors and Ligands* (eds. Ahmed, R. & Honjo, T.) 17–37 (Springer Berlin Heidelberg, 2011).
88. Fife, B. T. & Pauken, K. E. The role of the PD-1 pathway in autoimmunity and peripheral tolerance. *Ann. N. Y. Acad. Sci.* **1217**, 45–59 (2011).
89. Chang, H.-W. *et al.* The involvement of Fas/FasL interaction in porcine circovirus type 2 and porcine reproductive and respiratory syndrome virus co-inoculation-associated lymphocyte apoptosis in vitro. *Vet. Microbiol.* **122**, 72–82 (2007).
90. Fenaux, M., Opriessnig, T., Halbur, P. G., Elvinger, F. & Meng, X. J. Two Amino Acid Mutations in the Capsid Protein of Type 2 Porcine Circovirus (PCV2) Enhanced PCV2 Replication In Vitro and Attenuated the Virus In Vivo. *J. Virol.* **78**, 13440–13446 (2004).
91. Opriessnig, T., McKeown, N. E., Zhou, E.-M., Meng, X.-J. & Halbur, P. G. Genetic and experimental comparison of porcine circovirus type 2 (PCV2) isolates from cases with and without PCV2-associated lesions provides evidence for differences in virulence. *J. Gen. Virol.* **87**, 2923–2932 (2006).



92. Krakowka, S. *et al.* A nine-base nucleotide sequence in the porcine circovirus type 2 (PCV2) nucleocapsid gene determines viral replication and virulence. *Virus Res.* **164**, 90–99 (2012).
93. Huang, L. P., Lu, Y. H., Wei, Y. W., Guo, L. J. & Liu, C. M. Identification of one critical amino acid that determines a conformational neutralizing epitope in the capsid protein of porcine circovirus type 2. *BMC Microbiol.* **11**, 188 (2011).
94. Kroemer, G. *et al.* Classification of cell death. *Cell Death Differ.* **16**, 3–11 (2009).
95. Zhivotovsky, B. & Orrenius, S. Calcium and cell death mechanisms: A perspective from the cell death community. *Cell Calcium* **50**, 211–221 (2011).
96. Lin, C. *et al.* Caspase-Dependent Apoptosis Induction via Viral Protein ORF4 of Porcine Circovirus 2 Binding to Mitochondrial Adenine Nucleotide Translocase 3. *J. Virol.* **92**, e00238-18 (2018).
97. Hubbard, K. & Ozer, H. L. Mechanism of immortalization. *Age* **22**, 65–69 (1999).
98. Reed, L. J. & Muench, H. A simple method of estimating fifty per cent endpoints. *Am. J. Epidemiol.* **27**, 493–497 (1938).
99. Gillespie, J., Opriessnig, T., Meng, X. j., Pelzer, K. & Buechner-Maxwell, V. Porcine Circovirus Type 2 and Porcine Circovirus-Associated Disease. *J. Vet. Intern. Med.* **23**, 1151–1163 (2009).
100. Gao, Z. *et al.* ORF4-protein deficient PCV2 mutants enhance virus-induced apoptosis and show differential expression of mRNAs in vitro. *Virus Res.* **183**, 56–62 (2014).
101. Chae, J.-S. & Choi, K.-S. Proinflammatory cytokine expression in the lung of pigs with porcine circovirus type 2-associated respiratory disease. *Res. Vet. Sci.* **90**, 321–323 (2011).

102. Du, Q. *et al.* Porcine Circovirus Type 2 Suppresses IL-12p40 Induction via Capsid/gC1qR-Mediated MicroRNAs and Signalings. *J. Immunol.* ji1800250 (2018).  
doi:10.4049/jimmunol.1800250
103. Li, S., Kong, L. & Yu, X. The expanding roles of endoplasmic reticulum stress in virus replication and pathogenesis. *Crit. Rev. Microbiol.* **41**, 150–164 (2015).
104. Tait, S. W. G., Ichim, G. & Green, D. R. Die another way – non-apoptotic mechanisms of cell death. *J. Cell Sci.* **127**, 2135–2144 (2014).
105. Shi, Y. Mechanisms of Caspase Activation and Inhibition during Apoptosis. *Mol. Cell* **9**, 459–470 (2002).
106. Corcoran, J. A., Saffran, H. A., Duguay, B. A. & Smiley, J. R. Herpes Simplex Virus UL12.5 Targets Mitochondria through a Mitochondrial Localization Sequence Proximal to the N Terminus. *J. Virol.* **83**, 2601–2610 (2009).
107. Claros, M. G. & Vincens, P. Computational Method to Predict Mitochondrially Imported Proteins and their Targeting Sequences. *Eur. J. Biochem.* **241**, 779–786 (1996).
108. Rodríguez-Cariño, C., Sánchez-Chardi, A. & Segalés, J. Subcellular Immunolocalization of Porcine Circovirus Type 2 (PCV2) in Lymph Nodes from Pigs with Post-weaning Multisystemic Wasting Syndrome (PMWS). *J. Comp. Pathol.* **142**, 291–299 (2010).
109. Engle, T. B. *et al.* Variation in time and magnitude of immune response and viremia in experimental challenges with Porcine circovirus 2b. *BMC Vet. Res.* **10**, (2014).
110. Kreikemeier, C. A. *et al.* Genome-wide analysis of TNF-alpha response in pigs challenged with porcine circovirus 2b. *Anim. Genet.* **46**, 205–208 (2015).

111. Zhu, X., Bai, J., Liu, P., Wang, X. & Jiang, P. Suppressor of cytokine signaling 3 plays an important role in porcine circovirus type 2 subclinical infection by downregulating proinflammatory responses. *Sci. Rep.* **6**, (2016).
112. Byrd, A. L. & Segre, J. A. Adapting Koch's postulates. *Science* **351**, 224–226 (2016).
113. Falkow, S. Molecular Koch's postulates applied to microbial pathogenicity. *Rev. Infect. Dis.* **10 Suppl 2**, S274-276 (1988).